Title
Molecular Mechanism that Leads to Development of Epilepsy by a Sodium Channel Mutation

Author
Velazquez, Eric

Publication Date
2014

Peer reviewed|Thesis/dissertation

UNIVERSITY OF CALIFORNIA,
IRVINE

Molecular Mechanism that Leads to Development of Epilepsy by a Sodium Channel Mutation

DISSERTATION

submitted in partial satisfaction of the requirements
for the degree of

DOCTOR OF PHILOSOPHY

in Biomedical Sciences

by

Eric Velazquez

Dissertation Committee:
Professor Alan L. Goldin, Chair
Professor Emiliana Borrelli
Associate Professor David C. Lyon
Associate Professor Xiangmin Xu

2014

DEDICATION

To my parents, Salvador Velazquez and Esther Rivera, for their love, encouragement and endless support. Their strong work ethic has had a major influence both inside and outside my academic life.

To my brothers, Elias “Tito” and Joel. A special thanks to Joel for always continuing to inspire me, even to this day.

To all my old and new friends, who I consider to be part of my extended family. All of you have shaped my character and who I am as a person.

To my girlfriend, Christine, for her love, support and motivation during my graduate journey.

TABLE OF CONTENTS

LIST OF FIGURES

LIST OF TABLES

ACKNOWLEDGEMENTS

I would like to express my gratitude for the privilege of working under Professor Alan L. Goldin. His support, guidance and mentorship have truly been immeasurable. Al has not only provided me with the tools used to present the work in this dissertation, but his dedication has challenged and inspired me in many ways. It has been a privilege to learn and work under him in his laboratory.

I would like to thank current and previous members of the Goldin laboratory who have helped me in one way or another during all these years. Markus Ehrengruber, Annie Lee, AJ Barela, Joyce Iping, Radit Aur, Hai Nguyen, Christine Hong, Lauren Guy, Bryan Boubion, Jing Chen, Brian Tanaka and Karoni Dutt: thank for you for training me, providing technical assistance and encouraging scientific discussions. Without you, the lab would have never been the same.

I would like to thank my thesis committee members, Professor Emiliana Borrelli, Associate Professor David C. Lyon, Associate Professor Xiangmin Xu and now retired Professor Martin A. Smith for their time commitment, critiques and discussions in order to make me a better scientist.

I would like to thank my collaborators Dr. Andrew Escayg and his lab at Emory University for providing the Scn1a-D1866Y mouse. Thanks to Stacey Dutton from the Escayg lab for her contribution on seizure susceptibility for the dissertation.

In addition, I would like to thank the University of California, Irvine, NIH Grant NS065187, NS048336 for the financial support provided.

CURRICULUM VITAE

Eric Velazquez

Dept. of Microbiology & Molecular Genetics
Medical Sciences I, Room C266 Irvine, CA 92697-4025
(949) 824-8508, Email: velazque@uci.edu

EDUCATION

University of California, Irvine **Irvine, CA**
Ph.D., Biomedical Sciences November 2014
Dissertation: Molecular Mechanism that Leads to Development of Epilepsy by a Sodium Channel Mutation

University of Puerto Rico, Rio Piedras **Rio Piedras, PR**
B.S., Chemistry 2005

RESEARCH EXPERIENCE

University of California, Irvine **Irvine, CA**
Graduate Student Researcher; Advisor: Alan L. Goldin, M.D., Ph.D 2006-2014
Molecular Mechanism that Leads to Development of Epilepsy by a Sodium Channel Mutation

- Measured and determined biophysical properties of neurons by whole-cell patch clamp in hippocampal acute dissociated neurons and acute brain slices
- Analyzed activity of extracellular field potential recordings
- Acquired and maintained primary culture of rodent brain tissue
- Administered and assisted mouse colony of several strains
- Engineered and customized viral vector for transfection of sodium channel in primary and secondary mammalian cultures

University of Puerto Rico, Rio Piedras **Rio Piedras, PR**
Undergraduate Researcher; Advisor: Jose A. Lasalde, Ph.D 2004-2005

- Created and screened sequence of mutant plasmids before performing functional studies
- Collaborated and coordinated with the development of mutant plasmids library
- Assisted with establishment and optimization of techniques new to the lab

University of Puerto Rico, Rio Piedras **Rio Piedras, PR**
Undergraduate Researcher; Advisor: Reginal Morales, Ph.D 2003

- Helped with chromatography protein purification of toxin
- Collaborated and coordinated with local blood bank for the acquisition of blood samples
- Assisted with basic maintenance of lab equipment

PEER-REVIEWED PUBLICATIONS

Lizardi-Ortiz, J.E., Hyzinski-García, M.C., Fernández-Gerena, J.L., Osorio-Martínez, K.M., **Velázquez-Rivera, E.**, Valle-Avilés, F.L., Lasalde-Dominicci, J.A. Aromaticity at the water-hydrocarbon core interface of the membrane: consequences on the nicotinic acetylcholine receptor. Channels. 2008; 2:3, 191-201.

CONFERENCE PRESENTATIONS

Velazquez, E., Boubion, B., Escayg, A., Goldin, A.L. (2014). Epileptic *Scn1a* Mutation Reduces Action Potential Firing of Pyramidal cells. Society for Neuroscience meeting. Poster presentation. Washington, DC. November 2014.

Velazquez, E., Escayg, A., Goldin, A.L. (2013). An Epilepsy-Causing Mutation in SCN1A Causes Gain-of-Function in GABAergic Interneurons. Poster presentation at the UCI EpiCenter Symposium, Irvine, CA., March 2013.

Velazquez, E., Escayg, A., Goldin, A.L. (2012). An Epilepsy-Causing Mutation in SCN1A Causes Gain-of-Function in GABAergic Interneurons. Poster presentation at the American Epilepsy Society meeting, San Diego, CA., December 2012.

GRANTS AND AWARDS

Howard Hughes Medical Institute – UCI Graduate Fellow 2008-2009

TEACHING

University of California, Irvine
Teaching Assistant, Genetics Winter 2009

REFERENCES

Alan L. Goldin, M.D, Ph.D.
Professor, Department of Microbiology & Molecular Genetics
Director, Medical Scientist Training Program
Senior Associate Dean for Academic Affairs
University of California, Irvine
Irvine, CA 92697-4025
240 Medical Sciences B
(949) 824-5334
agoldin@uci.edu

ABSTRACT OF THE DISSERTATION

Molecular Mechanism that Leads to Development of Epilepsy
by a Sodium Channel Mutation

By

Eric Velazquez

Doctor of Philosophy in Biomedical Sciences

University of California, Irvine, 2014

Professor Alan L. Goldin, Chair

The number of mutations in the voltage-gated sodium channel Nav1.1, encoded by *SCN1A,* that have been associated with genetic epilepsy is extremely high compared to the other sodium channel genes. The crucial function of the voltage-gated sodium channels in the central nervous system (CNS) is to regulate the influx of sodium or sodium current into the neurons. Sodium currents are required for the generation and propagation of action potentials. Subsequently the action potentials cause the release of neurotransmitters that allow the communication and synchronization among neurons in a circuit. Most of the previous mouse models of *Scn1a* sodium channel mutations result in loss-of-function of sodium currents and decrease of excitability of interneurons. In this study, I investigate the mechanism by which a novel *SCN1A* mutation, D1886Y, causes epilepsy in a mouse model. Chapter 1

examines the activation, inactivation and dynamics of sodium currents in parvalbumin-expressing (PV+) interneurons from the hippocampus. The *Snc1a*-D1866Y mutation in these neurons resulted in gain-of-function of sodium current. Chapter 2 investigates how the *Snc1a*-D1866Y mutation affects the excitability of excitatory and inhibitory neurons to generate action potentials. In PV+ interneurons, the mutation reduced the excitability to fire action potentials. A reduction in action potential firing was also detected in pyramidal neurons, but to a lesser degree. Chapter 3 examines the seizure susceptibility *in vivo* and in the hippocampal circuit of mice expressing the *Snc1a*-D1866Y mutation. Our findings suggest the existence of different molecular mechanisms for how *Scn1a* mutations cause epilepsy. Identification of the molecular mechanisms that lead to epilepsy is crucial for the development of new anti-epileptic drugs.

INTRODUCTION

Epilepsy is a disease that has been described thousands of years ago since the first human civilizations (Wolf, 2010), and is one of the most common neurological disorders. It affects about 1% of the global population (Tuchman, Hirtz, & Mamounas, 2013) and over 3 million Americans of all ages – more than multiple sclerosis, cerebral palsy, muscular dystrophy, and Parkinson's disease combined. In the United States, almost 500 new cases of epilepsy are diagnosed every day, and it is estimated that up to 50,000 deaths occur annually associated with epilepsy (WHO, 2009). Most recent estimations predict that in United States, 1 in 26 people will develop epilepsy during some point in their life (CURE, 2013), and about 5–10% of all people will have an unprovoked seizure (Pallin et al., 2008).

Although it has been known for centuries that epilepsy results from dysfunction of the brain, we still don't have a cure or a complete understanding of the pathology, despite the advance of scientific tools that has helped to understand the function of both normal and epileptic brain. We know that seizures arise from abnormal electrical activity of neural networks (Berg et al., 2010). Some of the factors that have made it difficult to find a cure or better treatments are "intrinsic" to the nature of epilepsy. First, epilepsy affects the most complex organ in vertebrates, the brain. The brain contains tens of billions neurons, with great heterogeneity such that each neuron may contact tens of

thousands of other neurons (Silvestri, Sacconi, & Pavone, 2013). All this by itself could make a single human brain more complex than all the computer, routers and internet combined together. The intricacy is so vast that Nobel laureate physics and mathematician Sir Roger Penrose considered the brain as the most complex structure in the universe (Krulwich, 2012). If we consider this complexity in conjunction with the plasticity, dynamics and different patterns in the brain, it is not surprising how daunting it is to understand the brain. Second, epilepsy is not one but a group of neurological disorders that affect the brain, with the majority of the epileptic disorders being precipitated by multiple genetic, acquired and precipitating factors (Bladin, 2011; Lennox, 1947). This means that there are multiple phenotypes and multiple ways to produce seizures, with complex gene interactions and modifiers (epistatic) with the internal or external environment (epigenetic) taking place (Kim et al., 2011; Roopra, Dingledine, & Hsieh, 2012). This complexity makes it very difficult to determine the cause of epilepsy. For example, two patients with similar phenotype may have different neural circuits affected, with different mechanisms of seizure generation. Therefore, their prognosis and treatment could be very different despite the same set of symptoms (Wilmshurst, Berg, Lagae, Newton, & Cross, 2014).

Several of the factors that lead to the development of epilepsy include stroke, head trauma, brain tumors, and genetic mutations. The most common type of epilepsy comprising 40% of cases is considered idiopathic, meaning that the cause is unknown (Steinlein, 2002). It is likely that most of these idiopathic

epilepsies are due to genetic mutations (Hirose, Mitsudome, Okada, & Kaneko, 2005). Therefore, genetics is believed to be the main driving force, directly or indirectly, responsible for epilepsy. Mutations in some genes result in alterations of brain structure and development that lead to seizures (Guerrini & Dobyns, 2014), but the majority of the genes identified so far that are involved in seizure generation contribute in some way to the excitability or conductance of neurons. These genes can encode for neurotransmitter receptors, ion channels, or enzymes that affect either the production, release or removal of the neurotransmitters and channels (Calhoun & Isom, 2014).

Genetic Epilepsy with Febrile Seizures plus (GEFS+) is a genetic epileptic disorder that has an autosomal dominant pattern of inheritance (Scheffer & Berkovic, 1997). Individuals affected with GEFS+ can experience febrile seizure before age of six, and beyond this age they often experience afebrile seizures of many different types. Mutations in five genes have been shown to cause GEFS+, although mutations in *SCN1A* (Nav1.1) are the major cause of GEFS+ and other related epileptic disorders (L. R. F. Claes et al., 2009; Lossin, 2009). All of the genes that have been identified as causing GEFS+ are related to inhibition. The first two genes are *GABRG2* and *GABRD* that encode the gamma2 and delta subunits of the $GABA_A$ receptor (Baulac et al., 2001; Harkin et al., 2002; Wallace et al., 2001). The other 3 genes encode different subunits of the voltage-gated sodium channel (VGSC). VGSC are composed of one core α subunit and two modulatory or accessory β subunits. β subunits do not form the sodium channel

by themselves, but they modulate localization, cell surface expression and electrophysiological properties of the α subunit of VGSCs (Calhoun & Isom, 2014). Although there are 4 isoforms of the β subunits (β1-β4) that are expressed in the CNS of mammals, only mutations in the β1 subunit (*SCN1B*) have been associated with GEFS+. $Na_v1.1$ (*SCN1A*) and $Na_v1.2$ (*SCN2A*) are two of α subunit VGSC isoforms that are expressed in the adult central nervous system in mammals and that have been associated with GEFS+. Approximately 20 mutations in *SCN2A* have been associated with mild epileptic disorders including GEFS+, while over 800 mutations of *SCN1A* have been associated with epileptic disorders. Over 70% of *SCN1A* mutations cause Dravet syndrome (formally known as Severe Myoclonic Epilepsy of Infancy), a more severe epileptic disorder than GEFS+ (Catterall, 2014; Singh et al., 2001). About 29 missense mutations cause GEFS+, making *SCN1A* mutations the major cause of this syndrome.

The function of the VGSC is to initiate and propagate action potentials, by controlling the sodium influx. These pore-forming α subunits isoforms have about 80% homology and they therefore share the same structure (Catterall, 2000). Each isoform contains four homologous domains, where each domain has six transmembrane segments, as well as intracellular N and C domains (Catterall, 1993). The VGSCs are in a closed state when the membrane potential is at resting. When the membrane potential of a cell is raised above the resting potential, this change is sensed by the VGSCs, causing a conformational change

from closed to open that allows sodium ions to flow from the outside to inside of the cell (Hille, 2001). The influx of sodium causes further depolarization of the cell, causing more VGSCs to activate into the open state. After a few milliseconds, the positive membrane potential due to the sodium influx causes another conformational change of the VGSC from open to inactive that blocks the flow of Na^+. As VGSCs inactivate, potassium channels open, allowing the flow of potassium ions from the inside to the outside of the cell to repolarize the membrane potential. Once the resting potential is reestablished, the VGSCs go through another conformational change from the inactivated to the closed state, which is necessary for the VGSCs to fire another action potential (Armstrong & Hille, 1998). Therefore, the properties of the open, closed and inactive states and the transition kinetics from one state to another help to determine the shape and frequency of the action potentials. Thus, if a mutation causes changes in the properties of any of the VGSC states and/or kinetics, these changes are likely to affect the firing of action potentials. Erratic firing of action potentials disturbs the delicate excitatory and inhibitory balance in the CNS and can lead to an epileptic phenotype.

Since the identification of the first mutation associated with GEFS+, researchers have being trying to determine the molecular mechanisms that lead to epilepsy. The first approach that was used was to study the properties of the mutant channels and anti-epileptic drugs (AEDs) in heterologous expression systems such as *Xenopus* oocytes (Tomaselli, Marbán, & Yellen, 1989). In these

experiments, cDNA of the sodium channel subunit containing mutations that cause epilepsy were injected into the oocytes (Spampanato, Escayg, Meisler, & Goldin, 2001; Wallace et al., 1998). An alternative system was to express the mutant channels either transiently or stably in mammalian cell lines such as human embryonic kidney (HEK) cells (Alekov, Rahman, Mitrovic, Lehmann-Horn, & Lerche, 2000; Lossin, Wang, Rhodes, Vanoye, & George, 2002). Because of the relatively easy expression of mutant sodium channels in these systems, the heterologous systems have been very important for the characterization, development and screening of AEDs. Unfortunately, these systems do not model all the physiological aspects of the disease, for two reasons. First, a single mutation of *Scn1a* has been shown to have different effects among different expression system (Escayg & Goldin, 2010). Therefore, the results using heterologous systems may not reflect the real physiological effects of the mutations (Mantegazza, 2011). Second, the heterologous systems cannot replicate some of the basic characteristic of a neuron, which are the generation of action potentials, formation of circuits and seizures (Mantegazza, Rusconi, Scalmani, Avanzini, & Franceschetti, 2010).

More recently, genetically modified mice have been used to more accurately model epileptic human diseases (Noebels, 2001). Introduction of gene deletions or specific single point mutations makes it possible to use the mice to characterize the effects of the mutations at the molecular, tissue or organ, and *in*

vivo behavior level. Several models of GEFS+ and Dravet Syndrome (DS) had been produced in the last decade using mice.

About half of the mutations in *SCN1A* that result in DS encode for nonsense or frameshift mutations (Marini et al., 2007). These types of mutations result in non-functional $Na_v1.1$ sodium channels or haploinsufficiency (Bechi et al., 2012; Meisler & Kearney, 2005). Therefore, most of the mouse models with alterations in *Scn1a* have been exon removal or nonsense mutations, which eliminate expression of the sodium channel (Mistry et al., 2014; Ogiwara et al., 2007; Yu et al., 2006). The reduced expression of *Scn1a* in all these mouse models appears to affect only the sodium current of the interneurons at the age at which symptoms become apparent. The reduction of sodium current density consequently leads to a reduction in the excitability of the affected interneurons. Because interneurons are GABAergic, they cause inhibition of the neurons receiving their input (Babb, Pretorius, Kupfer, & Brown, 1988; Wallingford, Ostdahl, Zarzecki, Kaufman, & Somjen, 1973). These results have led to the current hypothesis concerning the mechanism of DS, which is that it results from loss of inhibition. This model of loss of inhibition was also supported by results with the *Scn1a*-R1648H mutation that causes GEFS+ (Martin et al., 2010). The *Scn1a*-R1648H mutation neutralizes one of the positively charged argentines located in the voltage-sensing transmembrane segment of the sodium channel. The R1648H mutation caused a reduction in the sodium current density in

inhibitory neurons (Martin et al., 2010; Tang et al., 2009), similar to the results for the DS mutations.

An important question is whether all mutations in *SCN1A* that are associated with GEFS+, DS or other related epileptic disorders cause seizures by the same pathological mechanism. Although there has been an expansion in the number of antiepileptic drugs (AEDs) in recent years, the percentage of epileptic patients with good seizure control has not improved. Seizures cannot be completely controlled in about 30% of epileptic patients, a percentage that has not changed over the past decades (Kwan & Brodie, 2000; Laxer et al., 2014). This lack of success in seizure control suggests that there are other molecular mechanisms responsible for causing seizures, and these mechanisms are not blocked by current AEDs. Uncontrolled seizures from refractory epilepsy are known to increase the risk of death (Sillanpaa 2010). Patients with epilepsy also suffer from a variety of other disorders and comorbidities (Helmstaedter et al., 2014), which contribute to a poor quality of life.

One of the mutations in *SCN1A* that causes GEFS+ is D1866Y (Spampanato et al., 2004). The D1866Y mutation is found in different domain from the GEFS+ mutations of the sodium channel that have been previously studied. This mutation is located in the C terminus of the VGSC, specifically in what is predicted to be an EF-hand domain (Chagot, Potet, Balser, & Chazin, 2009; Wingo et al., 2004) . Including D1866Y, there are 3 additional mutations in

the small EF-hand domain of *SCN1A* have been identified as causing GEFS+ (Annesi et al., 2003; Hindocha et al., 2009; Nagao et al., 2005), making this domain one of the most common sites of GEFS+ mutations. Mutations in the same domain in $Na_v1.5$ (*SCN5A*), the main cardiac VGSC isoform, have been associated with Long-QT syndrome (LQTS) and Brugada syndrome (Zimmer & Surber, 2009).

In this study, we investigated the mechanism of how the D1866Y mutation causes GEFS+. First, we determined the changes in the gating properties of the sodium channel due to the mutation. To accomplish this aim, we isolated and recorded sodium currents from dissociated interneurons in the hippocampus that express parvalbumin. We selected these neurons because they have been shown to express high levels of *Scn1a* (Ogiwara et al., 2007). Second, we determined the alterations of neuronal excitability resulting from the mutation. To accomplish this objective, we measured the ability of the same hippocampal interneurons and excitatory neurons to fire action potentials in brain slices. Third, we determined the effect of the mutation on the susceptibility for seizures. To accomplish this aim, we measured susceptibility to induced convulsions *in vivo* and the seizure-like activity in the hippocampal network in brain slices.

CHAPTER 1

Epileptic *Scn1a*-D1866Y Mutation Increases Sodium Current in Interneurons

Abstract

The D1866Y mutation in the *SCN1A* sodium channel gene is one of hundreds of mutations in the channel that can result in an epilepsy syndrome. Several heterologous expression systems have been used to determine the functional effects on the sodium currents of some of these mutations. However, conflicting results between those system and mammalian neurons from mouse models suggest that findings in heterologous systems may not reflect the results *in vivo*. To determine the physiological effects of one of these mutations (D1866Y), we analyzed the gating properties of the mutant sodium channels in parvalbumin-expressing interneurons from the hippocampus of knock-in mice. This population of neurons was selected because they have been shown to endogenously express high amounts of the *Scn1a* sodium channel. The sodium current density was unaffected by the expression of the *Scn1a*-D1866Y, suggesting that there is no trafficking defect due to the mutation. The *Scn1a*-D1866Y shifted the voltage-dependence of activation to depolarized voltages, consistent with a loss-of-function due the mutation. There was no effect on the voltage-dependence of inactivation. However, we observed acceleration in

recovery from inactivation, reduced use-dependent inactivation and the slower kinetics of inactivation, all of which are consistent with increased sodium channel activity. These findings suggest that the *Scn1a*-D1866Y mutation results in a net gain-of-function of the sodium channel.

Introduction

Mutations in *SCN1A* can be associated with several genetic epileptic disorders, one of them being Genetic Epilepsy with Febrile Seizures plus (GEFS+). GEFS+ is considerate to be part of a spectrum of genetic epileptic syndromes, including febrile seizures, severe myoclonic epilepsy, borderline severe myoclonic epilepsy (SMEB), intractable childhood epilepsy with generalized tonic-clonic seizures (ICEGTC) and Dravet Syndrome (DS), among others (Parihar & Ganesh, 2013). A common characteristic among these epileptic disorders is that they are inherited in an autosomal dominant fashion. Other similarities among these disorders are the phenotypes and the ages of onset of seizures, which occur during infancy. The phenotypic spectrum ranges from mild seizure as in febrile seizures to severe seizures in patients with Dravet Syndrome, with GEFS+ representing an intermediate phenotype.

The mutation D1866Y in *SCN1A* that causes GEFS+ is found in the predicted EF-hand domain in the sodium channel C-terminus (Babitch & Anthony, 1987; Chagot et al., 2009; Wingo et al., 2004). Although mutations in *SCN1A* that are associated with epilepsy are found throughout the whole sodium channel gene (http://www.scn1a.info/ and http://www.molgen.ua.ac.be/SCN1AMutations/Statistics/Mutations.cfm), mutations in the C-terminus in other homologous sodium channels have been associated with changes in sodium current properties that result in a wide range of diseases. Analysis of the effects of the D1866Y mutation in *Xenopus laevis*

oocytes suggested that the mutation produces a change in the interactions with the auxiliary subunit β1, encoded by *Scn1b* (Spampanato et al., 2004*)*. The consequences of this disrupted interaction were a depolarized shift in the voltage-dependence of inactivation, accelerated recovery from inactivation, increased persistent current and reduced use-dependent inactivation of the sodium current (Spampanato et al., 2004). These results suggest that the *Scn1a*-D1866Y mutation results in a gain-of-function of the sodium channel.

Previous studies in our lab and others have characterized the effects on the sodium current properties of a number of different mutations that also cause GEFS+ and DS. Not surprisingly, different mutations in *Scn1a* result in different changes in gating properties, although there has not been any correlation between the position of the mutation with the gating property modified or phenotype. Many of these studies were done using *Xenopus* oocytes or HEK cell heterologous expression systems (Escayg & Goldin, 2010). One of the most studied GEFS+ mutations in *SCN1A* is R1648H, a mutation found in the transmembrane segment that senses the membrane voltage (Escayg et al., 2000). First, the effects of the *Scn1a*-R1648H mutation were studied in *Xenopus* oocytes, in which the mutation resulted in gain-of-function of sodium channels due to acceleration of recovery from inactivation and reduced use-dependent inactivation of the sodium current (Spampanato et al., 2001). *Scn1a*-R1648H expressed in HEK cells also resulted in gain-of-function changes, although by a different mechanism involving increased persistent current (Lossin et al., 2002).

When the *Scn1a*-R1648H mutation was studied in a knock-in mouse model, which is most likely a more relevant model to determine physiological effects, the mutation resulted in reduced current density, increased use-dependent inactivation and slower recovery from inactivation in dissociated bipolar shaped cortical interneurons, which are inhibitory (Martin et al., 2010). The *Scn1a*-R1648H mutation's effects on dissociated cortical pyramidal neurons, which are excitatory, were minimal. These results suggest that the *Scn1a*-R1648H mutation results in loss-of-function of the sodium channel in inhibitory neurons, which would lead to decreased inhibition (Martin et al., 2010).

Taking into consideration all of these contradictory findings about the effects of the *Scn1a*-R1648H mutation in different expression systems, it appears that each expression system modified the effects of the mutation in different ways (Escayg & Goldin, 2010). This is not surprising because each system is likely to have different protein interactions, post translational modifications and other regulatory factors in the cell environment (Mantegazza et al., 2010). Therefore, to more accurately determine the effects of the D1866Y mutation *in vivo*, we examined sodium currents in a specific population of interneurons from knock-in mice. It is important to examine a specific neuronal subpopulation because of the heterogeneity of neurons in the hippocampus (Klausberger & Somogyi, 2008). Parvalbumin-expressing (PV+) inhibitory interneurons express a high level of *Scn1a* (Ogiwara et al., 2007), making them an excellent neuronal

target to detect changes of sodium current properties resulting from the D1866Y mutation.

Based on observations made in neurons from diverse mouse models of mutations in *Scn1a,* the mutations have a significant effect only on the properties of inhibitory interneurons at early ages (Martin et al., 2010; Mistry et al., 2014; Ogiwara et al., 2007; Yu et al., 2006). The goal of this research is to determine how the *Scn1a*-D1866Y mutation alters the function of the *Scn1a* sodium channel, for which it is crucial to analyze the sodium current properties in the native neuronal environment in which the sodium channel is expressed. Therefore, we isolated sodium currents from PV+ interneurons of the hippocampus from infant-juvenile mice of age P16-P17.

Materials and Methods

Animals

Generation of *Scn1a*-D1866Y mice was performed by our collaborator, Dr. Andrew Escayg in Emory University, Georgia, using homologous recombination. Once mice were received at the University of California, Irvine, the *Scn1a*-D1866Y mice were backcrossed to C57BL/6 mice for at least 8 generations. The G42 transgenic mice expressing enhanced green fluorescent protein (EGFP) specifically in PV+ interneurons (Chattopadhyaya et al., 2004), which is on the C57BL/6 genetic background, were crossed to the *Scn1a*-D1866Y mice. Heterozygous mice for the *Scn1a*-D1866Y mutation (*Scn1a*$^{D1866Y/+}$) were bred to obtain mice homozygous for *Scn1a*-D1866Y (*Scn1a*$^{D1866Y/D1866Y}$). Only one of the breeders is hemizygous for the expression of EGFP. Mice were maintained at 22 °C on a 12-h light/dark cycle. Food and water were available *ad libitum*. All experiments were performed in accordance with the Institutional Animal Care and Use Committees of University of California, Irvine.

Genotyping

To detect the presence of the *Scn1a*-D1866Y mutation, tail samples were taken from mice between postnatal days 4 and 14 (P4-P14) and digested overnight at 60°C. DNA from tails samples was amplified by PCR using a specific *Scn1a* primer pair in which the forward primer is ACATGTACATTGCTGTCATCCTG and the reverse primer is TTTCCCAACAGAAACCCTGC. PCR amplification was performed with 1 cycle at 94°C for 4 min, 38 cycles at 94°C for 30 sec, 64°C for

30 sec, 72°C for 1.5 min and 1 cycle at 72°C for 4 min. The 1163 base pairs (bp) band was digested with the restriction enzyme BsrGI overnight at 37°C. DNA fragments were resolved in 0.8% agarose gel. The wild-type band is 1163 bp and the mutant bands are 904 bp and 259 bp. To detect the presence of expression of EGFP on mice, we used goggles with light source and emission filters to visualize EGFP (Model:FHS/LS-1B from BLS Ltd., Budapest, Hungry) in the brains of mice between the ages P0-P4. After P4, the skin pigmentation and thickness of mice makes it impossible to detect EGFP with the goggles. If EGFP expression was not determined by P4, then EGFP expression was determined by PCR analysis. Amplification of EGFP was done using same DNA extracted from tail samples to determine the genotype of the D1866Y mutation. Primers AAGTTCATCTGCACCACCG and TCCTTGAAGAAGATGGTGCG with 1 cycle at 94°C for 4 min, 35 cycles at 94°C for 30 sec, 62°C for 30 sec, 72°C for 1 min and 1 cycle at 72°C for 4 min produced a 173 bp band. Forward Primer CTAGGCCACAGAATTGAAAGATCT and reverse primer GTAGGTGGAAATTCTAGCATCATCC were also used with EGFP primers as DNA positive control that produces a 324 bp band.

Preparation of dissociated cells

Dissociated cells were acquired using a slightly modified method previously described by Li et al. (Li, Massengill, O'Dowd, & Smith, 1997) (http://www.jove.com/video/562/preparation-of-dissociated-mouse-cortical-neuron-cultures). Briefly, EGFP-positive male mice between P16-P17 were

anesthetized with halothane and decapitated. The brains were removed and put quickly on oxygenated ice-cold dissociation solution and horizontally sliced with a vibrotome (300 microns) while oxygenating with 95% O_2 and 5% CO_2. Using a bright field microscope and capillary glass, the hippocampus was identified, removed from slices, minced and then digested for 30 min with a papain-containing solution at 37°C. Enzyme digestion was halted by washing the minced hippocampus once with ice-cold dissociation solution, 3 times with ice-cold high concentration of BSA/Trypsin Inhibitor solution (HI) and then 2 times with ice-cold low concentration BSA/Trypsin Inhibitor solution (LI). The minced hippocampus was transferred to neurobasal medium supplemented with B27 solution, in which cells were mechanically dissociated using a fire polished Pasteur pipette. Dissociated cells were plated on poly-L-Lysine (PDL)-coated coverslips and cultured at 37°C in 5% CO_2. After 1 hour, cells were fed with glial conditioned media previously warmed to 37°C.

Electrophysiological recordings

Voltage-clamp recordings on dissociated cells were done at 23°C in the whole-cell configuration within 2-36 hours after being plated to let them recover. This time allowed the cells to re-grow some of the processes lost during the dissociation while still limiting space clamp artifacts. Identification of parvalbumin-EGFP positive cells was done visually using an inverted Axiovert A100 microscope. Sodium currents were isolated and recorded by transferring coverslips with dissociated cells to bath (external) solution consisting (in mM):

150 NaCl, 3 KCl, 15 TEA-Cl, 4 $BaCl_2$, 0.1 $CdCl_2$ and 10 HEPES (pH 7.4). The electrode solution consisted of (in mM): 190 N-methyl-D-glucamine, 1 NaCl, 4 $MgCl_2$, 0.1 BAPTA, 4 Na_2-ATP, 1.6 phospocreatine-Na_2, 0.2 GTP-TRIS and 30 HEPES (pH 7.4). Patch pipettes with a resistance of 4-7 MΩ were pulled from borosilicate glass (1.5 mm OD, 0.86 mm ID; Sutter Instruments, Novato, CA) with a P-97 Flaming-Brown puller (Sutter Instruments, Novato, CA). Recordings were done using an Axopatch 1C patch clamp with Digidata 1322A interface and Clampex 10.2 software. After forming a gigaseal and breaking into the cell, fast capacitance and whole cell capacitance and resistance were compensated, followed by series resistance compensation to 40-80%. Corrections for leak and capacitance currents were done using P/4 subtraction. Currents were filtered at 5 kHz and sampled at 25 kHz.

Channel properties were examined using different pulse protocols based on the procedures previously described by Spampanato et al. (Spampanato et al., 2004). Voltage-dependence of activation and inactivation, kinetics of inactivation, persistent current and current density were determined using a two-step protocol, in which a conditioning pulse was applied from a holding potential of -80 mV to a range of potentials from -100 to 15 mV in 5 mV increments for 100 msec, immediately followed by a test pulse to -15 mV for 10 msec. The time between the end of the conditional step pulse and the start of the conditional step pulse of the next sweep was 3.8 sec, which was determined to be long enough for the sodium channels to completely recover from inactivation. To analyze the voltage-

dependence of activation, peak currents from the conditional pulse were normalized to the maximum peak current and plotted against voltage to calculate reversal potential. Current was converted to conductance and plotted against voltage and fit with a Boltzmann distribution. The equation used is $G = 1 / (1 + \exp(-0.03937z(V - V_{1/2}))$, in which G is conductance, z is the apparent gating charge, V is the potential of the conditional step pulse, and $V_{1/2}$ is the potential for half-maximal activation. The voltage-dependence of inactivation data were fit with the equation $I = 1 / (1 + \exp(V - V_{1/2}) / a)$, in which I is equal to the test pulse current amplitude, V is the potential of the conditioning pulse, $V_{1/2}$ is the voltage for half-maximal inactivation, and a is the slope factor. The peak current amplitudes during the test pulses were normalized to the maximum peak current amplitude of the test pulses, plotted against the potential of the conditioning pulse, and fit with a Boltzmann distribution. To analyze the kinetics of inactivation, the decaying sodium current were fit using the Chebyshev method with a double exponential equation $I = A_{Fast} \times \exp[-(t - K)/ \tau_{Fast}] + A_{Slow} \times \exp[-(t - K)/ \tau_{Slow}] + C$, in which I is the current, A_{Fast} and A_{Slow} are the relative proportions of current inactivating with the time constants τ_{Fast} and τ_{Slow}, K is the time shift, and C is the steady-state non-inactivating current. The time shift was selected manually from the point at which the macroscopic current began to inactivate exponentially until 7 msec after the pulse started.

Current density was analyzed by dividing the maximal peak current by the cell capacitance. Persistent current was analyzed by dividing the mean current during

the last 10 milliseconds of the conditional pulse at 0 mV by the maximal peak current. Recovery from inactivation was analyzed using a two-step protocol in which the conditional pulse and test pulse were changed from a holding potential of -80 mV to -15 mV for 50 and 5 msec, respectively. The initial time between the conditional pulse and test pulse was 25 msec and subsequently reduced by to 1 msec on each sweep until the time between pulses was 1 msec. Peak currents during the test pulses were normalized to the peak current of the corresponding conditional pulse. Normalized currents were plotted as a function of time between pulses. To determine use-dependent inactivation, a train of 100 depolarizations was applied, with each depolarization from a holding potential of -80 mV to -15 mV for 17.5 msec. The time between pulses was controlled by changing frequency of the pulses to 39 Hz, 20 Hz or 10 Hz. The peak current during each depolarization was normalized to the peak current during the first depolarization and normalized currents were plotted as function of the corresponding start time of each pulse. The start time of the first pulse was time 0.

Statistical Analysis

Pulse generation and data collection were done with pCLAMP 10.2. All data are reported as mean ± standard error of mean (SEM). All statistics analysis was performed with SigmaStat 3.10. Statistical significance was determine with p-values under 5% ($p<0.05$). When comparing only 2 genotypes with respect to a single parameter, data were analyzed using Student's t-test. When comparing 3

genotypes, we used analysis of variance (ANOVA) followed by post-hoc pairwise comparison using the Holm-Sidak correction. One way ANOVA was used when the genotype was the only variable with multiple levels. Two way ANOVA was used when the time or voltage variable also had multiple levels.

Results

Mice carrying the *Scn1a*-D1866Y mutation were identified by electrophoresis after PCR and BsrGI digests of DNA obtained from tail samples. Heterozygosity and homozygosity of the *Scn1a*-D1866Y mutation (Fig. 1.1A) and hemizygosity of EGFP expression (Fig. 1.1B) were detected in Mendelian ratios. Mice carrying the *Scn1a*-D1866Y mutation were undistinguishable from wild-type littermates, regardless of the genetic dose.

Figure 1.1. *Scn1a*-D1866Y mutation identification

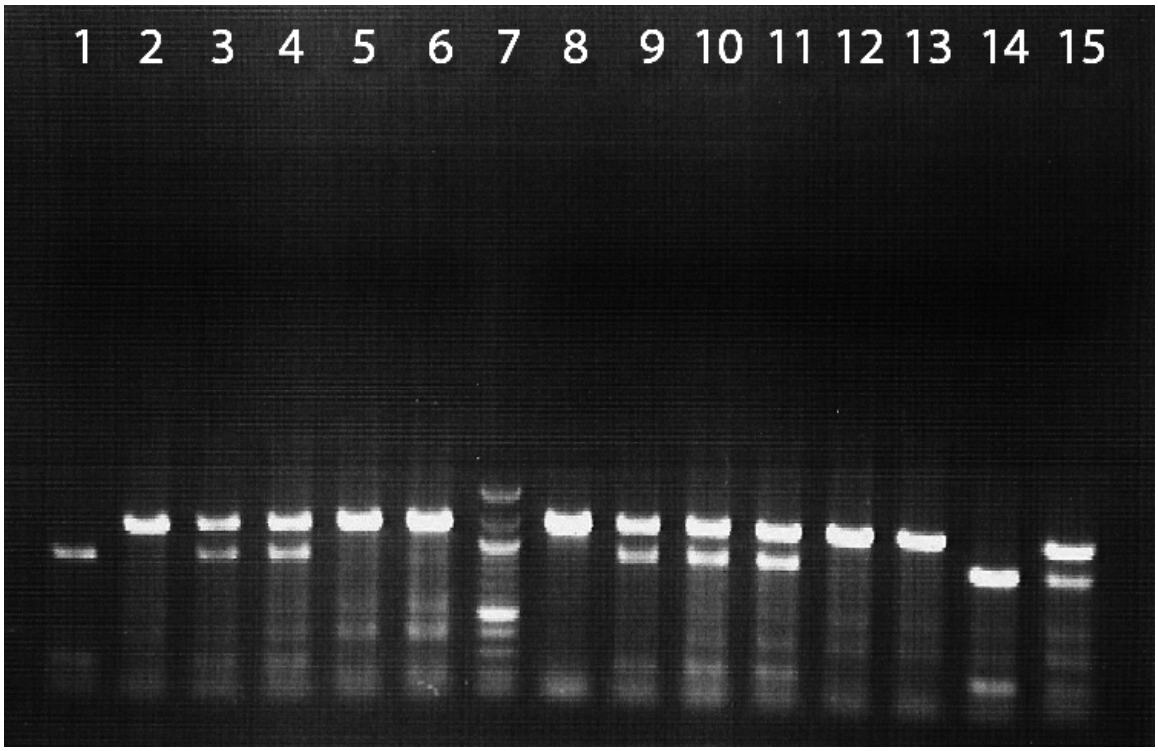

Figure 1.1. *Scn1a*-D1866Y mutation identification

Agarose gel electrophoresis of DNA from mice with the *Scn1a*-D1866Y mutation. Lanes 1 through 6 are from one litter and lanes 10 through 15 are from a second litter. Lanes 7-10 are controls. Lanes 2, 5, 6, 12 and 13 identify $Scn1a^{+/+}$ (wild-type) mice. Lanes 3, 4, 11 and 15 identify $Scn1a^{D1866Y/+}$ (heterozygous) mice. Lanes 1 and 14 identify $Scn1a^{D1866Y/D1866Y}$ (homozygous) mice. Lane 8 is a PCR control from heterozygous mice, while lane 9 is PCR-digested DNA from the same heterozygous control mouse. Lane 7 is a 100 bp ladder (NEB), with the brightest bands representing 1 Kb and 500 bp.

PV+ interneurons from Scn1a-D1866Y mice exhibit small changes in voltage-dependent properties

To investigate the mechanism(s) of how the *Scn1a*-D1866Y mutation in the voltage-gated sodium channel leads to seizures, we measured the peak sodium current amplitude in dissociated neurons from the hippocampus. Previous studies using other mouse models of GEFS+ and DS have suggested that the mutations only affect the properties of sodium currents of interneurons and not excitatory pyramidal neurons (Martin et al., 2010; Ogiwara et al., 2007; Yu et al., 2006). Those studies examined neurons during the second postnatal week, so we studied dissociated neurons from P16-P17 mice so we could compare the effects to those observed in the other mouse models. The hippocampus has more than twenty different populations of interneurons (Klausberger & Somogyi, 2008), and each one has different biochemical and electrophysiological properties. Therefore, it is critical to record sodium currents from a defined subpopulation of interneurons to compare mutant and wild-type properties. By crossing the *Scn1a*-D1866Y mice with the G42 transgenic mice (Chattopadhyaya et al., 2004), we were able to identify the subpopulation of PV+ interneurons by their EGFP expression. PV+ inhibitory interneurons are the subpopulation of interneurons with the most abundant expression of *Scn1a* during the age range of our experiments (Ogiwara et al., 2007).

Scn1a encodes the voltage-gated sodium channel $Na_v1.1$, which is important for regulating neuronal excitability. Therefore, we first examined the voltage-dependent gating properties of the mutant channels. Using a two-step voltage protocol, we measured the voltage-dependence of both activation and inactivation (Fig. 1.2A). Peak currents elicited during the conditional step voltages were analyzed to determine the voltage-dependence of activation. The voltage-dependence of activation in PV+ interneurons from homozygous mice was slightly shifted to depolarized voltages compare to wild-type littermates (Fig. 1.2B). PV+ interneurons from heterozygous mice were similar to wild-type. For quantification and comparison of the shift in the voltage-dependence of activation due to the D1866Y mutation, the data were fit with a Boltzmann distribution to determine the $V_{1/2}$ of activation (Fig 1.2C). The $V_{1/2}$ of activation for homozygous neurons was -28.6 ± 1 mV (n=6), which is significantly more positive than that of wild-type neurons (-35.3 ± 4 mV, n=6) (One way ANOVA; $p<0.05$). The $V_{1/2}$ of activation in heterozygous neurons was -33.2 ± 3 mV (n=4), which was not significantly different from either homozygous or wild-type neurons (Table 1).

We also examined the voltage-dependence of inactivation by plotting peak currents during the test pulse against the conditional step voltage. The *Scn1a*-D1866Y mutation did not have a significant effect on the voltage-dependence of inactivation (Fig. 1.2D). As for activation, a Boltzmann equation was used for a quantitative comparison (Fig 1.2E). The $V_{1/2}$ of inactivation for wild-type, heterozygous and homozygous neurons was -58.2 ± 4 mV (n=6), -57.0 ± 3 mV (n=4), -54.8 ± 2 mV (n=6), respectively (One way ANOVA; $p=0.22$) (Table 1).

Figure 1.2. *Scn1a*-D1866Y shifted the voltage-dependence of activation but not steady-state of inactivation

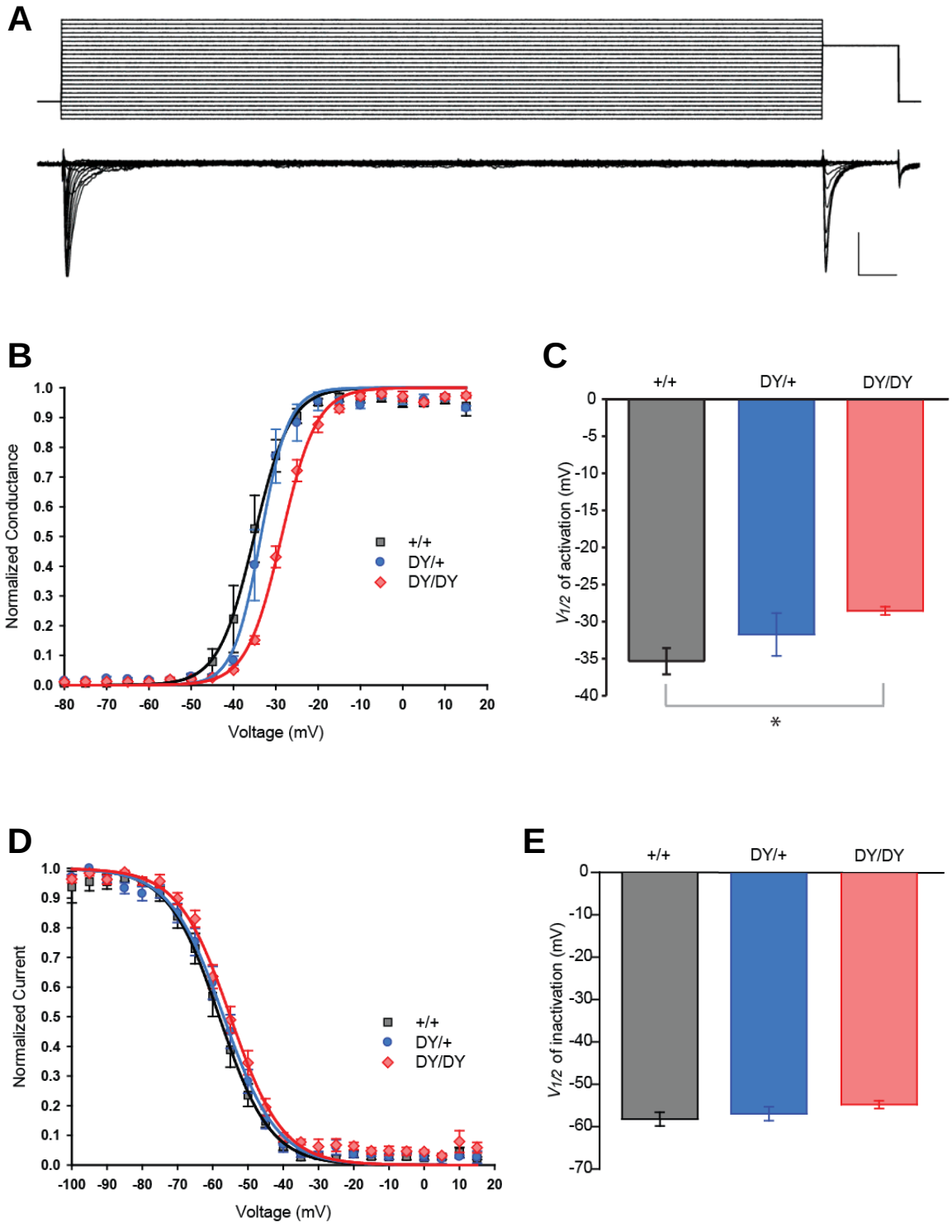

Figure 1.2. *Scn1a*-D1866Y shifted the voltage-dependence of activation but not steady-state of inactivation

A, Voltage protocol used for studying sodium channel activation and steady-state inactivation. Conditional pulses of 100 msec from a holding potential of -80 mV were applied, ranging from -100 to 15 mV in increments of 5 mV. The conditional pulses were immediately followed by a test pulse to -15mV for 10 msec (top graph). Representative voltage-clamp traces of currents obtained during the protocol are shown in the lower graph. **B**, Voltage-dependence of activation was determined by calculating the conductance from the peak current of the conditional pulse and plotted as function of the voltage of the conditional pulse. The voltage-dependence of activation was significantly shifted in the positive direction for homozygous (DY/DY) neurons compared to wild-type littermate (+/+), while heterozygous (DY/+) neurons had an intermediate phenotype. **C,** Potential for half-maximal ($V_{½}$) activation for wild-type, heterozygous and homozygous neurons was -35.3 ± 4 mV, -33.2 ± 3 mV and -28.6 ± 1 mV, respectively. **D**, The voltage-dependence of inactivation was determined by plotting peak current during the test pulse as a function of the conditioning pulse voltage. **E,** Potential for half-maximal ($V_{½}$) inactivation for wild-type, heterozygous and homozygous neurons was -58.2 ± 4 mV, -57.0 ± 3 mV and -54.8 ± 2 mV, respectively. The voltage-dependence of inactivation was similar among neurons of wild-type, heterozygous and homozygous (p=0.22). Wild-type n=5, heterozygous n=4 and homozygous n=5. The values shown are mean ± SEM. Statistical comparison of the half-maximums ($V_{1/2}$) of activation and inactivation by one way ANOVA followed by Hold-Sidak correction (Table 1). Asterisk (*) indicates significant difference ($p<0.05$) between (+/+) and (DY/DY).

PV+ interneurons with Scn1a-D1866Y exhibit slower kinetics of entry into inactivation

Scaling and superimposing the transient currents revealed that decay of sodium current in PV+ interneuron of homozygous was slower than that of PV+ interneurons of wild-type littermates (Fig. 1.3A). To quantify the kinetics of inactivation, the time constants of fast (τ_{Fast}) and slow (τ_{Slow}) inactivation were determined by fitting each trace with a two exponential equation. The time constants of fast inactivation of PV+ interneuron of homozygous (n=5) mice were significantly larger compared to the time constants of inactivation of wild-type (n=5) and heterozygous (n=4) littermates. There was no significant difference between wild-type and heterozygous mice (Fig. 1.3B). Likewise, the time constants of slow inactivation of PV+ interneuron of homozygous (n=5) mice were significantly larger compared to the time constants of inactivation of wild-type (n=5) and heterozygous (n=4) mice, but there is also a significant difference between wild-type and heterozygous mice (Fig. 1.3C). Differences in time constants among the three genotypes were smaller at greater membrane depolarizations.

Fig 1.3. *Scn1a*-D1866Y slowed the kinetics of inactivation

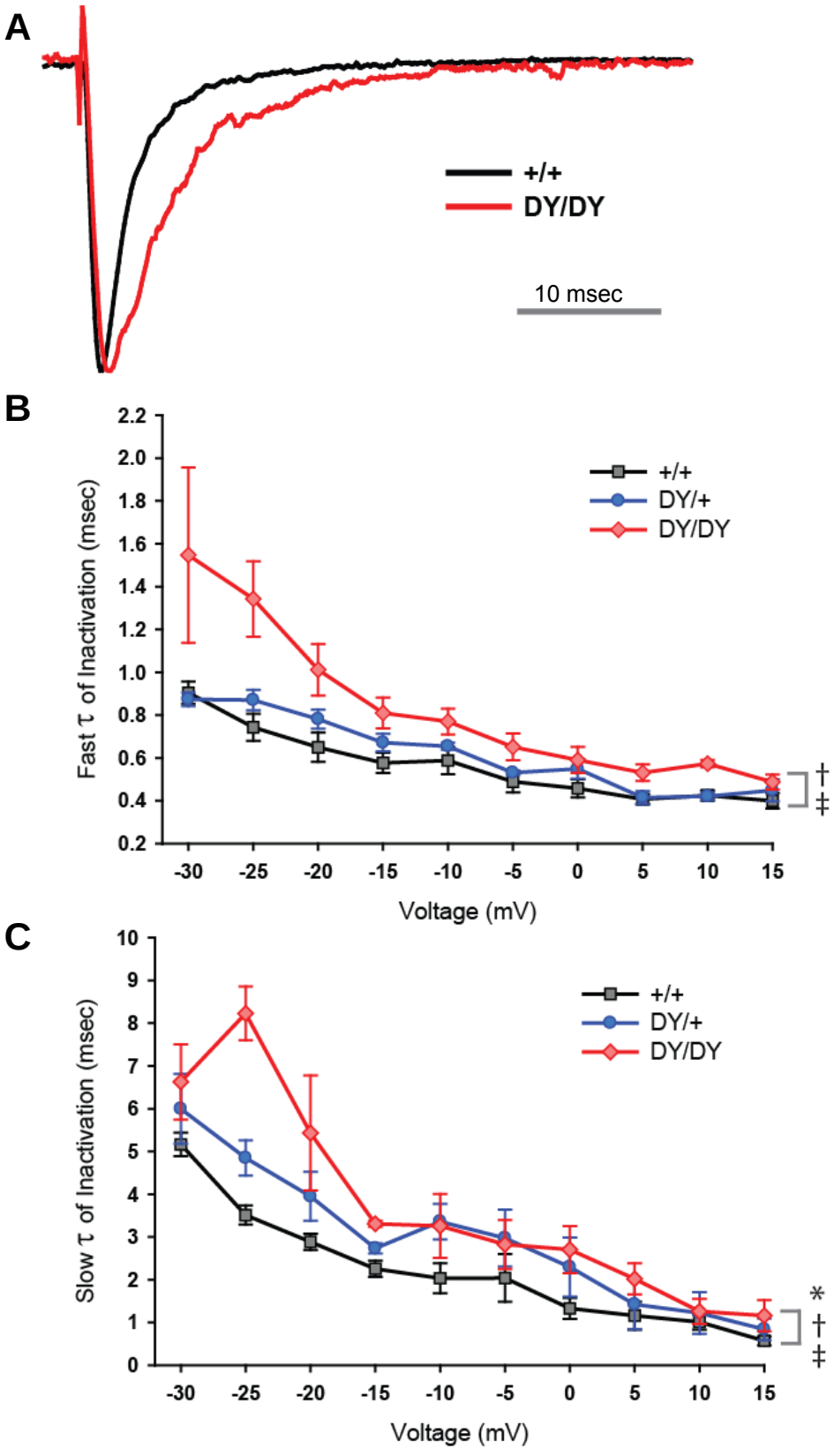

Fig 1.3. The *Scn1a*-D1866Y resulted in slower inactivation kinetics

A, Comparison of normalized current traces at -25 mV demonstrated subtle slowing in the kinetics of inactivation for neurons expressing *Scna1*$^{D1866Y/D1866Y}$ (DY/DY) compare to wild-type (+/+) neurons. Kinetics of inactivation were determined by fitting the decay of transient sodium currents with a double exponential equation. **B**, Kinetics of fast inactivation (τ_{Fast}) are slower for homozygous (DY/DY) compared to wild-type (+/+) and heterozygous (DY/+) neurons. **C**, Kinetics of slow inactivation (τ_{Slow}) followed a similar pattern, with slower kinetics for homozygous neurons compared to wild-type and heterozygous neurons. Heterozygous neurons also demonstrated significantly slower slow inactivation compared to wild-type. For both time constants, the largest differences are in the -30 mV to -20 mV range, and the differences were smaller at more depolarized potentials. The values shown are mean ± SEM. Wild-type n=5, heterozygous n=4, and homozygous n=5. Statistical comparison by two way ANOVA followed by Holm-Sidak test, statistical significant ($p<0.05$). Asterisk (*) indicates significant difference between (+/+) and (DY/DY), dagger (†) indicates significant difference between (+/+) and (DY/+) and double dagger (‡) indicates significant difference between (DY/+) and (DY/DY).

Once sodium channels inactivate, further activity is limited by the time it takes for the channels to recover from inactivation. Sodium channels need to return from the inactivated state to the closed state to be activated and open again (Bezanilla & Armstrong, 1977). Recovery from inactivation was determined by comparing the peak currents during test pulses to the peak currents of conditional pulses, where the time between the conditional and test pulse was changed to provide variable time for recovery from inactivation (Fig 1.4A). PV+ interneuron of homozygous mice (n=5) showed significantly faster recovery of sodium current compared to heterozygous (n=5) and wild-type (n=6) littermates. In addition, heterozygous neurons recovered faster than wild-type neurons (Two way ANOVA; $p<0.05$) (Fig 1.4B).

Fig 1.4. *Scn1a*-D1866Y accelerated recovery from inactivation

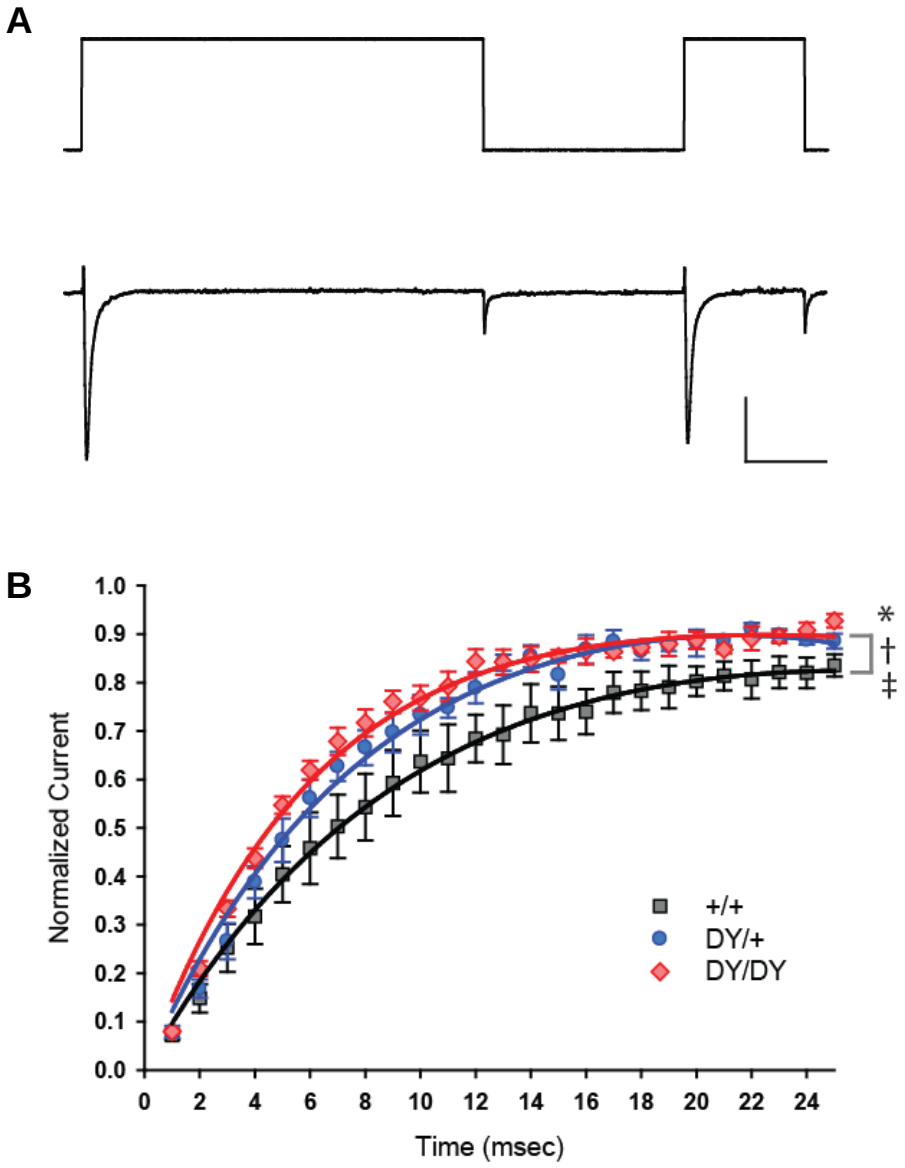

Fig 1.4. *Scn1a*-D1866Y accelerated recovery from inactivation

A, Voltage protocol used for measuring recovery from inactivation. Conditional pulses to -15 mV for 50 msec from a holding potential of -80 mV were followed by test pulses to -15 mV for 5 msec. The time between conditional and test pulses was reduced from 25 msec (above) to 1 msec in decrements of 1 msec. Representative voltage-clamp traces of currents obtained from the neuron are shown below. Scale bars indicate 400 pA and 10 msec. **B**, Recovery from inactivation was significantly faster in homozygous compared to wild-type and heterozygous littermates. Recovery in heterozygous neurons was significantly faster than wild-type. The values shown are mean ± SEM. Wild-type n=6, heterozygous n=5, and homozygous n=5. Statistical comparison with two way ANOVA followed by Holm-Sidak test, statistically significant ($p<0.05$). Asterisk (*) indicates significant difference between (+/+) and (DY/DY), dagger (†) indicates significant difference between (+/+) and (DY/+) and double dagger (‡) indicates significant difference between (DY/+) and (DY/DY).

To determine the effect of the *Scn1a*-D1866Y mutation on bursting behavior of sodium channels, we compared the peak currents obtained during each depolarization in a train of 100 depolarizations (Fig. 1.5A). This protocol provided information about use-dependent inactivation of the sodium channels. Use-dependent inactivation should correlate with recovery from inactivation, with less use-dependent inactivation corresponding to faster recovery from inactivation. PV+ interneurons of homozygous (n=6) and heterozygous (n=4) mice showed significantly less use-dependent inactivation compared to wild-type mice (n=5) during depolarization trains at 39 Hz (Fig. 1.5B), 20 Hz (Fig. 1.5C) and 10 Hz (Fig. 1.5D). In addition, homozygous PV+ interneurons showed significantly less use-dependent inactivation compared to heterozygous interneurons at 39 Hz, 20 Hz, and 10 Hz (Two way ANOVA; $p<0.05$).

Figure 1.5. *Scn1a*-D1866Y reduced use-dependent inactivation

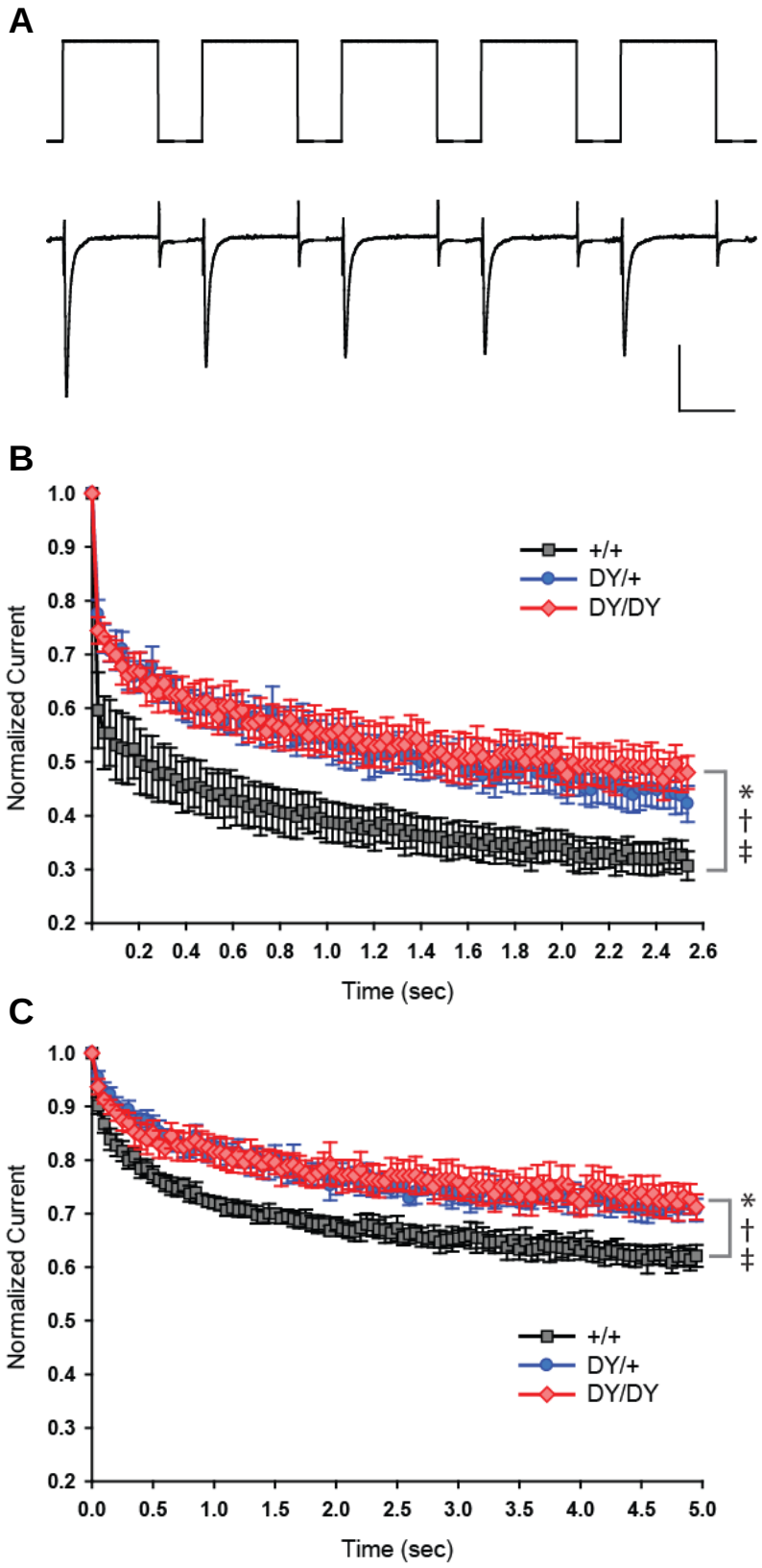

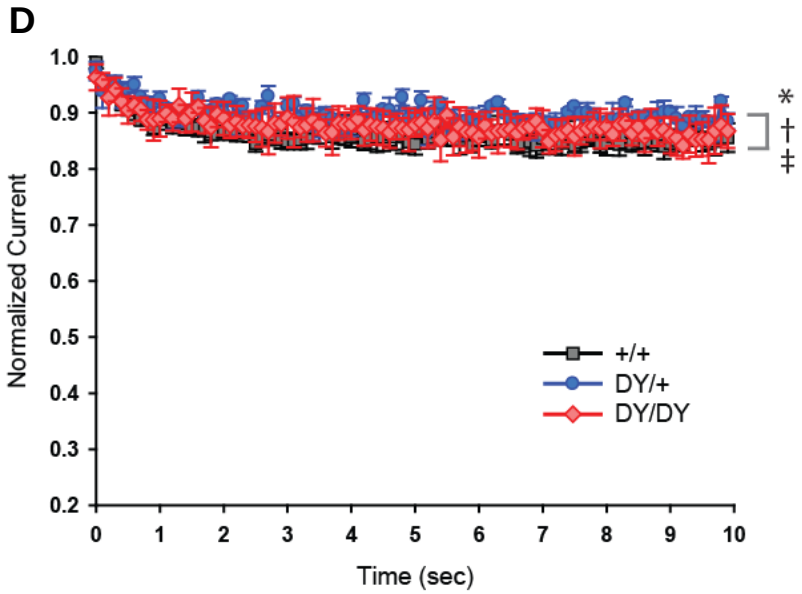

Figure 1.5. *Scn1a*-D1866Y reduced use-dependent inactivation

A, Protocol to determine use-dependent inactivation, showing just the first 5 of the 100 pulses (above) and representative voltage-clamp traces of currents obtained from the neuron at 39 Hz (below). **B**, **C** and **D,** Currents elicited at frequencies of 39 Hz, 20 Hz and 10 Hz, respectively. Neurons expressing the *Scna1*-D1866Y mutation, both heterozygous and homozygous, had significant less use-dependent inactivation at 39 Hz, 20 Hz and 10 Hz compared to neurons from wild-type littermates. Similarly, homozygous neurons demonstrated a significant decrease in use-dependent inactivation compared to heterozygous neurons at 39 Hz, 20 Hz, and 10 Hz. The values shown are mean ± SEM. Wild-type n=6, heterozygous n=5, and homozygous n=5. Statistical comparison with two way ANOVA followed by Holm-Sidak test, statistically significant ($p<0.05$). Asterisk (*) indicates significant difference between (+/+) and (DY/DY), dagger (†) indicates significant difference between (+/+) and (DY/+) and double dagger (‡) indicates significant difference between (DY/+) and (DY/DY).

PV+ interneurons with Scn1a-D1866Y have significantly increased persistent current but not current density

Previous studies have suggested that increased persistent current may contribute to the mechanism by which some GEFS+ mutations cause seizures (Lossin et al., 2002). Therefore, we measured the persistent current in mutant and wild-type neurons. Scaling and superimposing the transient currents indicated that the residual (persistent) current of PV+ interneurons from homozygous mice was higher than the current from PV+ interneuron from wild-type littermates (Fig. 1.6A). Normalized persistent current of PV+ interneurons from homozygous mice (DY/DY) was 0.036 ± 0.006 (n=6), which is higher than the persistent current of 0.010 ± 0.003 (n=5) from PV+ interneuron from wild-type mice (Fig. 1.6B). Persistent current from PV+ interneurons from heterozygous mice was 0.018 ± 0.005 (n=3), which is intermediate between wild-type and homozygous neurons (Table 1).

Another mechanism by which a mutation can increase excitability is to increase the sodium current density, which is the total current divided by the cellular capacitance (a measure of cell volume). We therefore determined the current density by normalizing the peak transient currents to cell capacitance. The current density of homozygous neurons was -99.6 ± 50 pA/pF (n=6), which is not statistically different compared to -122.7 ± 25 pA/pF of wild-type (n=4) littermates (Student's t-test; p=0.50) (Fig. 1.6C).

Figure 1.6. *Scn1a*-D1866Y increased persistent current but did not affect current density

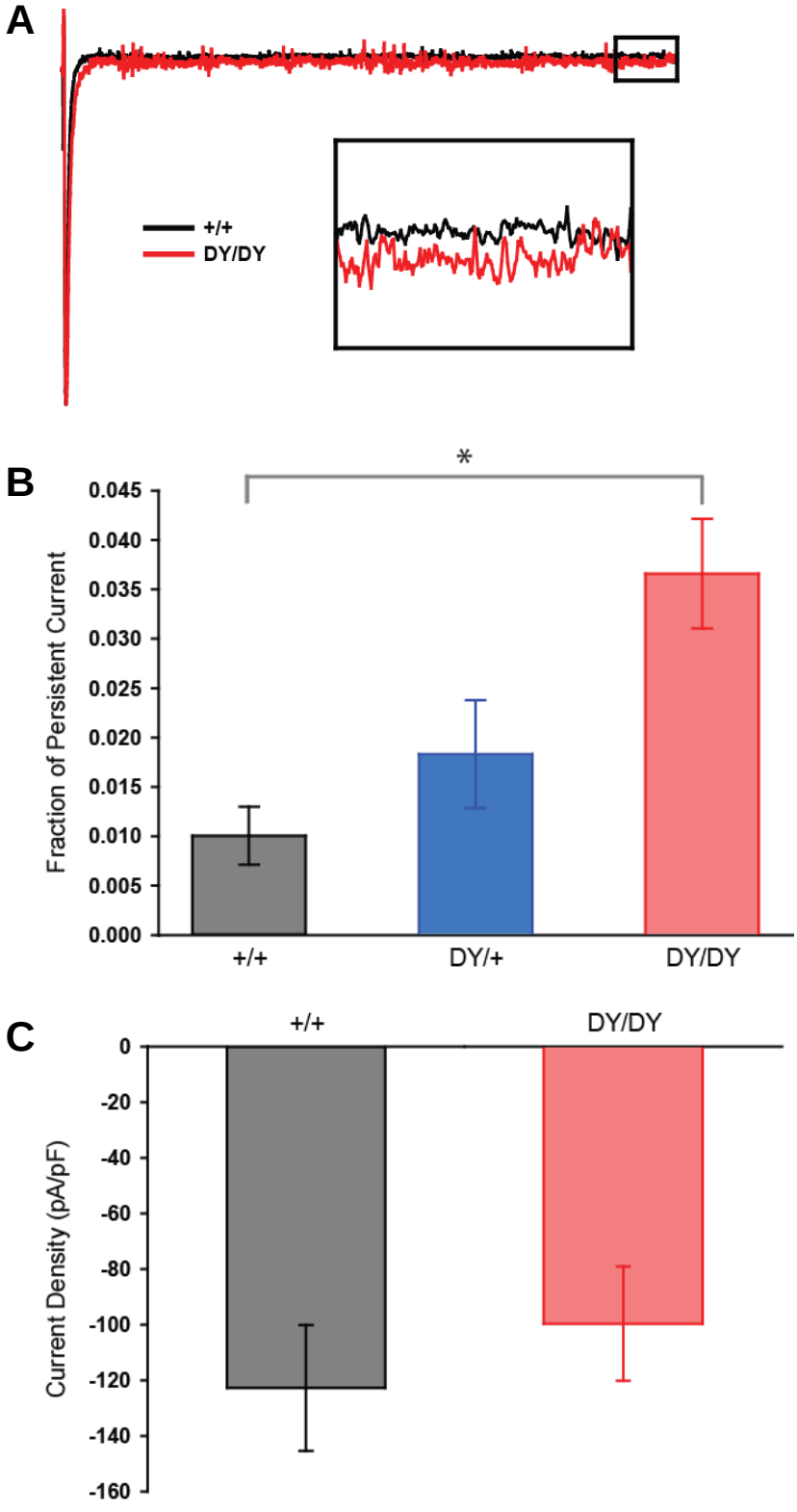

Figure 1.6. *Scn1a*-D1866Y mutation increased persistent current but did not affect current density

A, Comparison of normalized current traces at 0 mV for 100 msec. Inset shows persistent current during the last 10 msec. Persistent current was measured by taking the mean current during the last 10 msec of a 100 msec depolarization and normalizing it to the peak of the transient current. **B**, Persistent current was increased to 0.036±0.01 (n=6) in neurons from homozygous (DY/DY) mice from 0.010±0.008 (n=5) in wild-type (+/+) littermates. Heterozygous (DY/+) mice had an intermediate phenotype with 0.018±0.005 (n=3). Statistical analysis was performed using a one way ANOVA followed by Holm-Sidak test,. Asterisk (*) indicates significant difference ($p<0.05$) between wild-type and homozygous. **C**, Current density was not significantly different between neurons expressing wild-type or mutant channels, with -122.7 ± 50 pA/pF (n=4) for wild-type neurons and -99.6 ± 25 pA/pF (n=6) for homozygous neurons. The values shown are mean ± SEM. Statistical analysis was performed using the Student's t test; $p=0.50$.

Table 1.1 Parameters of sodium current in hippocampal PV+ interneurons of P16-P17 mice

	+/+	DY/+	DY/DY
Voltage-Dependence of Activation			
Gating Charge (z)	9.1 ± 1.3	10.3 ± 2	6.5 ± 0.6
$V_{½}$ (mV)	-35.3 ± 1.8	-31.7 ± 2.9	-28.6 ± 0.6*
n	6	4	6
Voltage-Dependence of Inactivation			
Slope (a)	7.0 ± 0.5	7.5 ± 0.6	7.3 ± 0.5
$V_{½}$ (mV)	-59.0 ± 1.8	-57.0 ± 1.6	-55.0 ± 1.1
n	6	4	5
Persistent Current			
Fraction	0.010 ± 0.003	0.018 ± 0.005	0.036 ± 0.006*
n	5	3	6
Current Density			
(pA/pF)	-122.7 ± 50	N.D.	-99.6 ± 25
n	4	-	6

Table 1.1 Parameters of sodium current in hippocampal PV+ interneurons of P16-P17 mice

The electrophysiological parameters were determined using the equations described in the Materials and Methods. The values shown are means ± SEM. Significant difference when $p<0.05$. One way ANOVA followed by Holm-Sidak test was performed to determine statistical difference between pairwise comparisons of genotypes for parameters with single values. Student's t test was performed to determine the statistical significance of the differences in current density. Asterisk (*) indicates significant difference between (+/+) and (DY/DY). Two way ANOVA followed by Holm-Sidak test was performed to determine statistical difference between genotypes for the kinetics of entry of inactivation (τ_{Fast} and τ_{Slow}), recovery from inactivation and use-dependence (not in table).

Discussion

Mutations in the *Scn1a* gene that result in GEFS+ have been previously studied using the heterologous expression system of *Xenopus* oocytes. Results from heterologous systems like *Xenopus* oocytes have been shown to be quite different from those obtained by studying mammalian neurons, suggesting that heterologous system are not a good model for determining the mechanisms of seizures in humans. The differences among systems can result from a variety of factors, including different protein interactions, post translational modifications and other regulatory factors in the cell environment (Mantegazza et al., 2010).

In the case of *Scn1a*-D1866Y, some of the effects of the mutation on sodium currents were very similar in the oocyte system compared to mammalian interneurons. The *Scn1a*-D1866Y effects between oocytes and neurons were comparable with respect to the time-dependent properties, but not with respect to the voltage dependent properties (Spampanato et al., 2004). The similarities in effects of the *Scn1a*-D1866Y mutation across different expression systems contrasts with the different effects of *Scn1a*-R1648H, which also results in GEFS+, but which has different effects on sodium channel properties in oocytes (Spampanato et al., 2001), HEK cells (Lossin et al., 2002), and mouse neurons (Martin et al., 2010).

One potential explanation for the different results with the *Scn1a*-D1866Y and the *Scn1a*-R1648H mutations is that they are located in different structural domains of the sodium channel. *Scn1a*-D1866Yis located in the C-terminus and

Scn1a-R1648H is located in the voltage sensing transmembrane segment. The oocyte might provide the basic and essential post-translational modifications and protein interactions for the C-terminus. *Scn1a*-D1866Y is located in a predicted EF-hand domain (Chagot et al., 2009; Wingo et al., 2004), which is a calcium binding domain. Calcium is a universal secondary messenger used by all eukaryotic cells, and the EF-hand domain is part of many calcium signaling proteins. Therefore, the results of expression in a heterologous system may be valid for a mutation in a domain or secondary structure for which the heterologous system utilizes the same endogenous proteins and pathways. On the other hand, oocytes may not provide all the modifications and interactions required for the voltage-sensing transmembrane segment to function correctly, as in mammalian neurons. Transmembrane segments or protein domains with the capacity to sense and change conformation in a voltage-dependent way are found only in excitable cells, which oocytes are not. This lack of voltage sensing in oocytes could also explain why the voltage-dependent properties of *Scn1a*-D1866Y specifically are the ones not comparable among expression systems.

Variability in the effects of different mutations in the same gene and in the same system or organisms are also frequently observed (Escayg & Goldin, 2010). The variability of the effects can result from diverse sources. Differences in the phenotype can be seen even among different mice strains, where some mice strains are more susceptible while other strains less susceptible to seizures (McKhann, Wenzel, Robbins, Sosunov, & Schwartzkroin, 2003; Schauwecker,

2011; Yu et al., 2006). The subtle differences in genetic background could give rise to higher expression of a gene or set genes in one mouse strain compared to the other strain (Meisler & Kearney, 2005). This variation is also true for GEFS+ in humans, where there is considerable variability in the epileptic phenotype, with some people being asymptomatic despite carrying a mutation that causes epilepsy in others (Scheffer & Berkovic, 1997).

The effects of the *Scn1a*-D1866Y and *Scn1a*-R1648H mutations were both analyzed in dissociated neurons from mice with same genetic background. Therefore genetic background is not responsible for the differences seen between *Scn1a*-D1866Y and *Scn1a*-R1648H mutations. Different neuronal subpopulations which most likely have different expression patterns, specifically PV+ interneurons of the hippocampus for *Scn1a*-D1866Y and bipolar shaped interneurons of the cortex for *Scn1a*-R1648H, can contribute to the differences seen between *Scn1a*-D1866Y and *Scn1a*-R1648H. However, it is unlikely that the different targeted inhibitory neuronal populations will be enough to elicit all the differences in the sodium current properties. The two mutations are found in different domains of the sodium channel, and each domain has its own role and contribution to the function of the channel.

The *Scn1a*-D1866Y mutation's effects on the voltage-dependent properties in PV+ interneurons are completely different from the effects in *Xenopus* oocytes. In oocytes, the voltage-dependence of activation was

unaffected, whereas in PV+ interneurons expressing only the mutant channel, activation was shifted to depolarized voltages. In neurons, a larger stimulus was required to activate a significant population of sodium channels when the mutant channel is expressed compared to wild-type channels. This change suggests that the *Scn1a*-D1866Y mutation results in a loss-of-function. In contrast, the *Scn1a*-D1866Y mutation did not have an effect on the voltage-dependence of inactivation in PV+ interneurons, but it was shifted in the depolarized direction in oocytes. The results in oocytes suggest that a comparable depolarization will shift a larger population of sodium channels into the inactive state, which was not observed in interneurons.

On the other hand, the *Scn1a*-D1866Y mutation's effects on the time-dependent properties are very similar between PV+ interneurons and oocytes. First, the kinetics of inactivation were significantly slower in cells expressing the *Scn1a*-D1866Y mutation compared to the ones expressing the *Scn1a* wild-type channel. This change in kinetics is easily noticeable in a voltage range of -30 mV to -20 mV, which is the range in which conductance through the sodium channel is maximal. The reduction in the difference of the time constants of inactivation as the voltage becomes more positive could be due to the fact that as the voltage step increases and gets closer to the reversal potential of sodium, the driving force for sodium to enter the cell is reduced. In addition, as the voltage becomes more depolarized, more sodium channels will enter the inactive state.

Consequently, the sodium current decreases comparably for the wild-type and mutant channels.

Second, recovery from inactivation is faster in cells expressing the D1866Y mutation compared to cells with the *Scn1a* wild-type channel. The faster recovery from inactivation suggests that the *Scn1a*-D1866Y mutation promotes the sodium channels to cycle back more rapidly to the closed state. The reduced time in the non-conductive state would allow more sodium channels to be available to re-open. The increase in time to enter together with the shorter time in the inactive state suggests that the mutation destabilizes the inactive conformation. It has been shown that the C-terminus domain of that sodium channel stabilize the inactivation state (Kass, 2004).

Furthermore, the *Scn1a*-D1866Y mutation resulted in reduced use-dependent inactivation at 10 Hz, 20 Hz and 39 Hz. Therefore, PV+ interneurons expressing *Scn1a*-D1866Y mutation expressed sodium currents that are more active than the sodium currents in PV+ interneurons expressing wild-type *Scn1a*. These results are exactly what is expected when slowed kinetics of inactivation are combined with faster recovery from inactivation in a population of sodium channels. This supports a gain-of-function resulting from the *Scn1a*-D1866Y mutation.

In addition to the increase of sodium current resulting from the changes in time-dependent properties, the *Scn1a*-D1866Y mutation also resulted in increased persistent sodium current in PV+ interneurons. Increased persistent current has been observed in several mutations in the EF-hand domain of the sodium channel (Rhodes et al., 2005). Increases in persistent current are caused by incomplete inactivation of the mutant channel, which leads to a proportion of channels either remaining open or re-opening (Crill, 1996). The increased persistent current due to the *Scn1a*-D1866Y mutation would also result in increased channel activity, adding to the effects of slower kinetics of inactivation and faster recovery from inactivation. The increased persistent current could reduce action potential subthreshold and may amplify the responses of neurons to excitation, leading to increased activity in an affected population of neurons and resulting in an epileptic phenotype (Stafstrom, 2007).

An alternative explanation for the increased persistent current and the increased sodium current could be that PV+ interneurons expressing the *Scn1a*-D1866Y mutation have more functional sodium channels in the membrane. GEFS+ and DS mouse models *Scn1a*-R1648H and *Scn1a*-kcockout, respectively, demonstrated reduced current densities in bipolar-shaped interneurons (Martin et al., 2010; Mistry et al., 2014; Ogiwara et al., 2007; Yu et al., 2006). This implies that the loss-of-function of the sodium current in these cells is responsible for the reduction of interneuron activity. However, we did not observe any effects of the *Scn1a*-D1866Y mutation on the current density of PV+

interneurons, suggesting that the *Scn1a*-D1866Y mutation doesn't decrease or increase the amount of functional sodium channels that are expressed. This result suggests that the mutation doesn't alter trafficking of the sodium channel, which has been suggested for other GEFS+ and DS mutations (Rusconi et al., 2009), and that the increase in persistent current is due to a change in the properties of the channels that are being expressed in the membrane.

While compensation by other sodium channel isoforms is a possibility that could affect the recorded sodium current properties, we believe that this kind of compensation is unlikely at the time when sodium currents were recorded. That is because compensation was not observed for other sodium channel mutations that have more severe phenotypes. The *Scn1a*-R1648H mutation and *Scn1a*-knockout mouse models for GEFS+ and DS, respectively, demonstrate more severe phenotypes during the second week of age. In both models, homozygosity of the mutations resulted in a strong phenotype, with death of the mice by P15. Northern blot, western blot and RT PCR analysis for $Na_v1.2$, $Na_v1.3$ and $Na_v1.6$, which are the other main sodium channel isoforms in the CNS, did not show an increase or compensation of the these sodium channels in the CNS in these mice (Martin et al., 2010; Mistry et al., 2014; Yu et al., 2006). Therefore, the decreased severity of the *Scn1a*-D1866Y mutation compared to these mouse models at the same age suggests that compensation is unlikely.

Single channel recordings can provide some light of how the *Scn1a*-D1866Y mutation increases sodium channel activity at the molecular level. One possibility is that once mutant channels enter the active state and open, they spend more time in the open conformation. This would explain the slower kinetics of inactivation observed in interneurons expressing *Scn1a*-D1866Y. The other possibility is that the mutation increases the probability of a single channel re-opening. This would also explain faster recovery from inactivation. It is possible that both effects could be present in a single mutant channel. Unfortunately, the *Scn1a* sodium channel isoform is not the only sodium channel expressed in PV+ interneurons, and combined with the current lack of a drug that could selectively block the other sodium channel isoforms, it is impossible to specifically examine the properties of the mutant channels in PV+ interneurons.

The *Scn1a*-D1866Y mutation differs from most of the GEFS+ and DS mutations in *Scn1a* that have been studies in previous mouse models. The majority of the effects of the *Scn1a*-D1866Y mutation, except for the voltage-dependence of activation, would result in increased sodium current. That suggests that the *Scn1a*-D1866Y mutation results in a more active sodium channel. The gain-of-function of sodium current by *Scn1a*-D1866Y contrasts with the theory of haploinsufficiency and loss-of-function of *Scn1a* mutations, like *Scn1a*-R1648H and *Scn1a*-knockout models, associated with epilepsy (Catterall, 2014). Autosomal dominant disorders like GEFS+ can result from gain-of-function or by haploinsufficiency of loss-of-function of the mutated protein. In

these other mouse models, loss-of function of the sodium channel generated loss-of-function of neuronal activity to fire action potentials. Increased sodium currents in inhibitory neurons also have been reported from induced pluripotent stem cells (iPSC)-derived neurons from DS patients (Jiao et al., 2013; Liu et al., 2013). These results must be interpreted with caution because the maturity of these induced neurons is unknown now is it known how similar they are to neurons in the CNS. It is possible that the gain-of-function of sodium current by the D1866Y mutation would result in increased action potential firing in PV+ interneurons. However, gain-of-function at the sodium channel level does not necessarily translate into gain-of-function at the cellular level. Either gain-of-function or loss-of-function can result in decreased cellular activity, depending on where the channel is expressed and the other channels expressed in the neuron (Ragsdale, 2008). Therefore, to completely understand the mechanism of how the *Scn1a*-D1866Y mutation leads to seizures and epilepsy, it is necessary to determine how the mutation affects the action potential firing in PV+ interneurons and pyramidal excitatory neurons, which are the main neurons in the hippocampus.

CHAPTER 2

Excitability of excitatory and inhibitory neurons is reduced by *Scn1a*-D1866Y mutation

Abstract

Voltage gated sodium channels (VGSC) are responsible for the initiation and propagation of action potentials in most neurons. Mutations in the voltage gated sodium channels that are expressed in the central nervous system (CNS) are known to be associated with the development of a wide variety of pathologies. Genetic epilepsy with febrile seizure plus (GEFS+) and other epileptic syndromes in the same spectrum have been shown to be caused by mutations in *SCN1A*, which encodes the VGSC $Na_v1.1$, and several mouse models had been constructed to study the epileptogenic mechanisms of these mutations. Modifications of *Scn1a* in previous mouse models resulted in loss-of-function of sodium channel activity, leading to the reduction of excitability of inhibitory interneurons in the cortex and hippocampus. In this study, we characterized how the *Scn1a*-D1866Y mutation, which results in gain-of-function of sodium current in parvalbumin-expressing (PV+) interneurons, affects the ability of the neurons of the hippocampus to fire action potentials. Firing of action potentials of PV+ interneurons expressing one copy of a mutant channel was decreased compared to wild-type littermates. On the other hand, the firing of

action potentials of excitatory pyramidal neurons was reduced by the mutation only in homozygous mice. These results support the hypothesis that *SCN1A* mutations affect mainly the GABAergic neuronal population.

Introduction

The excitability of a neuron is determined by the gating properties of all the functional ion channels that are expressed on its surface (Bean, 2007). Therefore, the combination of the properties of all the ion channels together with the proteins that modify and interact directly or indirectly with them shape the characteristics of excitability or action potential firing of a neuron. Mutations that can alter any of the properties of ion channels, including gating, permeability and trafficking, can result in diseases that are called channelopathies (Celesia, 2001). Channelopathies are defined as any of a wide array of conditions in which an altered ion channel causes the disease (S.G. Waxman, 2001). Channelopathies of the central nervous system may be the most serious ones because of the broad impact of the CNS, affecting other systems and organs, and effective treatment options are often limited.

Genetic epilepsy with febrile seizure plus (GEFS+) is a channelopathy in the CNS in which patients start to present at infancy (Scheffer & Berkovic, 1997). GEFS+ is considerate a spectrum, encompassing severe myoclonic epilepsy of infancy (SMEI) or Dravet Syndrome (DS), borderline SMEI (SMEB) and intractable epilepsy of childhood (IEC) (Scheffer, Zhang, Jansen, & Dibbens, 2009). The association between all these conditions is based on the phenotype, in which seizures are associated with fever and often refractory to treatment, and also with genetic factors. So far, 5 genes, *GABARD*, *GABARG*, *SCN1B*, *SCN2A*

and *SCN1A*, have been associated with GEFS+ and the other associated syndromes. Of those genes, *SCN1A* is the most prominent because more than 800 mutations that cause epilepsy have been identified in it (L. R. F. Claes et al., 2009; Lossin, 2009).

To provide insight about the mechanism of how mutations or alterations in *SCN1A* cause seizures, several mouse models had been created. Knockdown of *Scn1a* resulted not only in the reduction of *Scn1a* levels but also in an epileptic phenotype. In the first two *Scn1a*-knockout mouse models of DS, the gene was deleted in all the cells, but only the inhibitory interneurons from cortex and hippocampus demonstrated a reduction of sodium current in mice at an infant age (Ogiwara et al., 2007; Yu et al., 2006). The loss-of-function of sodium current in the interneurons resulted in a reduction in the ability of those neurons to fire action potentials. The loss-of-function of interneurons with reduced excitability is an excellent model for about the 50% of DS patients, who have a mutation that produces a non-sense mutation, frameshift or other change that prevents expression of the *SCN1A* channel (Mulley et al., 2005).

About 10% of DS patients have chromosomal rearrangements (Marini et al., 2009). However, there are about 40% of DS patients who have a point mutation in *SCN1A* (Marini et al., 2009), in which it is not clear if the mutation results in loss-of-function or some other alteration (Escayg & Goldin, 2010). In addition, all mutations that have been identified in *SCN1A* as causing GEFS+ are

point mutations. The hypothesis is that mutations in *SCN1A* that cause DS result in loss-of-function of sodium current, while the mutations that cause GEFS+ may result in loss-of-function or gain-of-function. Loss-of-function of sodium current causing reduced excitability of the interneurons has been shown with the R1648H point mutation of *Scn1a*, which models GEFS+ (Martin et al., 2010). In contrast, we have identified a mutation in *SCN1A* associated with GEFS+ that results in a net gain-of-function of sodium current in parvalbumin-expressing (PV+) inhibitory interneurons in mice. The *Scn1a*-D1866Y mutation resulted in faster recovery from inactivation, slower kinetics of inactivation, reduced use-dependent inactivation and increased persistent current (Chapter 1).

Though gain-of-function of sodium current had been shown to increase neuronal excitability in some cells (S. G. Waxman & Zamponi, 2014), in other cases gain-of-function can also decrease excitability (Burge & Hanna, 2012). Because the D1866Y mutation is the first *Scn1a* mutation shown to result in gain-of-function of sodium current in PV+ interneurons, we examined how the *Scn1a*-D1866Y mutation affects the firing properties of excitatory and inhibitory neurons in the CNS.

Materials and Methods

Animals

Mice generation, maintenance and identification (genotyping) was performed as previously described in Chapter 1. Briefly, generation of *Scn1a*-D1866Y mice was performed by Dr. Andrew Escayg at Emory University, GA using homologous recombination. Once mice were received at the University of California, Irvine, the *Scn1a*-D1866Y mice were backcrossed to C57BL/6J mice (JAX) for at least 8 generations. The G42 transgenic mice expressing enhanced green fluorescent protein (EGFP) specifically in parvalbumin-containing interneurons (Chattopadhyaya et al., 2004), which was also in the C57BL/6 genetic background, were crossed to the *Scn1a*-D1866Y mice. The EGFP gene was carried only in the hemizygous state and detected visually with a stimulating light source and emission filters in P0-P4 mice. Mice were maintained at 22 °C on a 12-h light/dark cycle. Food and water were available *ad libitum*. All experiments were performed in accordance with the Institutional Animal Care and Use Committee of University of California, Irvine.

Preparation and recordings from hippocampal slices

Mice were anesthetized with halothane, decapitated, and brains were rapidly placed in ice-cold sucrose artificial cerebrospinal fluid (ACSF) containing (in mM): 85 NaCl, 65 sucrose, 2.5 KCl, 25 glucose, 1.25 NaH_2PO_4, 4 $MgSO_4$, 0.5 $CaCl_2$, and 24 $NaHCO_3$ (oxygenated with 95% O_2, 5 % CO_2). Horizontal hippocampal

slices (300 μm) were cut using a Leica VT1200S vibrating blade microtome (Leica, Germany). Slices were incubated at 33°C for at least 1 h before electrophysiological recordings in oxygenated (95% O_2, 5% CO_2) standard ACSF containing (in mM): 126 NaCl, 2.5 KCl, 1.25 $NaHPO_4$, 1.2 $MgSO_4$, 10 glucose, 1.2 $CaCl_2$, and 26 $NaHCO_3$.

For the electrophysiological recordings, slices were submerged in a recording chamber and continuously perfused at 2 mL/min with oxygenated ACSF at 30°C. Cells were visualized with an upright microscope (Zeiss Axioskop Plus) equipped with infrared differential interference contrast optics and epifluorescence. Recording from PV+ interneurons were identified by expression of EGFP in the dentate gyrus. A Qimaging Iclick camera was used for the detection of the EGFP. Pyramidal cells were identified by localization of their soma and the distinctive morphology in the pyramidal cell layer in the CA1. Positive pressure of 5-9 inches of water (0.18-0.33 psi) in the electrode was used to approach the cells. Proximity was accessed by change of the response to a square pulse, at which point the positive pressure was reduced.

The electrode solution consisted of (in mM): 126 K-gluconate, 4 KCl, 10 HEPES, 2 Mg-ATP, 0.3 TRIS-GTP, 4 Na_2-ATP and 10 phospocreatine-Na_2 (pH 7.3). Patch pipettes with a resistance of 3-5 MΩ were pulled from borosilicate glass (1.5 mm OD, 0.86 mm ID; Sutter Instruments, Novato, CA) with a P-97 Flaming-Brown puller (Sutter Instruments, Novato, CA). Recordings were performed at 30°C. Cell

attachment and penetration to the inside of the cell were carried out in the voltage clamp mode, but the electrophysiological recordings were obtained in current clamp mode using a MultiClamp 700B amplifier (Molecular Devices, Union City, CA) and digitized with a Digidata 1322A digitizer (Molecular Devices). Data were analyzed offline with pClamp 10.2 software (Molecular Devices).

Action potential stimulation was done by injecting current for 2 seconds and reported as action potential frequency. Action potentials were counted if the membrane potential reached at least 0 mV. For PV+ interneurons, the number of action potential fired during the first 0.5 seconds of the stimulus was used to quantify excitability, while 2 seconds used to quantify excitability of the pyramidal cells. Action potential threshold was determined by the membrane potential at which the rate of change of depolarization (dV/dt) was 5 during the first fired action potential. To determine the point in which dV/dt was 5, we took the dV/dt point immediately below and above 5 from the phase plot and estimated the membrane potential value that will result in dV/dt=5. Input resistance was determined by the change in membrane potential due to negative current injection of -10 and -5 pA. This was calculated by subtracting the difference between the mean membrane potential value 100 milliseconds before the current stimulus from the mean membrane potential value 100 milliseconds during the stimulus. The 100 milliseconds during the stimulus were taken from the point at which the membrane potential reached a plateau. The changes in membrane

potential at these negative current injections were fitted with a straight line, in which the slope is the input resistance.

Statistical Analysis

Pulse generation and data collection were done with pCLAMP 10.2. All data are reported as mean ± standard error of mean (SEM). All statistics analysis was performed with SigmaStat 3.10. Statistical significance was determine with p-values under 5% ($p<0.05$). When comparing only 2 genotypes with respect to a single parameter, data were analyzed using Student's t-test. When comparing 3 genotypes, we used analysis of variance (ANOVA) followed by post-hoc pairwise comparison using the Holm-Sidak correction. One way ANOVA was used when the genotype was the only variable with multiple levels. Two way ANOVA was used when the time or voltage variable also had multiple levels.

Results

Mice were maintained and their genotypes were identified as described in Chapter 1. The *Scn1a*-D1866Y knock-in line was constructed and provided by our collaborator Dr. Andrew Escayg from the Human Genetics Department at Emory University. The different genotypes were obtained in Mendelian ratios regardless of whether they were crossed to the G42 transgenic mice.

Action potential firing is lower in PV+ interneurons from Scn1a-D1866Y mice compared to wild-type littermates

The excitability of PV+ interneurons was determined by recording action potential firing in slices from the hippocampus of P21-P24 mice. Current was injected for 2 seconds and the number of action potentials fired during the first half second was recorded. This protocol avoided the complication of trying to account for the accommodating nature of PV+ interneurons, in which the number of action potentials decreases with continued stimulation (Fig. 2.1). PV+ interneurons from *Scn1a*$^{D1866Y/+}$ (heterozygous) mice (n=4) fired fewer action potentials compared to *Scn1a*$^{+/+}$ (wild-type) mice littermates (n=3) (Two way ANOVA; $p<0.05$) (Fig 2.2).

Fig 2.1. Elicited action potentials of PV+ interneurons

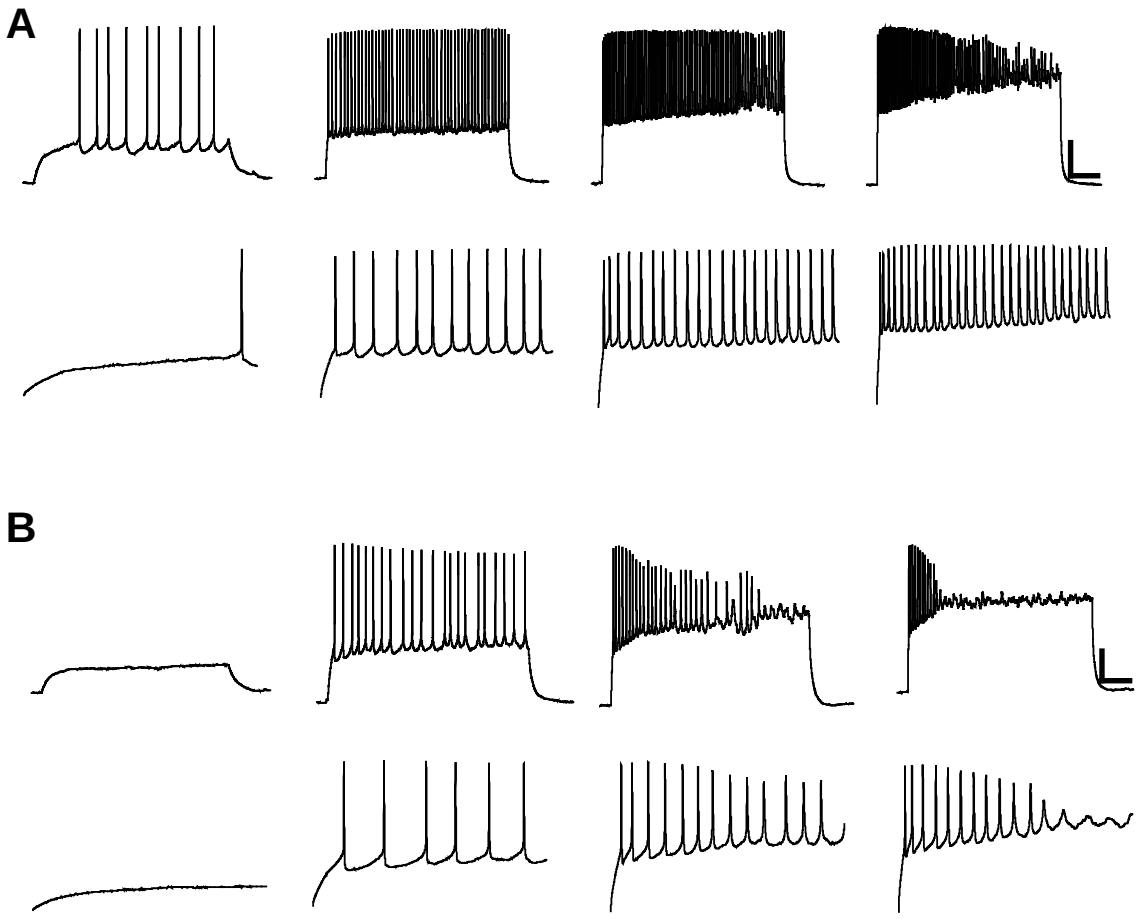

Fig 2.1. Elicited action potentials of PV+ interneurons

A, Representative firing of wild-type PV+ interneuron during 2 seconds (top) of current injection and zoom-in of the first 500 milliseconds of current injection (bottom). **B**, Representative firing of heterozygous PV+ interneuron during 2 seconds (top) of current injection and zoom-in of the first 500 milliseconds (bottom). Current injections from left to right are 10 pA, 50 pA, 100 pA and 150 pA. Scale bars indicate 250 ms and 20 mV.

Fig 2.2. *Scn1a*-D1866Y reduced action potential firing of PV+ interneurons

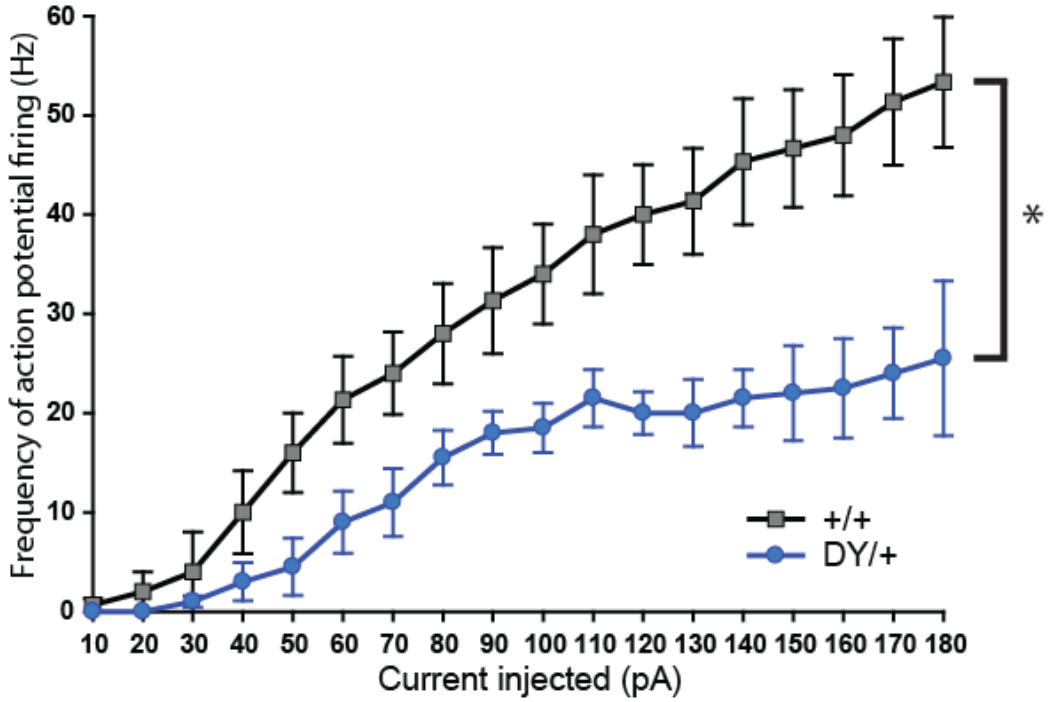

Fig 2.2. *Scn1a*-D1866Y reduced action potential firing of PV+ interneurons

Neuronal excitability measured as the frequency of action potential that were fired during the first 500 ms of the current injected. The frequency of action potential firing of heterozygous (DY/+) neurons was significantly lower than the frequency of wild-type (+/+) neurons. The values shown are mean ± SEM. Wild-type has n=3, and heterozygous has n=4. Asterisk (*) indicates statistical significance ($p<0.05$) between wild-type and heterozygous mice as determine by two way ANOVA followed by Holm-Sidak test, statistically significant ($p<0.05$).

Action potential firing frequency could be decreased because of an increase in the action potential threshold. We determined the action potential threshold as the membrane potential in which the dV/dt of the phase plot of the first elicited action potential was 5 (Fig. 2.3a). The action potential threshold of the PV+ interneurons in the dentate gyrus of P21-P24 mice was not altered by the D1866Y mutation (Fig 2.4b). Action potential thresholds for wild-type and heterozygous littermates were -39.1± 1.1 mV (n = 3) and -34.5± 2.9 mV (n=4), respectively (Student's t-test, p=0.62)

Fig 2.3. *Scn1a*-D1866Y did not affected action potential threshold of PV+ interneurons

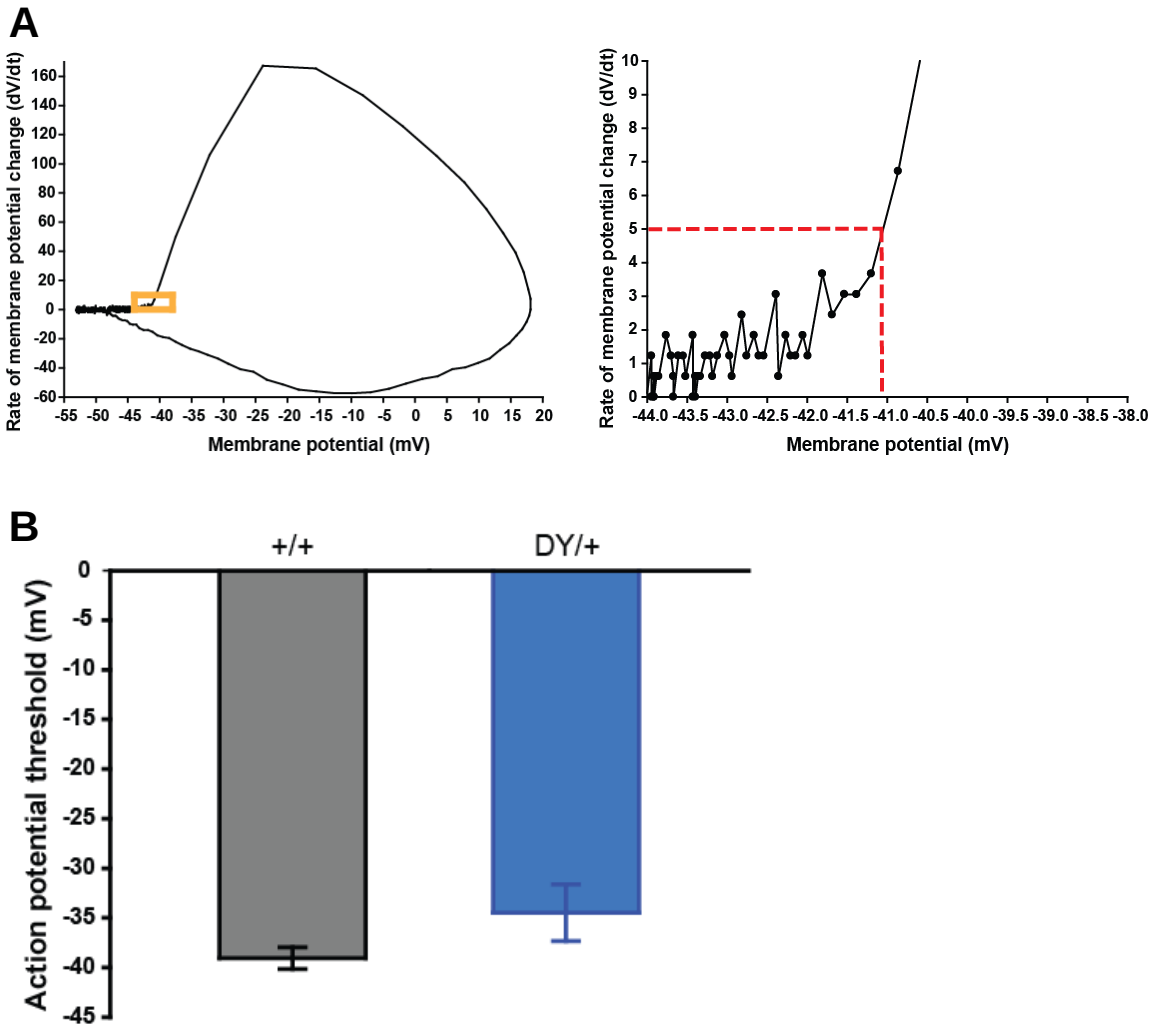

Fig 2.3. *Scn1a*-D1866Y did not affected action potential threshold of PV+ interneurons

A, On the right side, representative phase plot of the 1st fired action potential of PV+ interneurons. On the left side, zoom-in of phase plot region where dV/dt increases abruptly (orange box on right figure). Membrane potential where dV/dt equals 5 is considered the action potential threshold. **B**, Action potential threshold was -39.1 ± 1.1,mV (n=3) in wild-type neurons, and -34.5± 2.9 mV (n=4) in heterozygous neurons. The values shown are mean ± SEM. Statistical analyzes done by Student's t-test (p=0.62)

Another neuronal property that could affect the ability of the cell to fire action potentials is an alteration in the input resistance. To determine the input resistance, we plotted the change of the membrane potential as a function of the current injected (Fig. 2.4a). The input resistance of PV+ interneurons was 878 ± 286 MΩ (n=4) for interneurons from heterozygous mice and 870 ± 113 MΩ (n=3) for interneurons from wild-type littermates (Fig. 2.4b). Therefore, the input resistance of the PV+ interneurons from the dentate gyrus of P21-P24 mice was not altered by the D1866Y mutation (Student's t-test, p=0.98).

Fig 2.4. *Scn1a*-D1866Y did not altered the input resistance of PV+ interneurons

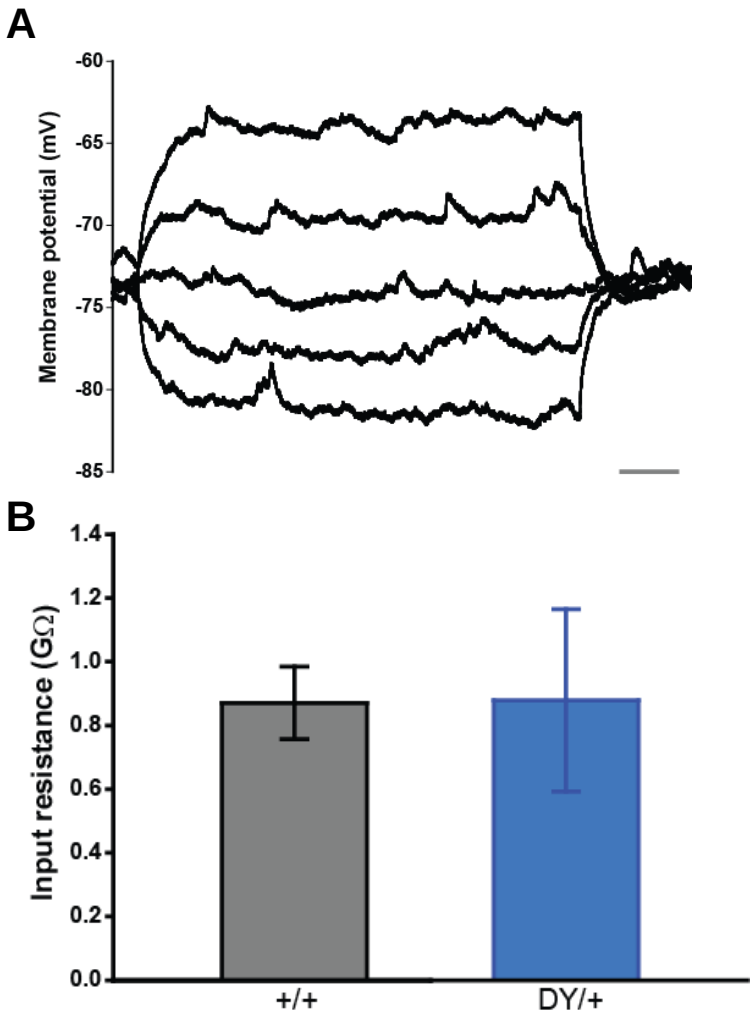

Fig 2.4. *Scn1a*-D1866Y did not altered the input resistance of PV+ interneurons

A, Subthreshold changes in the membrane potential as a result of small current injection of -10 pA, -5 pA, 0 pA, 5 pA and 10 pA during 2 s. Scale bar 250 ms. Input resistance was determined from the change in membrane potential as a function of the injected current producing the change. **B**, Input resistance was 870 ± 113 MΩ (n=3) in wild-type neurons, and 878 ± 286 MΩ (n=4) in heterozygous neurons. The values shown are mean ± SEM. Statistical analysis done by Student's t-test (p=0.98)

Excitability of the pyramidal cells from CA1 was decreased by the homozygous Scn1a-D1866Y mutation

To determine if the changes in excitability by the D1866Y mutation are specific to PV+ interneurons or if changes in excitability were more general, the excitability of pyramidal excitatory cells was determined (Fig 2.5). Because these neurons are abundant and easily identified by their morphology, we did not need to use a fluorescent marker to label this population. There was no differences in the action potential frequency between excitatory pyramidal neurons of heterozygous (n=7) and wild-type mice (n=5) from P21-P24. However, pyramidal neurons from homozygous mice (n=4) had a lower frequency of action potential firing compared to wild-type and heterozygous littermates at high current injections (Two way ANOVA) (Fig 2.6).

Fig 2.5. Elicited action potentials of pyramidal neurons

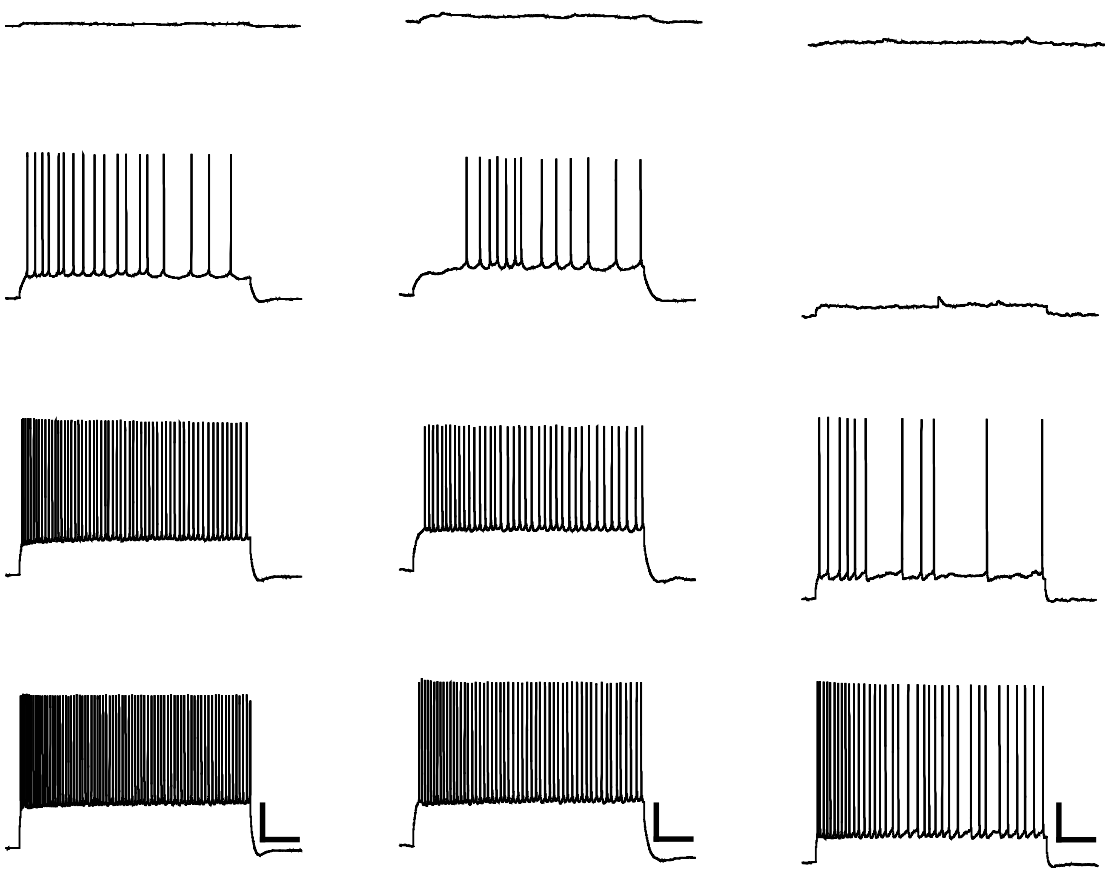

Fig 2.5. Elicited action potentials of pyramidal neurons

Representative action potential firing of CA1 pyramidal cells during 2 seconds of current injection from wild-type, heterozygous and homozygous *Scn1a*-D1866Y mice. Current injections from top to bottom are 10 pA, 50 pA, 100 pA and 150 pA. Scale bars indicate 250 ms and 20mV.

Fig 2.6. Pyramidal neurons from homozygous but not heterozygous *Scn1a*-D1866Y mice demonstrate reduced action potential firing

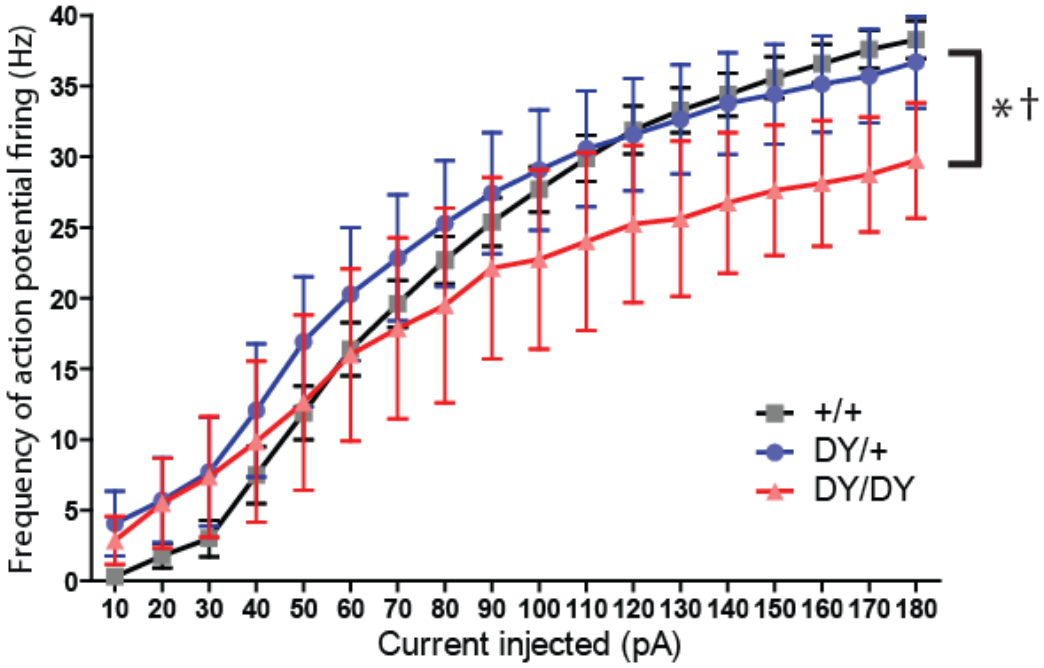

Fig 2.6. Pyramidal neurons from homozygous but not heterozygous *Scn1a*-D1866Y mice demonstrate reduced action potential firing

Neuronal excitability measured as the frequency of action potentials that were fired during 2 s of current injected (pA). Frequency of action potential firing of homozygous (DY/DY) neurons was significantly lower than frequency of wild-type (+/+) and heterozygous (DY/+) neurons at high current injections. The values shown are mean ± SEM. Wild-type n=5, heterozygous n=7, and homozygous n=4. Statistical comparison with two way ANOVA followed by Holm-Sidak test, statistically significant ($p<0.05$). Asterisk (*) indicates significant difference between (+/+) and (DY/DY), dagger (†) indicates significant difference between (DY/+) and (DY/DY) ($p<0.05$).

Since we observed a difference in action potential firing in pyramidal neurons from homozygous D1866Y mice, we tested the neuronal properties to determine which alteration was responsible for the effect. First, we determined the action potential threshold, which determines the initiation of the action potential. As for the PV+ interneurons, we converted the first fired action potential in a phase plot and determined the threshold as the membrane potential at which dV/dt was equal to 5. Action potential thresholds for wild-type, heterozygous and homozygous neurons were -48.4 ± 1.1 mV (n=5), -48.0 ± 2.7 mV (n=7) and -48.0 ± 4.7 mV (n=4), respectively (Fig 2.7). Therefore, the action potential threshold of the pyramidal neurons from CA1 of P21-P24 mice was not altered by the D1866Y mutation (One way ANOVA, p=0.99).

Fig 2.7. *Scn1a*-D1866Y did not altered the action potential threshold of pyramidal neurons

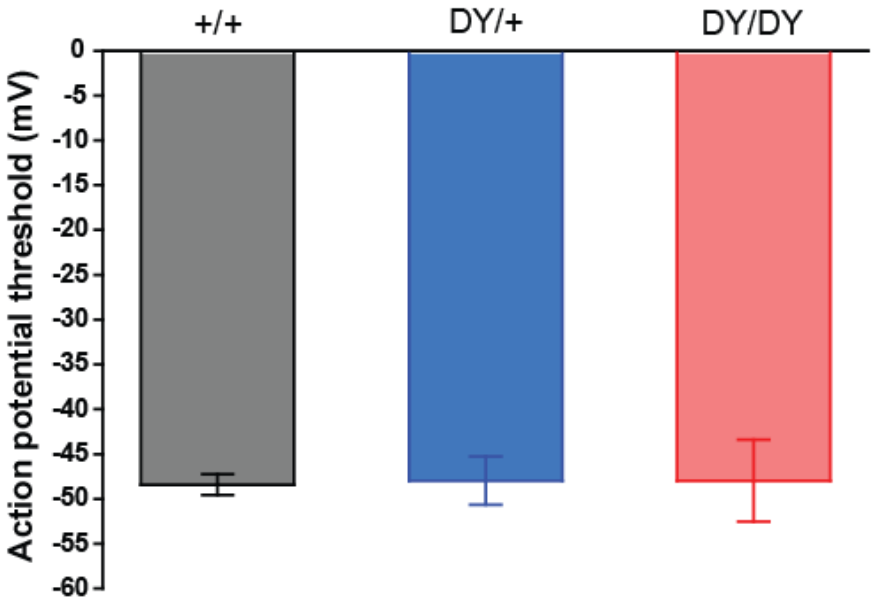

Fig 2.7. *Scn1a*-D1866Y did not altered the action potential threshold of pyramidal neurons

Action potential threshold was -48.4 ± 1.1 mV in wild-type neurons (n=5), -48.0 ± 2.7 mV in heterozygous neurons (n=7) and -48.0 ± 4.7 mV in homozygous neurons (n=4). The values shown are mean ± SEM. Statistical analysis done by one way ANOVA (p=0.99).

Finally, we determined the input resistance of the excitatory pyramidal neurons. The *Scn1a*-D1866Y mutation increased the input resistance of pyramidal cells in CA1 from 222 ± 10 MΩ for wild-type mice (n=5) mice to 316 ± 25 MΩ for heterozygous (n=7) mice. Homozygous littermates had an intermediate input resistance of 276 ± 33 MΩ (n=4) (Fig. 2.8). The values for both heterozygous and homozygous mice were increased, but only heterozygous mice were significantly different from wild-type mice (One way ANOVA, $p<0.05$).

Fig 2.8. *Scn1a*-D1866Y increased the input resistance of pyramidal neurons

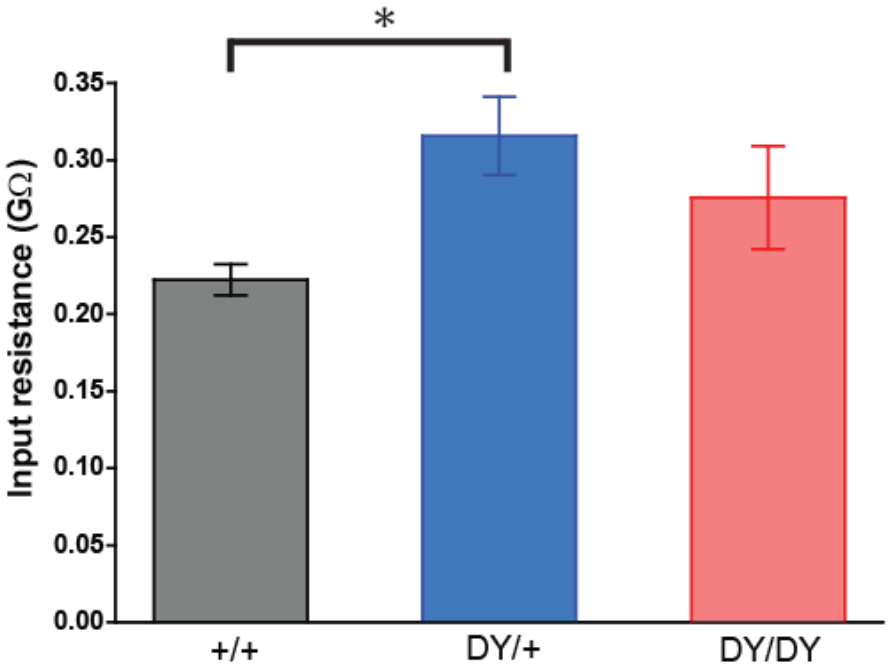

Fig 2.8. *Scn1a*-D1866Y increased the input resistance of pyramidal neurons

Input resistance of the pyramidal cells from wild-type neurons was 222 ± 10 MΩ (n=5). Input resistance was increased to 316 ± 25 MΩ in heterozygous neurons (n=7) and 276 ± 33 MΩ in homozygous neurons (n=4). The values shown are mean ± SEM. Statistical analysis was performed using a one way ANOVA followed by Holm-Sidak test. Asterisk (*) indicates significant difference ($p<0.05$) between wild-type (+/+) and heterozygous (DY/+) (Table 2.1).

Table 2.1. Excitability of neurons from the hippocampus of P21-P24 mice

	+/+	DY/+	DY/DY
PV+ interneurons in Dentate Gyrus			
Maximal frequency of action potential firing (Hz)	53.3 ± 6.6	25.5 ± 7.8 *	N.D.
Action potential threshold (mV)	-39.1± 1.1	-34.5± 2.9	N.D.
Input Resistance (MΩ)	870 ± 113	878 ± 286	N.D.
n	3	4	0
Pyramidal neurons in CA1			
Maximal frequency of action potential firing (Hz)	38.3 ± 1.3	36.7 ± 3.2	29.8 ± 4.0 * ‡
Action potential threshold (mV)	-48.4 ± 1.1	-48.0 ± 2.7	-48.0 ± 4.7
Input Resistance (MΩ)	222 ± 10	316 ± 25 *	276 ± 33
n	5	7	4

Table 2.1. Excitability of neurons from the hippocampus of P21-P24 mice

The procedures used to determine the neuronal properties were described in the Materials and Methods. The values shown are means ± SEM. Two way ANOVA test followed by Holm-Sidak test was performed to determine the statistical significance of the differences in action potential firing values between genotypes. Statistical significance of the action potential threshold and input resistance differences of PV+ interneurons was performed with Student's t test, while for pyramidal cells one way ANOVA followed by Holm-Sidak test was used. Asterisk (*) indicates significant difference ($p<0.05$) between wild-type (+/+) and homozygous (DY/DY) mice. Double dagger (‡) indicates significant difference ($p<0.05$) between heterozygous (DY/+) and homozygous (DY/DY) mice.

Discussion

The field of channelopathies is one that has been expanding in the last decades since the completion of sequencing the human genome. Because of the critical role and abundance of ion channels in some tissues, they have been linked with several disorders resulting from mutations in their genes (Schwartz, Ackerman, George, & Wilde, 2013; S.G. Waxman, 2013; Zaydman, Silva, & Cui, 2012). Although all systems are essential for proper development, function and simply survival of the human being, the nervous system is special because it controls other systems. A single neuron can express over a dozen different genes encoding ion channels, and all of these channels contribute to the function and excitability of the neuron (Bean, 2007). The high heterogeneity of the CNS means that the channelopathies of the nervous system are complex and difficult to fully understand. Dravet Syndrome (DS) and GEFS+ are two channelopathies that cause epilepsy. Both DS and GEFS+ have been associated mainly with mutations in the *SCN1A* gene that encodes the voltage-gated sodium channel $Na_v1.1$ (Hirose et al., 2013). In an effort to understand the mechanism by which mutations in *SCN1A* cause epilepsy, a number of mouse models have been constructed. Knockout of *Scn1a* provides a model for DS, in which about 50% of the human mutations cause a premature stop codon (Mulley et al., 2005). Premature stop codons generally result in nonfunctional proteins and hence the loss-of-function of the sodium channel. In contrast, mutations in *SCN1A* associated with GEFS+ are primarily missense mutations (L. R. F. Claes et al.,

2009; Lossin, 2009), which could result in either loss-of-function or gain-of-function of the sodium channel (Escayg & Goldin, 2010) .

Because of the high expression of *Scn1a* in PV+ interneurons during infant and juvenile stages in mice (Ogiwara et al., 2007), we wanted to determine which inhibitory neuronal subpopulations are most affected by the *Scn1a*-D1866Y mutation. We have previously shown that the *Scn1a*-D1866Y mutation results in an increase in sodium current in a heterologous expression system (*Xenopus* oocytes) as well in PV+ interneurons from primary neuronal culture (Chapter 1). These results suggested that the mutation resulted in a gain-of-function of the sodium channel, which is opposite to the loss-of-function caused by the *Scn1a*-knockout (Ogiwara et al., 2007; Yu et al., 2006) and *Scn1a*-R1648H mutation (Martin et al., 2010; Tang et al., 2009). In the mouse models of those alterations, the decrease of sodium currents resulted in the reduction of action potential firing by the affected inhibitory interneurons. Even though the effects on the sodium current due to alteration in *Scn1a* had been detected at the age of P14-P17 in those studies, we decided to characterize the effect on the excitability in mice from P21-P24, because at this age *Scn1a*-D1866Y mice have a more pronounced seizure phenotype and increased incidence of sudden death (Chapter 3).

We determined that the *Scn1a*-D1866Y mutation resulted in a significant reduction in the excitability of the PV+ interneurons in heterozygous mice

compared to wild-type littermates. We measured action potential firing during the first 500 milliseconds of the 2 seconds of stimulating current because action potential firing decreased in PV+ neurons after 500 milliseconds due to depolarization block. The depolarization block in the PV+ interneurons could be due in part to the small size of the soma. The small soma also explains the high values of input resistance seen in these neurons, in which even small injections of current result in strong depolarizations. The depolarization block was enhanced in heterozygous neurons.

Because the reduction of action potential firing could be due to an increase in the action potential threshold, we determined the threshold for neurons from mutant and wild-type mice. The action potential threshold of PV+ interneurons carrying the mutation was more depolarized compared to the wild-type neurons, although the difference was not statistically significant. Therefore, it is possible that small increase in the threshold voltage could contribute to the significant reduction in the frequency of the action potentials fired by the heterozygous PV+ interneurons.

In addition to the action potential threshold, the input resistance of a neuron can also affect action potential firing. The input resistance is a measure of how easy or difficult it is to change the membrane potential from its resting value. An input resistance that is very low or is reduced will result in a small change in the membrane potential for the same size stimulus, which may be insufficient to

reach the action potential threshold. The input resistance of PV+ interneurons of heterozygous mice was similar to the input resistance of wild-type littermates. All these findings suggest that changes in the input resistance and the action potential threshold are not responsible for the reduction of action potential firing of PV+ inhibitory interneurons.

The vast majority of neurons in the brain are not inhibitory interneurons but excitatory neurons. In fact, the hippocampus and neo-cortex are composed of about 20% inhibitory neurons (Markram et al., 2004). Despite the preponderance of excitatory neurons in the CNS, most alterations due to *Scn1a* mutations have been described to affect almost exclusively the inhibitory interneurons (Martin et al., 2010; Ogiwara et al., 2007; Yu et al., 2006), even though this channel can also be expressed in pyramidal cells (Westenbroek, Merrick, & Catterall, 1989). A recent study has shown that excitatory pyramidal neurons can also have altered excitability resulting from mutations in *Scn1a* (Mistry et al., 2014), which prompted us to examine the excitability of the pyramidal neurons. The action potential firing frequency of pyramidal neurons from heterozygous mice was not significantly different from that of wild-type littermates. However, there was a reduction in the frequency of action potential firing in pyramidal neurons from homozygous mice.

This result is different from what was observed in one of the *Scn1a*-knockout mouse models, in which there was increased action potential firing in

pyramidal neurons from heterozygous mice. This difference could be due to several reasons. First, the effects of the *Scn1a* mutations in our model and the *Scn1a*-knockdown are very different. *Scn1a*-D1866Y most likely results in a functional sodium channel while the knockout results in complete loss-of-function. Second, the results were obtained under different sets of conditions. Excitability of pyramidal neurons in the *Scn1a*-D1866Y model was determined in cells from the pyramidal cell layer of CA1 in brain slices, while the excitability of pyramidal neurons in the *Scn1a*-knockdown was determined from acutely dissociated cells. It is possible that the variation of the neuronal environment in the different preparation is responsible for difference in the excitability. Third, the genetic background of the *Scn1a*-D1866Y was C57BL/6, whereas the background for the *Scn1a*-knockdown was 129S6/SvEvTac (129) or the F1 generation of the C57BL/6 x 129. The influence of the genetic background on the variability of genetic epilepsy mouse models has been well-demonstrated, including for *Scn1a* mutations (Mistry et al., 2014; Yu et al., 2006). Other studies have shown an increase in action potential firing of excitatory and inhibitory neurons from *SCN1A* deletions using neurons derived from induced pluripotent stem cells (iPSC) from DS patients (Jiao et al., 2013; Liu et al., 2013). Although this technique has considerable potential for individualized screening and therapeutics, it is difficult to determine if the neurons derived from iPSCs are comparable to the actual neurons in the patient.

In the same way that we looked at the action potential threshold and input resistance with respect to the excitability of PV+ interneurons, we also examined these properties in pyramidal cells. There were no significant differences among the action potential thresholds of pyramidal neurons from wild-type, heterozygous and homozygous mice. However, the input resistance of pyramidal neurons form heterozygous mice was significantly higher than that of wild-type mice. Pyramidal neurons from homozygous mice also had an increased input resistance, although this difference was not statistically significant. The effect of the mutation on the input resistance of pyramidal neurons was quite different than for PV+ interneurons, in which the input resistance was unaltered. Although we do not know the reasons for this difference, the increased input resistance in pyramidal neurons did not alter the ability of those neurons to fire action potentials. The opposite was true in the heterozygous PV+ interneurons, in which there was no change in the input resistance but there was a decreased frequency of action potential firing. The discrepancy in the correlation of input resistance and action potential firing suggests two conclusions. First, the mechanisms involved in determining the input resistance and the firing of action potentials are different. Although the input resistance and the action potential threshold are determined by the ion channels expressed in the membrane, the type of ion channels activated at subthreshold levels differs from the channel activated during action potential firing. Therefore, once a neuron reaches its action potential threshold, its excitability changes and it is no longer linear, as it is at subthreshold levels.

Second, the subthreshold and threshold activity behavior of the channels seem to be affected differently by the *Scn1a*-D1866Y mutation.

The most widely accepted model of the pathology of DS and GEFS+ is that reduction of the activity or firing of inhibitory neurons is responsible for the pathology. It is interesting to note that the *Scn1a*-D1866Y mutation resulted in decreased action potential firing in both PV+ interneurons as well as in the excitatory pyramidal cells. However, the defect in PV+ interneurons is much larger than that in excitatory neurons. These results are consistent with the high levels of *Scn1a* expression in PV+ interneurons. Because of the low level of expression of *Scn1a* in pyramidal cells, the effects of the *Scn1a*-D1866Y mutation were not detected in heterozygous but only in homozygous mice. Therefore, our results concerning the *Scn1a*-D1866Y mutation support the model that reduced inhibition is the primary pathology in DS and GEFS+.

CHAPTER 3

Scn1a-D1866Y Mutation Increases Seizure Susceptibility and Hippocampal Network Activity

Abstract

Epilepsy is one of the most common neurological disorders. Its high prevalence is a major incentive for the development of more effective anti-epileptic drugs, better known as AEDs. Even with the development of new AEDs, there are about 30% of epileptic patients who suffer from intractable epilepsy. Uncontrolled seizures can lead to death and increase the risk of Sudden Unexpected Death of Epilepsy (SUDEP). To provide better treatment options for this population, it is necessary to develop new models that can be used to test potential drugs. Numerous mutations that cause epilepsy have been identified in the sodium channel *SCN1A* gene, making it an excellent candidate to study generalized genetic epilepsy. Several mouse models had been constructed to mimic human Dravet Syndrome (DS) and Genetic Epilepsy with Febrile Seizures Plus (GEFS+), which are two epileptic disorders caused by mutations in *SCN1A*. The main effect of the *Scn1a* mutation in these mouse models was a reduction of the sodium current in interneurons at an early age, which resulted in less excitable interneurons. These findings gave rise to a hypothesis that reduction of inhibition is responsible for the seizure phenotype. In

this study, we characterized the *in vivo* and hippocampal network effects of *Scn1a*-D1866Y, a mutation associated with GEFS+ that resulted in gain-of-function of parvalbumin-expressing (PV+) interneurons. Heterozygous mice had lower thresholds for chemically, electrically and thermally induced seizures and had an increase in mortality during the first year of life. Local field recordings of the hippocampus network of heterozygous mice demonstrated reduced latency and higher frequency of burst firing activity. These results suggest that the gain-of-function of sodium currents of interneurons can also lead to seizures and could serve as alternative model for AED development.

Introduction

Epilepsy is one of the most common neurological disorders. The worldwide population affected with epilepsy is estimated to be 50 to 65 million, with about 3 million in the United States (CURE). 80% of the worldwide population with epilepsy is found in developing countries. A primary cause of epilepsy is brain injury, including brain tumors (Goonawardena, Marshman, & Drummond, 2014), strokes (Menon & Shorvon, 2009), severe head trauma (Gallentine, 2013), fever (Cross, 2012), congenital brain malformation, and infections (Marchi, Granata, & Janigro, 2014). In addition to structural abnormalities, epilepsy can result from genetic factors. However, the cause is not known for approximately 40% to 60% of people suffering with epilepsy (Organization, 2012). It is thought that most of the unknown cases, known as idiopathic epilepsies, result from genetic mutations (Hirose et al., 2005).

People suffering from epilepsy also have a high risk of suffering other pathologies (Helmstaedter et al., 2014). The comorbidities of epilepsy include migraine, intellectual deficit, schizophrenia, ADHD and other psychiatric disorders (Pellock, 2004). An important risk is death from either Sudden Unexpected Death in Epilepsy (SUDEP) or other causes. It's estimated that about 50,000 deaths annually in the United States alone are associated with epilepsy (CURE, 2011). These deaths can be the direct result of seizures or accidents and injuries resulting from seizures. When sudden death is not due to

injuries nor directly resulting from seizures, it is classified as SUDEP. SUDEP accounts for 34% of the deaths of children with epilepsy (CURE, 2011). Therefore, more effective anti-epileptic drugs (AEDs) are necessary to alleviate seizures, comorbidities and death in patients with epilepsy.

Genetic mutations are a major cause of epilepsy, accounting for 40% of all epilepsies (Steinlein, 2002). This number includes both cases in which the gene or mutation is known and unknown (idiopathic). Most of the mutations that have been identified as causing epilepsy are in genes encoding ion channels (Lerche et al., 2013). Of these ion channel genes, the one in which the most epilepsy-causing mutations has been identified is the sodium channel *SCN1A* gene, with over 800 mutations identified to date (L. R. F. Claes et al., 2009; Lossin, 2009). For this reason, the *SCN1A* gene is a promising target for AEDs (Meisler & Kearney, 2005; Mulley et al., 2005). Dravet Syndrome (DS) is one of the epileptic disorders caused by mutations in *SCN1A*. About 40% of the mutations resulting in DS are nonsense mutations (Marini et al., 2011). People with DS suffer from severe, generalized tonic-clonic seizures, along with other symptoms (L. Claes et al., 2001). Genetic epilepsy with febrile seizures plus (GEFS+) is another epilepsy syndrome associated with mutations in *SCN1A* and resulting in a slightly less severe phenotype than DS (Scheffer & Berkovic, 1997).

To understand the mechanism that is responsible for these disorders, three mouse models have been constructed. These models included a knockout

of *Scn1a* (Ogiwara et al., 2007; Yu et al., 2006), a knock-in of an *Scn1a* nonsense mutations, and a knock-in of an *Scn1a* missense mutations (R1648) (Martin et al., 2010). All these models produce a similar effect at the molecular and cellular level. The common feature of these models is the reduction in the current density in interneurons expressing the *Scn1a* mutation. This loss-of-function of sodium current results in a decrease of excitability in the interneurons. The fact that all three of these models have the same effect suggests that cell-type selective loss-of-function of sodium current is a common mechanism for reduced of inhibition and seizure susceptibility.

Efforts to establish any correlation between phenotype and the mutations in *Scn1a* have not been informative so far (Kanai et al., 2004). Nevertheless, it is generally accepted that mutations in different domain of the sodium channel could alter sodium current properties in different ways (Lossin, 2009). One such mutation is *SCN1A*-D1866Y, which causes GEFS+ (Spampanato et al., 2004). GEFS+ is in the same spectrum as DS, in which DS can be considered to be the most severe phenotype of GEFS+ (Scheffer et al., 2009).

The goal of this research is to determine the effects of the *Scn1a*-D1866Y mutation on seizure susceptibility and hippocampus network activity. Chapter 1 presented data showing that the *Scn1a*-D1866Y resulted in a gain-of-function of the channel in PV+ interneurons. This increase of sodium influx resulted in decreased excitability of PV+ interneurons so they fired fewer action potentials.

The excitability of the pyramidal neurons to fire action potentials was unchanged by the *Scn1a*-D1866Y mutation in the heterozygous mice (Chapter 2). We hypothesize that these effects of the *Scn1a*-D1866Y mutation result in increased seizure susceptibility. To test this hypothesis, we determined the latency to and thresholds for behavioral seizures induced in mice by chemical, electrical or elevated body temperature. In addition, we measured micro-EEG or Local Field Potential (LFP) to assess the propensity of the hippocampus network to produce synchronous electrical seizure-like events, also known as bursting activity.

Materials and Methods

Animals

Mice generation, maintenance and identification (genotyping) was done as previously described in Chapter 1. Briefly, generation of *Scn1a*-D1866Y mice was performed by Dr. Andrew Escayg at Emory University, GA using homologous recombination. Once mice were received at the University of California, Irvine, the *Scn1a*-D1866Y mice were backcrossed to C57BL/6J mice (JAX) for at least 8 generations. Mice at Emory University were independently backcrossed to the same strain. The *Scn1a*-D1866Y mice were crossed to G42 transgenic mice, which express enhanced green fluorescent protein (EGFP) in pavalbumin-expressing (PV+) interneurons (Chattopadhyaya et al., 2004). The EGFP gene was carried only in the hemizygous state. Mice were maintained at 22 °C on a 12-h light/dark cycle. Food and water were available *ad libitum*. All experiments were performed in accordance with the Institutional Animal Care and Use Committees of Emory University and the University of California, Irvine.

Hyperthermia-induce seizure paradigm

Mice from P22-25 age were put individually in a chamber for 10 minutes to allow body temperature to acclimatize at 37.5°C. Core body temperature was monitored with a rectal temperature probe connected to heating lamp via temperature controller (TCAT 2DF, Physitemp). Using a heating lamp, the core body temperature of the mouse was increased by 0.5 degrees every two minutes

starting at 37.5°C until the mouse experienced a behavioral partial seizure or until a maximum temperature of 42.5°C. If a behavioral seizure was recorded, the experiment was stopped immediately.

Flurothyl-induced seizure paradigm

Mice from 3 to 5 months of age were put individually in a chamber and flurothyl (2,2,2-trifluroethylether, Sigma-Aldrich) was introduced at a rate of 20 µl/min. Latencies to the first myoclonic jerk (MJ) and to the generalized tonic-clonic seizure (GTCS) were recorded.

Psychomotor 6 Hz-induced seizure paradigm

Mice from 3 to 5 months of age were subjected to electrical pulses of 0.2 ms duration at 6 Hz for 3 seconds. Prior to the testing, a topical anesthetic was applied to the cornea. Each animal in a group was stimulated at a selected current intensity. Mice were manually restrained during stimulation. Immediately following stimulation, mice were placed in their home cage and examined for seizures. Seizures were characterized by forelimb clonus, rearing and falling and/or staring behaviors. Mice were left to recover for a week before being stimulated again with higher current.

Preparation of hippocampal slices

Brain slice preparation was done as previously described in Chapter 2. Briefly, mice were anesthetized with halothane or isoflurane, decapitated, and brains

were rapidly placed in ice-cold artificial cerebrospinal fluid (ACSF) containing (in mM): 85 NaCl, 65 sucrose, 2.5 KCl, 25 glucose, 1.25 NaH_2PO_4, 4 $MgSO_4$, 0.5 $CaCl_2$, and 24 $NaHCO_3$ (oxygenated with 95% O_2, 5 % CO_2). Transverse hippocampal slices (350 μm) were cut using a VT1200S vibrating blade microtome (Leica, Germany). Slices were incubated at 33°C for at least 1 h before electrophysiological recordings in oxygenated (95% O_2, 5% CO_2) standard ACSF containing (in mM): 126 NaCl, 2.5 KCl, 1.25 $NaHPO_4$, 0.5 $MgSO_4$, 10 glucose, 1.2 $CaCl_2$, and 24 $NaHCO_3$.

Electrophysiological recordings

Slices were submerged in a recording chamber and continuously perfused at 2 mL/min with oxygenated ACSF at 30°C during electrophysiological experiments. Cells were visualized with an upright microscope (Zeiss Axioskop Plus) equipped with infrared differential interference contrast optics and epifluorescence.

Patch pipettes with a resistance of 3-5 MΩ were pulled from borosilicate glass (1.5 mm OD, 0.86 mm ID; Sutter Instruments, Novato, CA) with a P-97 Flaming-Brown puller (Sutter Instruments, Novato, CA). Recordings were conducted at 30°C using a MultiClamp 700B amplifier (Molecular Devices, Union City, CA) and digitized with a Digidata 1322A digitizer (Molecular Devices). Data were analyzed offline with pClamp 10.2 software (Molecular Devices).

Micro-EEG or Local Field Potential recordings

For extracellular recordings, pipettes were filled with 150 mM NaCl and positioned in the CA3 stratum pyramidal layer. Field recordings were obtained in current clamp mode at 100X AC. Continuous extracellular recordings were acquired at 10 kHz and population spikes were acquired at 50 kHz. All extracellular field recordings were low-pass filtered at 1 kHz. ACSF with elevated potassium was prepared by supplementing standard ACSF with 3 M KCl to raise the external potassium concentration ($[K^+]_O$) to 8.5 mM. The experimental paradigm consisted of a control recording for 2-5 min in standard ACSF, followed by 20-25 min with 8.5 mM $[K^+]_O$, in which burst activity was recorded.

To evoke population spikes, constant-current stimuli (100 µsec) were applied via a stimulus isolator (A365D; WPI, Sarasota, FL) using a bipolar tungsten electrode (50 µm in diameter; A-M Systems, Carlsborg, WA) positioned in the mossy fiber tract. Population spikes were evoked in physiological 2.5 mM $[K^+]_O$ before and after exposing the slice to 8.5 mM $[K^+]_O$. Slices in which population spike amplitudes did not change more than 20% after exposing the slice to 8.5 mM $[K^+]_O$ were used for analysis.

Statistical Analysis

Pulse generation and data collection were done with pCLAMP 10.2. All data are reported as mean ± standard error of mean (SEM), except for age of deceased breeders reported as mean ± standard deviation (SD). Due to the preliminary

small *n* of homozygous mice in local field potential recordings, 2 slices from 1 mouse; all statistics analysis did not include data from homozygous mice during that portion. The preliminary data from homozygous are reported as the average of those 2 slices. Therefore, all statistical analysis was performed with SigmaStat 3.10 using Student's t-test between wild-type and heterozygous mice. Statistical significance was determine with p-values under 5% ($p<0.05$).

Results

*Scn1a-D1866Y m*ice utilized for the micro-EEG or local field potential recordings and life span statistics were maintained and identified as described in Chapter 1. All mice were backcrossed to C57Bl/6J at least 8 generations and crossed to G42 transgenic mice (Chattopadhyaya et al., 2004). Generation of the different genotypes was obtained in Mendelian ratios. Mice utilized in the hyperthermia, flurothyl and 6 Hz induced seizure were maintained at Emory University, and were also backcrossed at least 8 generations to C57BL/6J.

Scn1a-D1866Y facilitated spontaneous seizure and reduced life span

After the *Snc1a*$^{D1866Y/+}$ (heterozygous) mice were backcrossed to C57BL/6J, they exhibited an increased number of seizures compared to the original strain. Generalized tonic-clonic seizures were observed in mice as young as postnatal day 21 (P21). Behavioral seizures were also observed in adult mice and ranged from motionlessness to death, corresponding to seizure severity of 1 to 7 on the modified Racine scale (Racine, 1972). Although some heterozygous mice demonstrated a normal life span, there was 56% mortality during the first year (Fig. 3.1A). The mean age of heterozygous breeder mice that died was 4 months (Fig. 3.1B). There were twice as many females (n=214) as males (n=100) in the breeding colony, and most of the dead mice (84%) were female (Fig. 3.1C). Mice that were hemizogous for the EGFP gene, which was acquired

from the G42 transgenic strain, had the same percentage of mortality as those without the EGFP gene (Table 3.1). We did not observe any seizures in *Scn1a*$^{D1866Y/D1866Y}$ (homozygous) mice, although they started to die at the age of P21 and their life span was reduce to less than 2 months (Fig. 3.1D). The death of homozygous mice was not due to lack of nutrition or obvious movement disorders.

Fig. 3.1. Reduction of life span of *Scn1a*-D1866Y mice

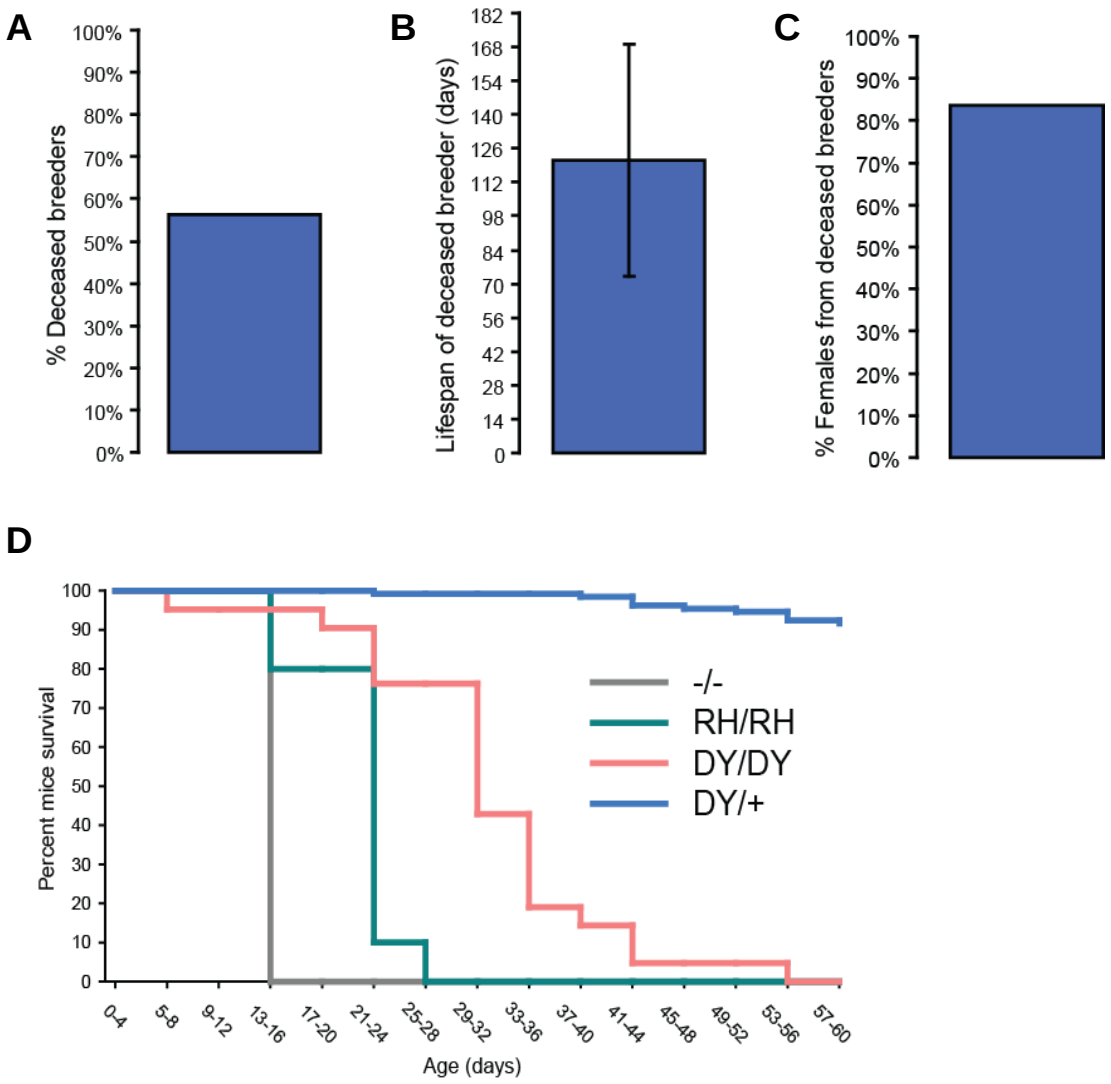

Fig. 3.1. Reduction of life span of *Scn1a*-D1866Y mice

A, Mortality of *Scn1a*-D1866Y heterozygous breeder mice was 56% (179 deceased out of 319). Mortality was measured from date of birth up to 1 year during the first year of age. **B,** The mean age of breeders at death was 121 ± 48 days (n=179). **C,** Percentage of deceased mice that were female was 84%. (Table 3.1). **D**, *Scna1*-D1866Y homozygous mice (DY/DY) started to die around P21. The majority died around P30, although some survived up to 7 weeks. Homozygous *Scn1a* Knockdown (-/-) and *Scn1a*-R1648H (RH/RH) mice had a shorter life span. Ages are presented as mean ± SD.

Reduction in latency to flurothyl-induced seizures in Scn1a-D1866Y mice

To determine the susceptibility of seizures resulting from the *Scn1a*-D1866Y mutation, the mice were first exposed to the chemiconvulsant flurothyl. There was no significant difference in the latency to the myoclonic jerk between wild-type mice (254.2 ± 7.8 seconds, n= 24) and heterozygous mice (253.2 ± 11.5 seconds, n= 25) (Fig. 3.2A). The latency to the first tonic-clonic seizure was significantly shorter for heterozygous mice (344.4 ± 10.1 seconds, n= 25) compared to wild-type littermates (392.7 ± 13.0 seconds, n= 24) (Fig 3.2B).

Fig 3.2. *Scn1a*-D1866Y reduced latency to flurothyl-induced seizures

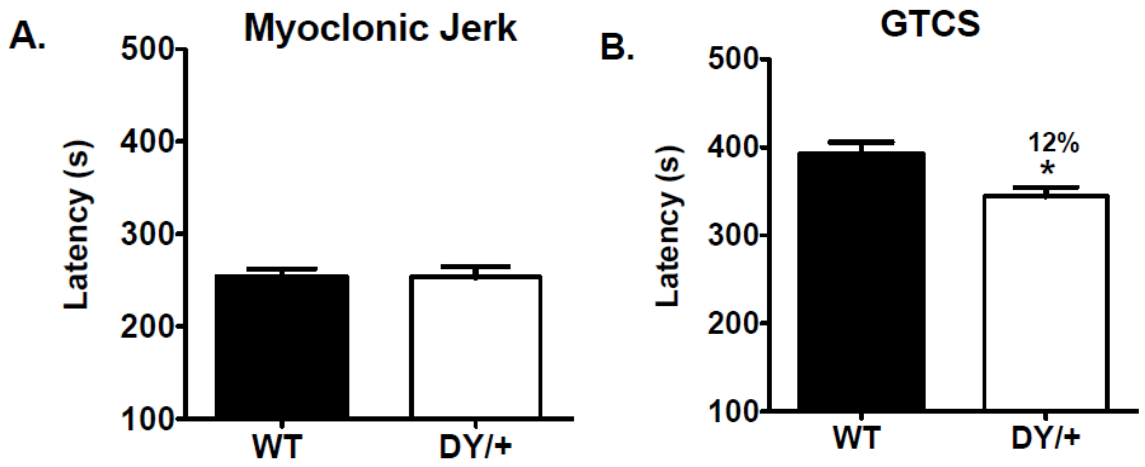

Fig 3.2. *Scn1a*-D1866Y reduced latency to flurothyl-induced seizures

A, Latency in seconds to the myoclonic jerk induced by flurothyl in wild-type mice (+/+) was 254.2 ± 7.8 (n=24) compared to 253.2 ± 11.5 (n=25) in heterozygous mice (DY/+). **B**, Latency in seconds to generalized tonic-clonic seizure (GTCS) induced by flurothyl in wild-type mice (+/+) was 392.7 ± 13.0 (n=24), while in heterozygous mice (DY/+) the latency was 344.4 ± 10.1 (n=25). The values shown are mean ± SEM. Asterisk (*) indicates statistical significance ($p<0.05$) between wild-type and heterozygous mice with Student's t test (Table 3.2).

Scn1a-D1866Y mice had psychomotor-induced seizures at lower current injections compared to wild-type mice

To determine if the susceptibility to experience seizures was specific for one paradigm or common to multiple seizure paradigms, we also induced psychomotor seizures by injecting current pulses at 6 Hz in the cornea of the mice. Increased current injection increased the fraction or percentage of mice in any group that experienced a seizure, but heterozygous mice required less current to induce seizures at any level compared to wild-type littermates (Fig 3.3).

Fig 3.3. ***Scn1a-D1866Y mice had 6 Hz-induced seizures at lower current injections compared to wild-type mice***

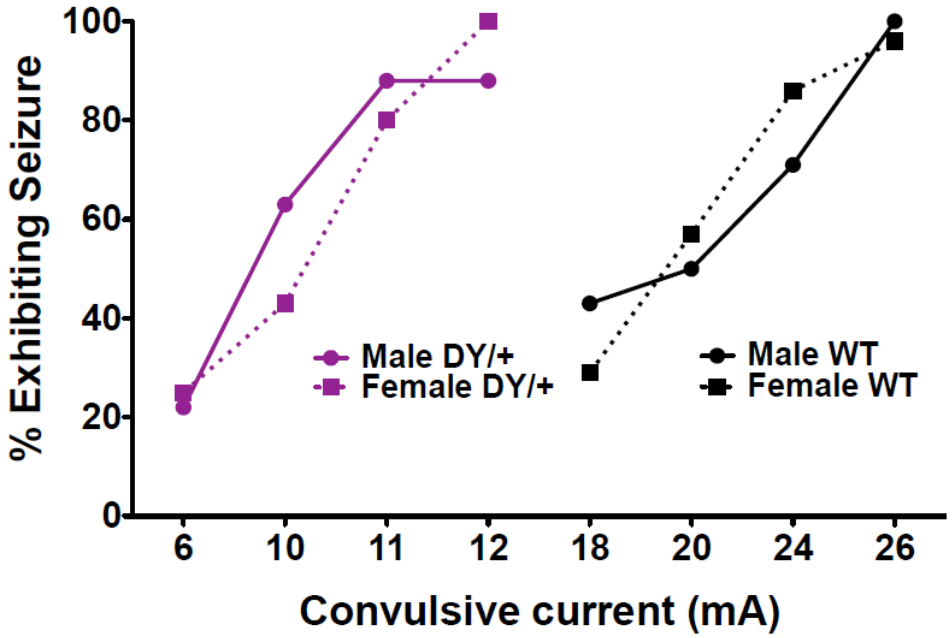

Fig 3.3. ***Scn1a-D1866Y mice had 6 Hz-induced seizures at lower current injections compared to wild-type mice***

The percentage of mice exhibiting a seizure phenotype is plotted against the amount current in milliamperes (mA) applied to the cornea at 6 Hz. About 20% of heterozygous mice (DY/+) experienced a seizure with 6 mA of current for both males (n=6) and females (n=11). With 12 mA of current, all heterozygous females seized, but not all males. Wild-type (WT) littermates required 18 mA of current to induce a seizure in about 30% of males (n=6) and females (n=9). Seizures were induced in all wild-type mice with 26 mA of current (Table 3.2).

Scn1a-D1866Y mice displayed hyperthermia-induced seizures at lower temperature than wild-type mice

Because GEFS+ in children has been associated with febrile seizures, we tested if increased body temperature induced seizures in juvenile mice. Body temperature was increased up to 42.5°C. The fraction or percentage of mice that did not exhibit a seizure decreased for mice expressing the *Scn1a*-D1866Y mutation as temperature was increased. Some homozygous mice exhibited seizures at the normal body temperature of 37.5°C, and by 40.5°C all the mice seized (n=12). Heterozygous mice started to exhibit seizures at 41.0°C and by 42.5°C all of them seized (n=12). Wild-type littermates never exhibited a seizure in this paradigm (n=12) (Fig 3.4).

Fig 3.4. *Scn1a*-1866Y reduced threshold of hyperthermia-induced seizures

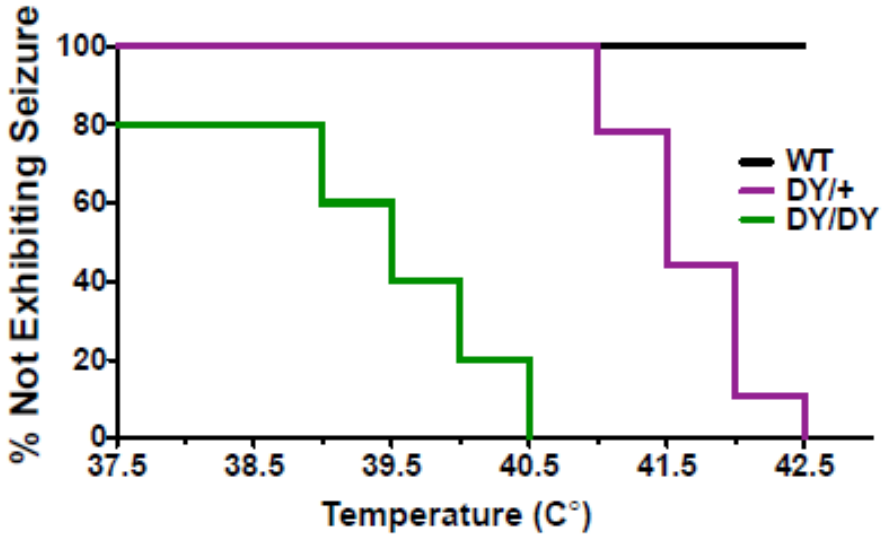

Fig 3.4. *Scn1a*-1866Y reduced threshold of hyperthermia-induced seizures

The percentage of mice not exhibiting a seizure phenotype is plotted against the increase in body temperature. About 20% of homozygous mice (DY/DY) exhibited seizures at normal temperature of 37.5°C. All homozygous mice experienced seizures by 40.5°C. About 20% of heterozygous mice (DY/+) exhibited seizures starting at 40.0°C and by 42.5°C all of them seized. Wild-type littermates (WT) never exhibited seizures. For each group n=12 (Table 3.2).

Hippocampal slices from Scn1a-D1866Y mice exhibited reduced latency and higher frequency of seizure-like activity

To determine if the *Scn1a*-D1866Y mutation had an effect on the neuronal network of the hippocampus, micro EEG or LFP recordings were performed. The recording electrode was placed in the pyramidal cell layer of the CA3 region. In normal ACSF, neuronal activity was at the basal level with a field potential at 0 mV. Perfusion of ACSF with an elevated concentration of 8 mM potassium resulted in seizure-like or burst activity, in which a group of neurons were activated at the same time. This was reversible by reintroducing regular ACSF (Fig 3.5A). The slices from wild-type mice had a latency to burst activity of 5.5 ± 0.5 min (n=4), while slices from heterozygous mice had a significantly shorter latency to burst activity of 3.7 ± 0.4 min (n=6) (Fig 3.5B). To determine if the health of the slices was affected by the procedure, population spikes before and after the recordings were performed in all slices, and were not significantly different before and after bursting (Fig 3.5C).

Fig 3.5. *Scn1a*-D1866Y reduced latency of bursting

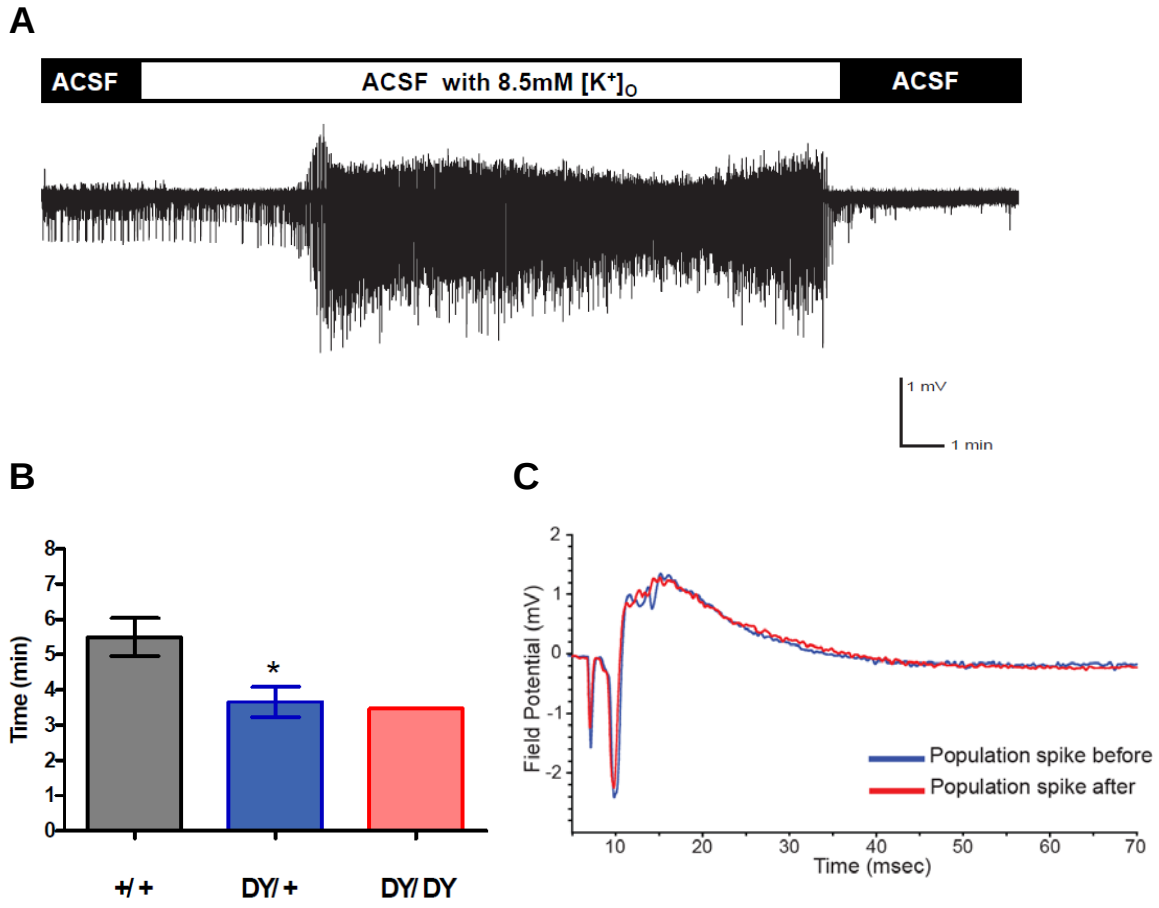

Fig 3.5. *Scn1a*-D1866Y reduced latency of bursting

A, Representative trace of brain slice perfused for 2 min in regular ACSF, then in ACSF with potassium elevated to 8.5 mM $[K^+]_O$, and finally washed with regular ACSF. **B**, Latency in minutes (min) to the beginning of the bursting events in CA3. The latency in wild-type mice (+/+) was 5.5 ± 0.5 (n=4), the latency in heterozygous mice (DY/+) was 3.7 ± 0.4 (n=6), and the latency in homozygous mice (DY/DY) was 3.5 ± 0.4 (n=2). The values shown are mean ± SEM. Statistical comparison was performed with Student's t test. Asterisk (*) indicates statistical significance ($p<0.05$) between slices from wild-type and heterozygous mice (Table 3). Slices from homozygous mice were not included in the statistical analysis because of the small sample size. **C**, The health of the slice was assessed by comparing population spikes before and after the recordings.

Because the *Scn1a*-D1866Y mutation caused epilepsy in mice, we wanted to determine if more neurons were recruited in the seizure-like events during bursting in hippocampal slices from mutant mice. Using the previous paradigm of recording micro-EEG from the pyramidal cell layer of CA3 with ACSF containing a high concentration of potassium, we measured the total amplitude of the burst event during one minute (Fig 3.6A). The bursting amplitude of slices of wild-type slices was 1.9 ± 0.2 mV (n=4), which was not significantly different from heterozygous slices, which was 1.8 ± 0.4 mV (n=6) (Student's t-test; p=0.85) (Fig 3.6B).

Fig 3.6. *Scn1a*-D1866Y did not affect bursting amplitude

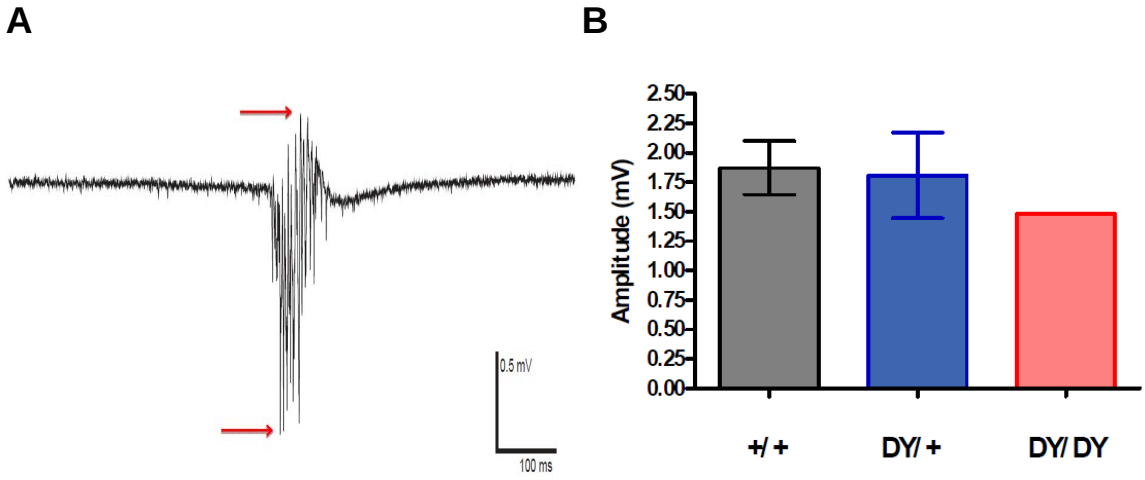

Fig 3.6. *Scn1a*-D1866Y did not affect bursting amplitude

A, Bursting amplitude was measured from the peak of the positive deflection to the peak of the negative deflection of all the events during 1 minute of bursting. **B**, Bursting amplitude in millivolts (mV) of the bursting event in CA3. Bursting amplitude of CA3 from wild-type slices (+/+) was 1.9 ± 0.2 (n=4). Bursting amplitude from heterozygous slices (DY/+) was 1.8 ± 0.4 (n=6), while for homozygous slices (DY/DY) it was 1.5 ± 0.2 (n=2). The values shown are mean ± SEM. Statistical analysis done with Student's t test (p=0.85) (Table 3.3). Slices from homozygous mice were not included in the statistical analysis due to the small sample size.

Another way in which the *Scn1a*-D1866Y mutation could have an effect on hippocampal network excitability is by changing the frequency of the bursting activity. Using the previous paradigm of high potassium ACSF in the pyramidal cell layer of CA3, we measured the number of bursting events during one minute. The slices from wild-type mice had a bursting frequency of 0.57 ± 0.07 Hz (n=4), while slices from heterozygous mice had a significantly higher bursting frequency of 0.86 ± 0.9 Hz (n=6) (Student's t-test; $p<0.05$) (Fig. 3.7).

Fig. 3.7. *Scn1a*-D1866Y increased bursting frequency

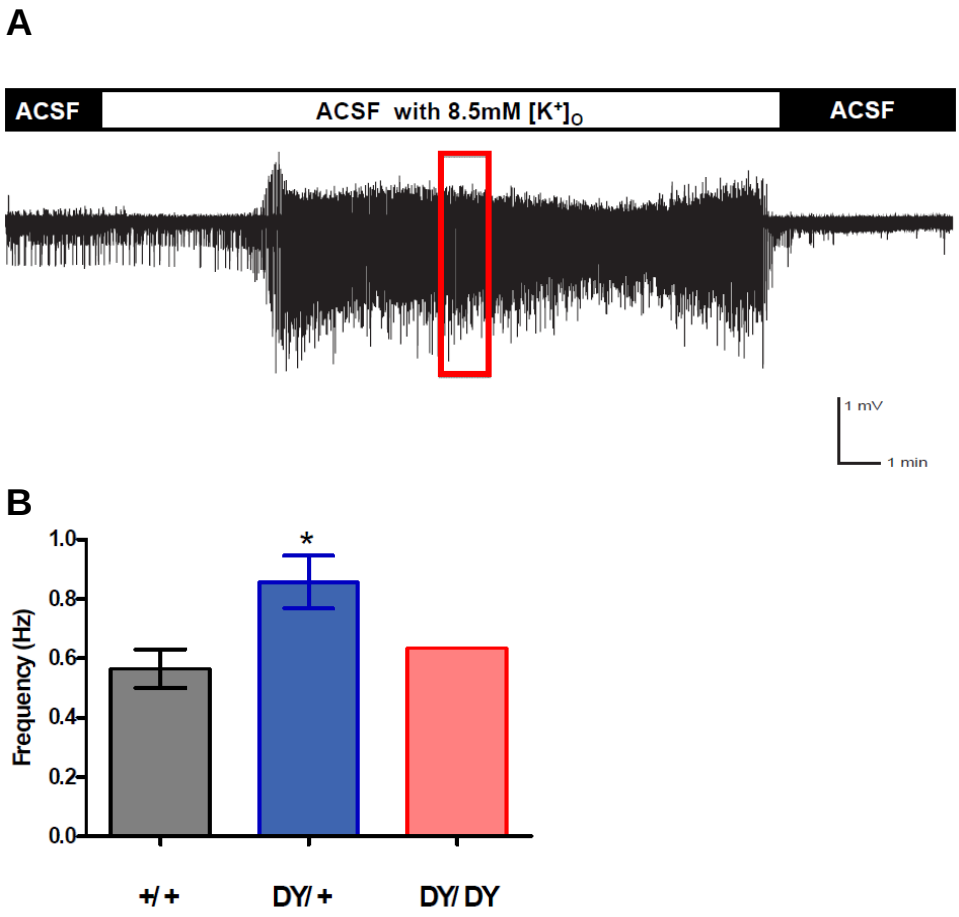

Fig. 3.7. *Scn1a*-D1866Y increased bursting frequency

A, Bursting frequency was measured by counting the amount of bursting during 1 minute of activity during the 8.5 mM $[K^+]_O$ stimulation. **B**, The frequency(Hz) of bursting events in the CA3. The bursting frequency of CA3 in wild-type slices (+/+) was 0.57 ± 0.07 (n=4). The bursting frequency in heterozygous slices (DY/+) was 0.86 ± 0.09 (n=6), while the bursting frequency in homozygous slices (DY/DY) was 0.63 ± 0.05 (n=2). The values shown are mean ± SEM. Asterisk (*) indicates statistical significance ($p<0.05$) between wild-type and heterozygous mice with Student's t test (Table 3.3). Slice from homozygous mice were not included in the statistical analysis due to small sample size.

It was possible to separate the frequency of bursting into two main components. One component is the duration of the event, known as intra-burst duration, while the second component is the time between events, known as the inter-burst duration (Fig. 3.8A). We wanted to determine which of these components was responsible for the change in frequency. Slices from wild-type mice had an intra-burst duration of 165 ± 10 msec (n=4), which was comparable to the intra-burst duration of slices from heterozygous mice (162 ± 8 msec, n=6) (Student's t-test; p=0.82) (Fig. 3.8B). On the other hand, inter-burst duration from wild-type mice was 1560 ± 180 msec (n=4), which was significantly longer than the inter-burst duration of 1050 + 105 msec (n=6) from heterozygous mice (Student's t-test; $p<0.05$) (Fig 3.8C).

Fig. 3.8. *Scn1a*-D1866Y effects on intra-burst and inter-burst duration

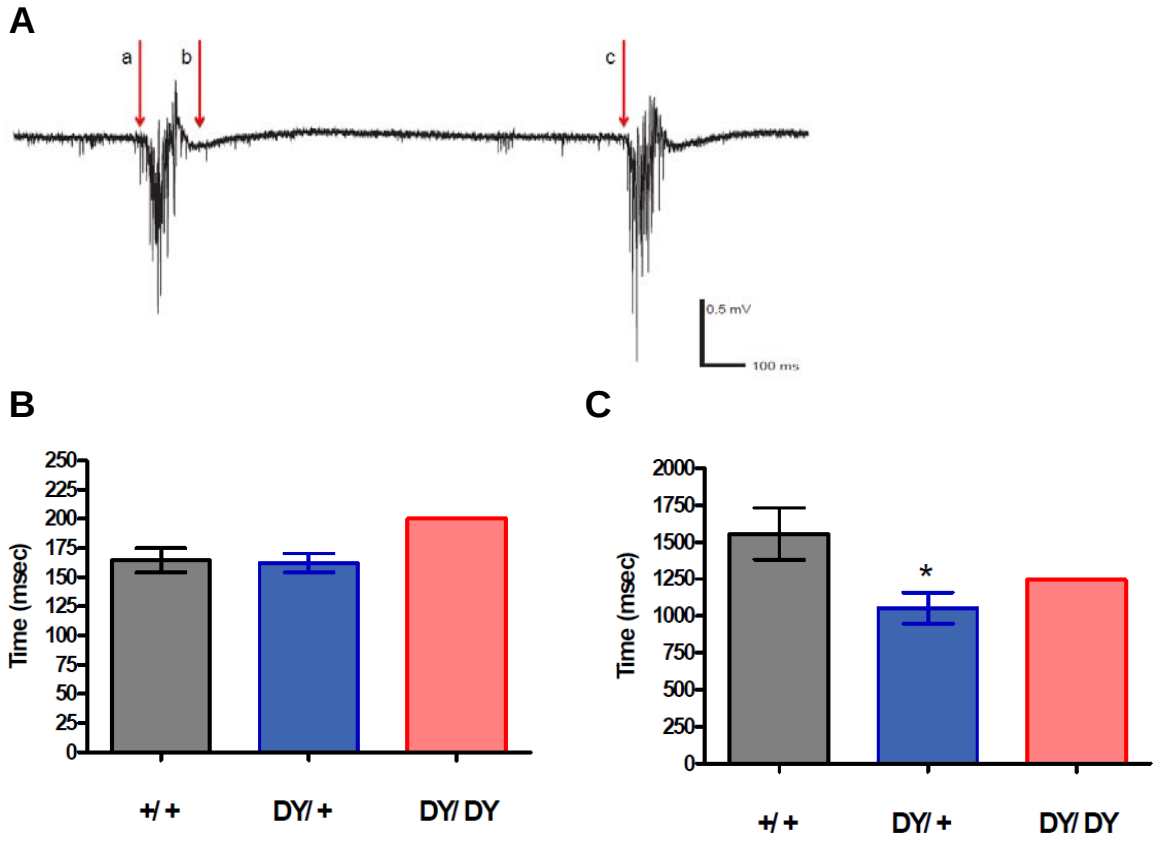

Fig. 3.8. *Scn1a*-D1866Y effects on intra-burst and inter-burst duration

A, Intra-burst duration was measured from the beginning (a) to the end (b) of a single bursting event, while the inter-burst duration was measured from the end of one bursting event to the beginning of the next one. **B**, Intra-burst duration in milliseconds (msec) in the CA3 of wild-type (+/+), heterozygous and homozygous slices was 165 ± 10, 162 ± 8, and 200 msec, respectively. Student's t-test between wild-type and heterozygous (p=0.82). **C**, Inter-burst duration in the CA3 of wild-type, heterozygous and homozygous slices was 1560 ± 180 msec, 1050 ± 105 msec , and 1250 msec, respectively. The values shown are mean ± SEM. Asterisk (*) indicates statistical significance ($p<0.05$) between wild-type and heterozygous mice as determine by Student's t test (Table 3.3). Slice from homozygous mice were not included in the statistical analysis due to the small sample size.

Table 3.1. Life span of deceased of *Scn1a*$^{D1866Y/+}$ breeders

	Males	Females	Total
Breeders with the EGFP gene			
Life span (days)	141 ± 15	116 ± 5	120 ± 5
n	16	82	98
Ratio of gender	0.163	0.837	-
Breeders without the EGFP gene			
Life span (days)	137 ± 9	120 ± 6	122 ± 6
n	13	68	81
Ratio of gender	0.160	0.840	-
Total Breeders			
Life span (days)	139 ± 9	118 ± 4	121 ± 4
n	29	150	179
Ratio of gender	0.162	0.838	-

Table 3.1. Life span of deceased of *Scn1a*$^{D1866Y/+}$ breeders

Female breeders had a higher mortality rate than male breeders, independent of whether the breeders carried the EGFP gene. Life span and ratio of deceased females was not affected by being hemizygous for the EGFP gene. The same effect was true for the males, for which hemizygosity for EGFP did not change the mortality rate. Therefore, the numbers of mice with and without EGFP were pooled for analysis. The values shown are mean ± SEM. No statistical differences ($p<0.05$) were detected using Student's t test. Homozygous mice were not included in the statistical analysis due to the small sample size.

Table 3.2. Thresholds for induced seizures

	+/+	DY/+	DY/DY
Latency to Flurothyl-Induced Seizure			
MJ (sec)	254.2 ± 7.8	253.2 ± 11.5	n/a
GTCS (sec)	392.7 ± 1.8	344.4 ± 10.1*	n/a
n	24	25	0
Current for 6 Hz-Induced Seizures			
Current to induce seizure in at least 1 mouse (mA)	18	6	n/a
Current to induce seizure in all mice (mA)	26	12	n/a
n	14	17	0
Temperature for Hyperthermia-Induced Seizures			
Lowest temperature to induce seizure (°C)	N.D.	41.0	37.5
Temperature to induce seizure in all mice (°C)	N.D	42.5	40.5
n	12	12	12

Table 3.2. Thresholds for induced seizures

The procedures to determine the threshold for induced seizures were described in the Materials and Methods. The values shown for the flurothyl-induced seizures are means ± SEM. Asterisk (*) indicates statistical significance ($p<0.05$) with Student's t test. No statistics were performed for the threshold for hyperthermia or 6 Hz induced seizures. Not detectable (N.D.) indicates that data were not measured because the paradigm did not induce a seizure. Not applicable (n/a) indicates that data could not be obtained because the mice did not survive to the age for testing.

Table 3.3. Properties of CA3 bursting activity

	+/+	DY/+	DY/DY
Bursting latency (min)	5.5 ± 0.5	3.7 ± 0.4 *	3.5
Bursting amplitude (mA)	1.9 ± 0.2	1.8 ± 0.4	1.5
Bursting frequency (Hz)	0.57 ± 0.07	0.86 ± 0.09 *	0.63
Intra-burst duration (msec)	165 ± 10	162 ± 8	200
Inter-burst duration (msec)	1560 ± 180	1050 ± 105 *	1250
n (slice; mice)	4; 2	6; 2	2;1

Table 3.3. Properties of CA3 bursting activity

The values shown are mean ± SEM. Asterisk (*) indicates statistical significance ($p<0.05$) between wild-type and heterozygous mice with Student's t test.. The preliminary data from the homozygous comes from 2 brain slices from same mice. Therefore the homozygous mice were not included in the statistical analysis due to the small sample size. Value shown of homozygous is the average of the 2 slices.

Discussion

Epilepsy syndromes, including those caused by monogenetic mutations, can have multiple phenotypes. While some individuals experience severe seizures, others can suffer mild seizures and others can be completely asymptomatic (Scheffer et al., 2009). This is due in part to differences in genetic background, although it is not completely understood how the expression of genetic modifiers is related to differences in pathology (Scheffer & Berkovic, 1997). This genetic background influence on seizures has been known for many years and it has been exploited recently by the use different strains of mice, in which a particular mutation in different mouse strains results in different seizure susceptibility (Mohajeri et al., 2004; Schauwecker, 2011). To avoid the influence of modifier genes in modeling the human epileptic phenotype caused by the *SCN1A*-D1866Y mutation, we backcrossed mice with the mutation to the C57BL/6J strain, which is commonly used for analyzing mouse models of epilepsy.

As we backcrossed the *Scn1a*-D1866Y mice on the C57BL/6J genetic background, mice carrying the mutation started to exhibit a more severe epileptic phenotype. Carriers started to experience spontaneous generalized tonic-clonic seizures on a regular basis. Generalized tonic-clonic seizures lasted from a few seconds up to half a minute. After a generalized tonic-clonic seizure, the mice were abnormally lethargic and immobile, which is commonly seen in patients

right after they experience a generalized seizure (R. S. Fisher & Schachter, 2000). Mice carrying the *Scn1a*-D1866Y mutation also exhibited abnormal behaviors that resembled other types of seizures, including stillness and repetitive motions related to absence seizure and myoclonic jerks (Scheffer & Berkovic, 1997).

The most extreme or severe phenotype was death, which we observed in almost 60% of heterozygous mice for the *Scn1a*-D1866Y mutation by the age of 4 months. Almost all the dead mice were found in the morning, which is very similar to the SUDEP phenotype in humans (Smithson, Colwell, & Hanna, 2014). Although in humans the cases of SUDEP are not as high as the incidence of sudden death observed in our mice, SUDEP can account for up to 17% of deaths in patients with epilepsy (Sperling, 2001). SUDEP is the leading cause of premature death in patients with severe epilepsy, with a frequency ranging from 10-50% (Shorvon & Tomson, 2011). The difference in the risk between mice and humans could be in the heterogeneity of genetic background in the human population in addition to differences in the brain network (R.S. Fisher, 1989).

When we looked at gender in the population of the deceased mice that are heterozygous for the *Scn1a*-D1866Y mutation, we found that females comprised almost 90% of the mice that died. This gender difference could be due to the differences in the hormones produced by the females, which have been shown to exacerbate an epileptic phenotype (Savic & Engel, 2014; Verrotti et al., 2010). In

addition, it has been shown that the levels of PV+ interneurons continue to increase in the hippocampus of female mice during the first three months of age (Wu, Du, van den Buuse, & Hill, 2014). This increase of the affected neuronal population in females could be contributing to the high mortality seen in *Scn1a*-D1866Y females.

Because the mice were not monitored by video-EEG, we cannot define the location of the seizure focus, the electrographic signature, the duration, or the frequency of seizures in mice that survived compared to those that did not survive during the first year of life. In addition, we cannot determine if the seizures were the direct cause of death in these mice or if cardio-respiratory failure contributed to it (Auerbach et al., 2013; Kalume, 2013). However, we do know that the incidence of both severe seizures and death became evident at P21, which is about one week after the expression of *Scn1a* is detected (Ogiwara et al., 2007). Conditional knockdown of *Scn1a* only in PV+ interneurons has shown that loss of *Scn1a* in only that specific neuronal population is sufficient to elicit spontaneous and induced seizures (Cheah et al., 2012; Dutton et al., 2013; Ogiwara et al., 2013) that are comparable to those seen in mouse models with global knockdown of *Scn1a* (Ogiwara et al., 2007; Yu et al., 2006) and in patients with DS and GEFS+ (Scheffer et al., 2009).

To determine if the *in vivo* effects of the *Scn1a*-D1866Y mutation were similar to the *Scn1a*-knockout (Ogiwara et al., 2007; Yu et al., 2006) and *Scn1a*-

R1648H mutation (Martin et al., 2010), we determined the seizure thresholds for several paradigms commonly used to elicit seizures. First, heterozygous mice for *Scn1a*-D1866Y mutation had a 12% reduction in the latency to GTCS but not to MJ compared to wild-type littermates when exposed to flurothyl. These results are comparable to the latency reduction in GTCS of 19% in the heterozygous *Scn1a*-R1648H (Martin et al., 2010) and the 15%-19% reduction in the heterozygous conditional *Scn1a* knockout (Dutton et al., 2013) under similar conditions. To more closely mimic the seizures observed in DS patients, we used the paradigm of psychomotor seizures elicited by current pulses at 6 Hz, which models intractable seizures (Barton, Klein, Wolf, & White, 2001). In this paradigm, wild-type mice required more current to induce seizures compare to the heterozygous mice. This result suggests that mice expressing the D1866Y mutation are more likely to develop intractable seizures. One of the main characteristics of children under the age of 6 years that suffer from GEFS+ is that fever or warm baths have been associated with their seizures. About 2-5% of human infants experience febrile seizures, but most of those individuals don't develop epilepsy (Improvement & Management, 2008). When we elevated the body temperature of young mice, we observed that mice expressing the *Scn1a*-D1866Y mutation were more susceptible to seizures. On the other hand, wild-type littermates never experienced any type of behavioral seizure when body temperature was increased up to 42.5°C. Taking the observations made in all the induced seizure paradigms together, we conclude that the *Scn1a*-D1866Y mutation increases seizure susceptibility and reproduces some of the main

seizure characteristics found in patients on the GEFS+ spectrum. Those characteristics include “intractable” seizures and susceptibility to hyperthermia or fever-induced seizures (Scheffer & Berkovic, 1997). Therefore, identification of the changes in the neurological network activity of mice carrying the *Scn1a*-D1866Y mutation can provide insight about the increased seizure susceptibility in GEFS+ patients.

Evaluation of the network activity of epileptic patients requires electroencephalogram (EEG) recordings. EEG allows monitoring of brain function and neuronal networks activity. The seizure or ictal period is characterized by hypersynchronous activity of the neurons in the network (R. S. Fisher et al., 2014). Because the *Scn1a*-D1866Y mutation resulted in changes in the PV+ interneurons at the molecular (Chapter 1) and cellular levels, but no changes in the pyramidal neurons of the hippocampus in heterozygous mice (Chapter 2), we wanted to determine if those changes could lead to an increase in the neuronal network activity of the hippocampus that could explain the increased seizure susceptibility. To determine the effects of the *Scn1a*-D1866Y mutation that are specific to the hippocampal network in young mice, we used local field potential recording as micro EEG (Bedard, Kroger, & Destexhe, 2004). In regular ACSF, action potential firing activity of the hippocampal network was minimal and similar for both slices expressing the *Scn1a*-D1866Y mutation and wild-type. When we stimulated brain slices by increasing the extracellular concentration of potassium, the hippocampal network produced oscillations in the field potential. The

oscillations in the field potentials induced by the higher potassium concentration in CA3 are similar to the population spike during the electric stimulation of the mossy fiber tract. Increasing the external concentration of potassium depolarizes the resting potential of the neurons, bringing it closer to the threshold for action potential initiation (Baylor & Nicholls, 1969; Somjen, 2002). Excitation of the mossy fiber tract results in excitation of the CA3 pyramidal cells (Andersen, Bliss, & Skrede, 1971) as well as inhibitory interneuron in the hilus, which in turn projects to CA3 (Acsády, Kamondi, Sík, Freund, & Buzsáki, 1998). Excitation of pyramidal cells results in depolarization of the individual membrane potentials due to an influx of sodium (Hodgkin & Huxley, 1952). The collective and synchronous depolarization of membrane potentials translates into a downward or negative shift of the field potential. Once the membrane potentials of the pyramidal cells are repolarized, the field potential increases. These oscillations in the field potential resulting from synchronous neuronal activity of neurons are defined as seizure-like activity or bursting events.

The hippocampal network from both wild-type and *Scn1a*-D1866Y mutant mice produced bursting events when stimulated by increasing extracellular potassium. However, the time to develop bursting events in slices from the *Scn1a*-D1866Y mice was shorter compared to wild-type littermates. These results are consistent with those from flurothyl-induced seizures in that although both mutant and wild-type mice exhibited behavioral seizures, the latency for the onset of GTCS was shorter in *Scn1a*-D1866Y mice compared to wild-type mice.

In addition to the reduction in latency for the bursting events, the hippocampal network of the *Scn1a*-D1866Y mice also showed a higher frequency of bursting events. The increase in the bursting event frequency in slices with the mutation could be the result of the reduction of time between two bursting events, the reduction of time of the bursting events, or a combination of both. Analysis of the time between bursting events, known as inter-burst duration, demonstrated that this duration was reduced in the *Scn1a*-D1866Y hippocampus. In contrast, the time of the bursting events, known as intra-burst duration, was unaffected by the mutation. These results suggest that under our stimulating conditions, each independent synchronous event in the hippocampal network was similar between mutant and wild-type, but the reappearance of the events was facilitated by the *Scn1a*-D1866Y mutation. The increased frequency in conjunction with the reduced latency of bursting events in the hippocampus could predispose to the increase in seizure susceptibility as well as the spontaneous seizures *in vivo*. Bursting event amplitude remains unaffected by the *Scn1a*-D1866Y mutation, suggesting that there are no differences in the number of neurons that are participating during synchronous firing or activation. However, it is possible that the limitation of a single pipette measuring field potential at a single location in CA3 makes it impossible to detect differences in the quantity of the neurons participating during the bursting event in other regions of the network.

In conclusion, the mouse model of the *Scn1a*-D1866Y mutation was able to recapitulate many of the characteristics of GEFS+ and intractable epilepsies,

including spontaneous seizures, SUDEP and a reduced threshold for hyperthermia-induced seizures. Increased neuronal activity was also observed at the hippocampal network level, where the *Scn1a*-D1866Y mutation increased the frequency and reduced the latency to bursting events. These results, in conjunction with the gain-of-function in sodium current and loss-of-function of action potential firing in PV+ interneurons with no changes in the excitability of pyramidal neurons by the *Scn1a*-D1866Y mutation, suggest that not all *Scn1a* mutations that cause GEFS+ or DS have the same molecular mechanism. The reduction in the excitability of PV+ interneurons supports the model of reduction of inhibition leading to a hypersynchronous neuronal circuit.

The development of new epileptic models, like the *Scn1a*-D1866Y mouse model, are important for the development of new AEDs or the re-evaluation of current AEDs that are contraindicated in some patients. The mechanism of action of many AEDs like valproate, phenobarbital, carbamazepine, phenytoin, and lamotrigine includes block of sodium channels. In many instances, these AEDs exacerbate seizures in patients with mutations that result in loss-of-function of *Scn1a* (Guerrini et al., 1998). Because *Scn1a*-D1866Y results in gain-of function instead of loss-of-function, the use of specific sodium channel blockers for *Scn1a* might be beneficial in patients with this mutation or other mutations that increase *Scn1a* function. Consistent with this prediction, valproate and phenobarbital have been effective drugs to control seizures in some family members with the *Scn1a*-D1866Y mutation (Spampanato et al., 2004).

CHAPTER 4

Discussion

The goal of this study was to characterize and understand the mechanism by which the sodium channel *Scn1a*-D1866Y mutation results in the development of epilepsy and seizures. An additional goal was to determine if all mutations in the voltage-gated sodium channel $Na_v1.1$, encoded by *Scn1a,* that cause GEFS+ or DS do so by a similar molecular mechanism. This goal is particularly important for the current and future development of AEDs, since different mechanisms are likely to require different therapeutic approaches.

Previous research characterizing the effects of *Scn1a* mutations that cause epilepsy can be divided into two main groups. The first group consists of studies using heterologous expression systems (Alekov et al., 2000; George, 2004; Lehmann-Horn & Jurkat-Rott, 1999; Spampanato et al., 2001; Sugawara et al., 2002; Vanoye, Lossin, Rhodes, & George, 2006), and the second group consists of studies using mammalian neurons. Studies using heterologous expression have the advantage of being high-throughput (Goldin, 2006). This is beneficial for the screening and development of new AEDs. However, the alterations in the electrophysiological properties characterized in heterologous systems can be markedly different from the alterations in neurons (Lossin et al.,

2002; Martin et al., 2010; Spampanato et al., 2001; Tang et al., 2009). Therefore the results in the heterologous systems may not be directly relevant to the situation *in vivo*. In addition, heterologous systems are not able to produce action potentials or electrical communication like neurons, which are required for seizure activity (Mantegazza et al., 2010). Hence, the determination of the molecular mechanisms that lead to seizure using heterologous systems may not be accurate (Avanzini, Franceschetti, & Mantegazza, 2007). On the other hand, studies that use actual neurons to determine the electrophysiological alterations are more relevant to the *in vivo* situation. This is in part because the sodium channel is not overexpressed and it has experienced the normal post-transcriptional processing (Lossin, 2009), post-translational modifications and functional interactions with other proteins (Cantrell & Catterall, 2001). Additionally, in the neuronal system the characterization of the effect by the mutation can include an analysis of cell and network excitability, which provides a better understanding of the complexity of seizure generation.

A third smaller group of studies that have been carried out in recent years include the use of non-mammalian animals such as *Drosophila melanogaster* (Sun et al., 2012) and *Danio rerio* (Baraban, Dinday, & Hortopan, 2013). Each of these systems has the advantage that they can be used to obtain high-throughput drug screening based on *in vivo* behavior. Because these models use whole animals, they can provide a framework to study the neuronal system from the molecular level to behavior. Unfortunately, it is unknown if the seizure-like

behaviors in these models really involves the same mechanisms and neuronal networks that are responsible for seizures in mammals. Hence, to be able to better understand the pathological mechanisms in humans caused by the D1866Y mutation, we used a mouse model.

The gating properties of an ion channel determine how the channel fires and how much current it conducts. The gating mechanisms of $Na_v1.1$ and the other mammalian homologs and orthologs are similar (Catterall, 1996). When a neuron is at rest, the voltage-gated sodium channels are in a closed conformation. When there is a stimulus that depolarizes the membrane, the sodium channel transitions from the closed to the open, conductive conformation. This results in further depolarization of the membrane. If the depolarization of the membrane reaches the action potential threshold, all available sodium channels will transition to the open conformation, which results in the rising phase of the action potential. The strong depolarization of the membrane then causes the sodium channels to go into the non-conductive, inactivated state. Once the membrane potential is re-polarized by the potassium channels, sodium channels can then return to the closed state from which they can be reactivated.

In Chapter 1, we examined the effects on the gating properties of the sodium channel by the *Scn1a*-D1866Y mutation. To study the alterations in the sodium current properties, we selected a neuronal population that has very high levels of $Na_v1.1$. PV^+ inhibitory interneurons have the highest levels of $Na_v1.1$

expressed in the hippocampus (Ogiwara et al., 2007), and these neurons can be identified in the G42 transgenic mice (Chattopadhyaya et al., 2004). In these neurons, the *Scn1a*-D1866Y mutation resulted in a positive shift in the voltage-dependence of activation, slower kinetics of inactivation, faster recovery from inactivation, reduced use-dependent inactivation and increased persistence current. The positive shift in activation in homozygous mice suggests a loss-of-function because of the higher threshold for firing an action potential, but all the other gating alterations are consistent with a gain-of-function of the sodium channel.

The activation of sodium channels is essential for the generation of action potentials (Hodgkin & Huxley, 1952). Action potentials mediate the phasic release of neurotransmitters, which in turn modulates electrical propagation in the postsynaptic neurons (Hall, 1972; Miledi & Slater, 1966). The firing of an action potential initiates when the membrane potential reaches the action potential threshold. At that point, available resting voltage-gated sodium channels will activate. However, during subthreshold depolarizations, most of the sodium channels are closed and other channels are more active. Therefore, membrane excitability is determined by the entire population of ion channels, and action potential firing of each neuron is shaped and influenced by the whole set of functional ion channels expressed in that neuron (Bean, 2007; Carter, Giessel, Sabatini, & Bean, 2012).

In Chapter 2, we analyzed the effect of the *Scn1a*-D1866Y mutation on the firing of action potentials and membrane excitability of neurons. First, we looked at the effect of the mutation on PV^+ interneurons. Action potential firing was greatly reduced in heterozygous mice. The reduction in the firing appeared to be the consequence of an early onset of depolarization block. The action potential threshold was increased by the mutation, but this change was not statistically significant. The membrane excitability at subthrehold levels was analyzed by the input resistance, which was not altered in PV+ interneurons. The mutation also resulted in a slight reduction of action potential firing of excitatory pyramidal cells from CA1, although this reduction was only seen in the homozygous mice. Action potential threshold were not affected but the input resistance was increased in pyramidal neurons from heterozygous mice.

Abnormal activity of a neuronal population can lead to the pathological phenotype of seizures. GEFS+ and DS are considered to be part of the same epileptic spectrum, with similar symptoms but varying in severity. Children with GEFS+ as well as those with DS experience seizures that are precipitated by fever (Scheffer & Berkovic, 1997), although as the patient grows older, fever is no longer required to initiate seizures. Patients with GEFS+ or DS are also commonly affected by other comorbidities. Lack of effective treatment can result in the most severe symptom of GEFS+ or DS, which is SUDEP (sudden unexplained death in epilepsy). Both seizures and their comorbidities are the

result of irregular and hypersynchronous network activity, which is driven by the abnormal firing activity of the neurons in the network.

In Chapter 3, we characterized the seizure susceptibility of *Scn1a*-D1866Y mice as well as the susceptibility of the hippocampal network to generate seizure-like activity. Mice carrying the mutation experienced generalized seizures more quickly when exposed to flurothyl. They also required less corneal current stimulation and less of an increase in body temperature to evoke seizures. Heterozygous mice not only were more susceptible to evoked seizures, but they demonstrated spontaneous seizures. Heterozygous mice demonstrated a high mortality rate due to SUDEP, while the life span of homozygous mice was dramatically reduced to less than 2 months. Local field potentials from the hippocampal network of heterozygous mice demonstrated a higher degree of neural synchronization. Bursting events were generated with less time and they had a higher frequency in the mice carrying the mutation.

Although our findings from heterozygous mice are more relevant to human pathology because GEFS+ is dominant, the results from homozygous mice can provide valuable information. Specifically, the pyramidal cells from homozygous mice demonstrated a reduction in action potential firing. This result supports the hypothesis that *Scn1a* is also expressed in excitatory neurons, although not at the level of PV^+ interneurons. Homozygosity probably increases the percentage of mutant channels to sufficient levels to produce alterations in the excitability of

the pyramidal cells. The reduction of action potential firing in the pyramidal cell population could contribute to the life span reduction of homozygous mice, although the increase of *Scn1a* in other brain regions with age is also probably an important factor.

The findings from heterozygous mice in Chapter 2 in conjunction with the findings in Chapter 1 suggest that *Scn1a*-D1866Y leads to epilepsy by a mechanism that is different from that described for other GEFS+ and DS mutations. A model of loss of inhibition has been proposed from several mouse models of GEFS+ and DS, in which reduced sodium channel function was observed. The D1866Y mutation resulted in the reduction of action potential firing in PV+ interneurons, which supports the model of loss of inhibition as the cause of epilepsy in DS and GEFS+. However, the *Scn1a*-D1866Y mutation also resulted in gain-of-function of the sodium currents, as shown in Chapter 1. It has been suggested in other epilepsy models that gain-of-function of sodium channels can reduce the activity of the cell. In the case of D1866Y, we propose that the increase of sodium influx in the heterozygous PV^+ interneurons results in the early onset of depolarization block, thus reducing the action potential firing of these inhibitory cells. Delays in the repolarization required to fire action potentials have been associated with a range of human diseases (Keating & Sanguinetti, 2001; Lossin et al., 2002; Q. Wang et al., 1995; Weiss et al., 2003; Yang et al., 1994).

The working model of the molecular mechanism of Scn1a-D1866Y we are proposing considers the effects on channel gating, cellular excitability and network excitability. The D1866Y mutation caused a destabilization of the inactivated state of the sodium channel, leading to increased persistent current, slower kinetics of inactivation and reduced use-dependent inactivation. This increase of sodium channels in the open state then reduced the availability of closed channels. Sodium channels need to be in the closed state in order to be able to be activated for the firing of more action potentials. PV+ interneurons expressing the mutant channels are able to fire action potentials but they cannot sustain action potential firing because of the unavailability of sodium channels in the closed state. The reduction of action potential firing of PV+ interneurons then reduced the inhibition that keeps the hippocampal circuit in normal synchrony. The less inhibited neuronal circuit became hyper-synchronous, which was manifest as seizures. This supports the idea that the C-terminal domain is critical for inactivation of the sodium channel (Irie, Shimomura, & Fujiyoshi, 2012; Mantegazza, Yu, Catterall, & Scheuer, 2001; Nguyen & Goldin, 2010), and is consistent with the delay in myocardial repolarization seen in Long QT Syndrome (Schwartz et al., 1995) by mutations in same region of the cardiac sodium channel (Dumaine et al., 1996; D. W. Wang, Yazawa, George, & Bennett, 1996; Zimmer & Surber, 2009).

This model of gain-of-function of the sodium channel as the molecular mechanism reducing the activity of PV^+ interneurons and leading to GEFS+ is

supported by clinical data. First, it has been reported that some epileptic patients contain *SCN1A* gene duplications rather than missense, non-sense or deletion mutations. The fact that these patients have more than two copies of the gene suggests a possible gain-of-function of the sodium channel due to over expression. On the other hand, it is possible that genetic modifiers in these patients modulate expression of the sodium channels. A second line of evidence supporting the hypothesis of gain-of-function leading to GEFS+ comes from the family expressing the D1866Y mutation. Phenobarbital and valproate are two of the AEDs widely used to treat epilepsy (Rogawski & Löscher, 2004), and both of these drugs function by enhancing inhibition. While these drugs are not contraindicated in GEFS+ and DS (like lamotrigine or carbamazepine), they are not very effective in DS patients with severe seizures. However, in the family carrying the D1866Y mutation, phenobarbital and valproate were effective in suppressing seizures in 2 of 4 family members (Spampanato et al., 2004). The suppression over 12 years of febrile seizures and 9 years of afebrile seizures in one patient with these drugs suggests that the seizures resulted from a reduction in the inhibitory system. GEFS+ is also associated with mutations in subunits of the $GABA_A$ receptor, further supporting the loss of inhibition model (Meisler, Kearney, Ottman, & Escayg, 2001). However, it is possible that the efficacy of these drugs in the D1866Y family could be due in part to effects on other targets or pathways.

In recent years, new unconventional treatments had been proposed to provide seizure control. Optogenetics has been used to successfully stop seizures in mice by controlling inhibitory output (Krook-Magnuson, Armstrong, Oijala, & Soltesz, 2013). Similarly, transplantation of inhibitory neurons has been shown to be efficaceous in reducing seizures in mice (Henderson et al., 2014). However, the dentate gyrus is one of the two regions in the brain in which neurogenesis continues during adult life. As the dentate produces more defective inhibitory neurons, the fraction of treated or implanted neurons will decrease with time. Hence, seizure control could be transient. Therefore, conventional treatment with a drug might be more beneficial in the long term.

In conclusion, our results have important implications for the development of new and improved treatments for epilepsy. First, not all alterations in *SCN1A* that results in DS or GEFS+ have the same molecular mechanism. This could explain the reason why some patients are refractory to treatment. It is important to note that, although most patients with epilepsy due to *SCN1A* mutations have deletion or nonsense mutations, mouse models may not necessarily reveal other molecular mechanism that lead to DS or GEFS+. Second, it is necessary to use different and new epileptic models to find rare or unusual mechanisms responsible for seizures. New models of epilepsy could reveal new potential targets or could provide systems for the development of new AEDs that are more specific. For example, the *Scn1a*-D1866Y mouse could be used in the screening of sodium blockers that are specific to $Na_v1.1$ that can restore the activity of PV^+

interneurons. In addition, new epileptic models in conjunction with well-established models can provide information about whether specific AEDs are effective in treating seizures resulting from different mechanisms.

Reference List

Acsády, L., Kamondi, A., Sík, A., Freund, T., & Buzsáki, G. (1998). GABAergic cells are the major postsynaptic targets of mossy fibers in the rat hippocampus. *J.Neurosci., 18*, 3386-3403.

Alekov, A. K., Rahman, M. M., Mitrovic, N., Lehmann-Horn, F., & Lerche, H. (2000). A sodium channel mutation causing epilepsy in man exhibits defects in fast inactivation and activation *in vitro*. *J.Physiol.(Lond.), 529*, 533-539.

Andersen, P., Bliss, T. V., & Skrede, K. K. (1971). Lamellar organization of hippocampal pathways. *Exp Brain Res, 13*(2), 222-238.

Annesi, G., Gambardella, A., Carrideo, S., Incorpora, G., Labate, A., Pasqua, A. A., . . . Quattrone, A. (2003). Two novel SCN1A missense mutations in generalized epilepsy with febrile seizures plus. *Epilepsia, 44*, 1257-1258.

Armstrong, C. M., & Hille, B. (1998). Voltage-gated ion channels and electrical excitability. *Neuron, 20*, 371-380.

Auerbach, D. S., Jones, J., Clawson, B. C., Offord, J., Lenk, G. M., Ogiwara, I., . . . Isom, L. L. (2013). Altered Cardiac Electrophysiology and SUDEP in a Model of Dravet Syndrome. *PLoS ONE, 8*(10), e77843. doi: 10.1371/journal.pone.0077843

Avanzini, G., Franceschetti, S., & Mantegazza, M. (2007). Epileptogenic channelopathies: experimental models of human pathologies. *Epilepsia, 48 (suppl. 2)*, 51-64.

Babb, T. L., Pretorius, J. K., Kupfer, W. R., & Brown, W. J. (1988). Distribution of glutamate-decarboxylase-immunoreactive neurons and synapses in the rat and monkey hippocampus: light and electron microscopy. *J Comp Neurol, 278*(1), 121-138. doi: 10.1002/cne.902780108

Babitch, J. A., & Anthony, F. A. (1987). Grasping for calcium binding sites in sodium channels with an EF hand. *J Theor Biol, 127*(4), 451-459.

Baraban, S. C., Dinday, M. T., & Hortopan, G. A. (2013). Drug screening in Scn1a zebrafish mutant identifies clemizole as a potential Dravet syndrome treatment. *Nat Commun, 4*. doi: 10.1038/ncomms3410

Barton, M. E., Klein, B. D., Wolf, H. H., & White, H. S. (2001). Pharmacological characterization of the 6 Hz psychomotor seizure model of partial epilepsy. *Epilepsy Res., 47*(3), 217-227. doi: S0920121101003023 [pii]

Baulac, S., Huberfeld, G., Gourfinkel-An, I., Mitropoulou, G., Beranger, A., Prud'homme, J.-F., . . . LeGuern, E. (2001). First genetic evidence of $GABA_A$ receptor dysfunction in epilepsy: a mutation in the γ2-subunit gene. *Nat.Genet., 28*, 46-48.

Baylor, D. A., & Nicholls, J. G. (1969). Changes in extracellular potassium concentration produced by neuronal activity in the central nervous system of the leech. *J Physiol, 203*(3), 555-569.

Bean, B. P. (2007). The action potential in mammalian central neurons. *Nat.Rev.Neurosci., 8*, 451-465.

Bechi, G., Scalmani, P., Schiavon, E., Rusconi, R., Franceschetti, S., & Mantegazza, M. (2012). Pure haploinsufficiency for Dravet syndrome $Na_v1.1$ (*SCN1A*) sodium channel truncating mutations. *Epilepsia, 53*, 87-100.

Bedard, C., Kroger, H., & Destexhe, A. (2004). Modeling extracellular field potentials and the frequency-filtering properties of extracellular space. *Biophys J, 86*(3), 1829-1842. doi: 10.1016/s0006-3495(04)74250-2

Berg, A. T., Berkovic, S. F., Brodie, M. J., Buchhalter, J., Cross, J. H., van Emde Boas, W., . . . Scheffer, I. E. (2010). Revised terminology and concepts for organization of seizures and epilepsies: report of the ILAE commission on classification and terminology, 2005-2009. *Epilepsia, 51*, 676-685.

Bezanilla, F., & Armstrong, C. M. (1977). Inactivation of the sodium channel - sodium current experiments. *J.Gen.Physiol., 70*, 549-566.

Bladin, P. F. (2011). Pioneering concepts in epileptology: the cerebral dysrhythmia of Frederic Gibbs (1903-92) and William Lennox (1884-1960). *J Clin Neurosci, 18*(8), 1038-1043. doi: 10.1016/j.jocn.2010.12.051

Burge, J. A., & Hanna, M. G. (2012). Novel insights into the pathomechanisms of skeletal muscle channelopathies. *Curr Neurol Neurosci Rep, 12*(1), 62-69. doi: 10.1007/s11910-011-0238-3

Calhoun, J., & Isom, L. (2014). The Role of Non-pore-Forming β Subunits in Physiology and Pathophysiology of Voltage-Gated Sodium Channels. In

P. C. Ruben (Ed.), *Voltage Gated Sodium Channels* (Vol. 221, pp. 51-89): Springer Berlin Heidelberg

Cantrell, A. R., & Catterall, W. A. (2001). Neuromodulation of Na^+ channels: an unexpected form of cellular plasticity. *Nat.Rev.Neurosci., 2*, 397-407.

Carter, B. C., Giessel, A. J., Sabatini, B. L., & Bean, B. P. (2012). Transient sodium current at subthreshold voltages: activation by EPSP waveforms. *Neuron, 75*, 1081-1093.

Catterall, W. A. (1993). Structure and function of voltage-gated ion channels. *Trends Neurosci., 16*, 500-506.

Catterall, W. A. (1996). Molecular properties of sodium and calcium channels. *J Bioenerg Biomembr, 28*(3), 219-230.

Catterall, W. A. (2000). From ionic currents to molecular mechanisms: the structure and function of voltage-gated sodium channels. *Neuron, 26*, 13-25.

Catterall, W. A. (2014). Sodium Channels, Inherited Epilepsy, and Antiepileptic Drugs. In P. A. Insel (Ed.), *Annual Review of Pharmacology and Toxicology, Vol 54* (Vol. 54, pp. 317-338). Palo Alto: Annual Reviews

Celesia, G. G. (2001). Disorders of membrane channels or channelopathies. *Clin.Neurophysiol., 112*, 2-18.

Chagot, B., Potet, F., Balser, J. R., & Chazin, W. J. (2009). Solution NMR structure of the C-terminal EF-hand domain of human cardiac sodium channel $Na_v1.5$. *J.Biol.Chem., 284*, 6436-6445.

Chattopadhyaya, B., Di Cristo, G., Higashiyama, H., Knott, G. W., Kuhlman, S. J., Welker, E., & Huang, Z. J. (2004). Experience and activity-dependent maturation of perisomatic GABAergic innervation in primary visual cortex during a postnatal critical period. *J.Neurosci., 24*, 9598-9611.

Cheah, C. S., Yu, F. H., Westenbroek, R. E., Kalume, F. K., Oakley, J. C., Potter, G. B., . . . Catterall, W. A. (2012). Specific deletion of $Na_v1.1$ sodium channels in inhibitory interneurons causes seizures and premature death in a mouse model of Dravet syndrome. *Proc.Natl.Acad.Sci.USA, 109*, 14646-14651.

Claes, L., Del-Favero, J., Cuelemans, B., Lagae, L., Van Broeckhoven, C., & De Jonghe, P. (2001). De novo mutations in the sodium-channel gene *SCN1A* cause Severe Myoclonic Epilepsy of Infancy. *Am.J.Hum.Genet., 68*, 1327-1332.

Claes, L. R. F., Deprez, L., Suls, A., Baets, J., Smets, K., Van Dyck, T., . . . De Jonghe, P. (2009). The *SCN1A* variant database: a novel research and diagnostic tool. *Hum.Mutat., 30*, E904-E920.

Crill, W. E. (1996). Persistent sodium current in mammalian central neurons. *Annu.Rev.Physiol., 58*, 349-362.

Cross, J. H. (2012). Fever and fever-related epilepsies. *Epilepsia, 53 Suppl 4*, 3-8. doi: 10.1111/j.1528-1167.2012.03608.x

CURE. (2011, 2011). Epilepsy facts. from http://www.cureepilepsy.org/about/epilepsy_facts.asp

CURE. (2013). State of Research in the Epilepsies. In CURE (Ed.). Chicago, IL: CURE.

Dumaine, R., Wang, Q., Keating, M. T., Hartmann, H. A., Schwartz, P. J., Brown, A. M., & Kirsch, G. E. (1996). Multiple mechanisms of Na^+ channel-linked long-QT syndrome. *Circ.Res., 78*, 916-924.

Dutton, S. B., Makinson, C. D., Papale, L. A., Shankar, A., Balakrishnan, B., Nakazawa, K., & Escayg, A. (2013). Preferential inactivation of *Scn1a* in parvalbumin interneurons increases seizure susceptibility. *Neurobiol.Dis., 49*, 211-220.

Escayg, A., & Goldin, A. L. (2010). Sodium channel *SCN1A* and epilepsy: mutations and mechanisms. *Epilepsia, 51*, 1650-1658.

Escayg, A., MacDonald, B. T., Meisler, M. H., Baulac, S., Huberfeld, G., An-Gourfinkel, I., . . . Malafosse, A. (2000). Mutations of *SCN1A*, encoding a neuronal sodium channel, in two families with GEFS+2. *Nat.Genet., 24*, 343-345.

Fisher, R. S. (1989). Animal models of the epilepsies. *Brain Res.Rev., 14*, 245-278.

Fisher, R. S., Acevedo, C., Arzimanoglou, A., Bogacz, A., Cross, J. H., Elger, C. E., . . . Wiebe, S. (2014). ILAE official report: a practical clinical definition of epilepsy. *Epilepsia, 55*(4), 475-482. doi: 10.1111/epi.12550

Fisher, R. S., & Schachter, S. C. (2000). The Postictal State: A Neglected Entity in the Management of Epilepsy. *Epilepsy Behav, 1*(1), 52-59. doi: 10.1006/ebeh.2000.0023

Gallentine, W. B. (2013). Utility of continuous EEG in children with acute traumatic brain injury. *J Clin Neurophysiol, 30*(2), 126-133. doi: 10.1097/WNP.0b013e3182872adf

George, A. L., Jr. (2004). Molecular basis of inherited epilepsy. *Arch.Neurol., 61*, 473-478.

Goldin, A. L. (2006). Expression of ion channels in *Xenopus* oocytes. In J. J. Clare & D. J. Trezise (Eds.), *Expression and Analysis of Recombinant Ion Channels* (pp. 1-25). Weinheim: Wiley-VCH. (Reprinted from: In File)

Goonawardena, J., Marshman, L. A., & Drummond, K. J. (2014). Brain tumour-associated status epilepticus. *J Clin Neurosci*. doi: 10.1016/j.jocn.2014.03.038

Guerrini, R., & Dobyns, W. B. (2014). Malformations of cortical development: clinical features and genetic causes. *Lancet Neurol, 13*(7), 710-726. doi: 10.1016/s1474-4422(14)70040-7

Guerrini, R., Dravet, C., Genton, P., Belmonte, A., Kaminska, A., & Dulac, O. (1998). Lamotrigine and seizure aggravation in severe myoclonic epilepsy. *Epilepsia, 39*, 508-512.

Hall, Z. W. (1972). Release of neurotransmitters and their interaction with receptors. *Annu Rev Biochem, 41*, 925-952. doi: 10.1146/annurev.bi.41.070172.004425

Harkin, L. A., Bowser, D. N., Dibbens, L. M., Singh, R., Phillips, F., Wallace, R. H., . . . Petrou, S. (2002). Truncation of the GABAA-receptor γ2 subunit in a family with generalized epilepsy with febrile seizures plus. *Am.J.Hum.Genet., 70*, 530-536.

Helmstaedter, C., Aldenkamp, A. P., Baker, G. A., Mazarati, A., Ryvlin, P., & Sankar, R. (2014). Disentangling the relationship between epilepsy and its behavioral comorbidities - the need for prospective studies in new-onset epilepsies. *Epilepsy Behav, 31*, 43-47. doi: 10.1016/j.yebeh.2013.11.010

Henderson, K. W., Gupta, J., Tagliatela, S., Litvina, E., Zheng, X., Van Zandt, M. A., . . . Naegele, J. R. (2014). Long-Term Seizure Suppression and Optogenetic Analyses of Synaptic Connectivity in Epileptic Mice with Hippocampal Grafts of GABAergic Interneurons. *The Journal of Neuroscience, 34*(40), 13492-13504. doi: 10.1523/jneurosci.0005-14.2014

Hille, B. (2001). *Ion channels of excitable membranes* (3 ed.). Sunderland, MA: Sinauer Associates, Inc.

Hindocha, N., Nabbout, R., Elmslie, F., Makoff, A., Al-Chalabi, A., & Nashef, L. (2009). A case report of a family with overlapping features of autosomal dominant febrile seizures and GEFS+. *Epilepsia, 50*, 937-942.

Hirose, S., Mitsudome, A., Okada, M., & Kaneko, S. (2005). Genetics of idiopathic epilepsies. *Epilepsia, 46 Suppl 1*, 38-43. doi: 10.1111/j.0013-9580.2005.461011.x

Hirose, S., Scheffer, I. E., Marini, C., De Jonghe, P., Andermann, E., Goldman, A. M., . . . Epilepsy, T. G. C. o. t. I. L. A. (2013). *SCN1A* testing for epilepsy: application in clinical practice. *Epilepsia, 54*, 946-952.

Hodgkin, A. L., & Huxley, A. F. (1952). A quantitative description of membrane current and its application to conduction and excitation in nerve. *J.Physiol.(Lond.), 117*, 500-544.

Improvement, S. C. o. Q., & Management, S. o. F. S. (2008). Febrile Seizures: Clinical Practice Guideline for the Long-term Management of the Child With Simple Febrile Seizures. *Pediatrics, 121*(6), 1281-1286. doi: 10.1542/peds.2008-0939

Irie, K., Shimomura, T., & Fujiyoshi, Y. (2012). The C-terminal helical bundle of the tetrameric prokaryotic sodium channel accelerates the inactivation gate. *Nat.Commun., 3*, 793.

Jiao, J., Yang, Y. Y., Shi, Y. W., Chen, J. Y., Gao, R., Fan, Y., . . . Gao, S. R. (2013). Modeling Dravet syndrome using induced pluripotent stem cells (iPSCs) and directly converted neurons. *Human Molecular Genetics, 22*(21), 4241-4252. doi: 10.1093/hmg/ddt275

Kalume, F. (2013). Sudden unexpected death in Dravet syndrome: Respiratory and other physiological dysfunctions. *Respiratory Physiology & Neurobiology, 189*(2), 324-328. doi: 10.1016/j.resp.2013.06.026

Kanai, K., Hirose, S., Oguni, H., Fukuma, G., Shirasaka, Y., Miyajima, T., . . . Kaneko, S. (2004). Effect of localization of missense mutations in *SCN1A* on epilepsy phenotype severity. *Neurology, 63*, 329-334.

Kass, R. S. (2004). Sodium channel inactivation goes with the flow. *J.Gen.Physiol., 124*, 7-8.

Keating, M. T., & Sanguinetti, M. C. (2001). Molecular and cellular mechanisms of cardiac arrhythmias. *Cell, 104*, 569-580.

Kim, M. K., Moore, J. H., Kim, J. K., Cho, K. H., Cho, Y. W., Kim, Y. S., . . . Shin, M. H. (2011). Evidence for epistatic interactions in antiepileptic drug resistance. *J Hum Genet, 56*(1), 71-76. doi: 10.1038/jhg.2010.151

Klausberger, T., & Somogyi, P. (2008). Neuronal diversity and temporal dynamics: the unity of hippocampal circuit operations. *Science, 321*, 53-57.

Krook-Magnuson, E., Armstrong, C., Oijala, M., & Soltesz, I. (2013). On-demand optogenetic control of spontaneous seizures in temporal lobe epilepsy. *Nat.Commun., 4*, 1376.

Krulwich, R. (2012). Which is bigger: a human brain or the universe. *Krulwich wonders.* from http://www.npr.org/blogs/krulwich/2012/07/24/157282357/which-is-bigger-a-human-brain-or-the-universe

Kwan, P., & Brodie, M. J. (2000). Early identification of refractory epilepsy. *N.Engl.J.Med., 342*(5), 314-319. doi: 10.1056/NEJM200002033420503 [doi]

Laxer, K. D., Trinka, E., Hirsch, L. J., Cendes, F., Langfitt, J., Delanty, N., . . . Benbadis, S. R. (2014). The consequences of refractory epilepsy and its treatment. *Epilepsy Behav, 37c*, 59-70. doi: 10.1016/j.yebeh.2014.05.031

Lehmann-Horn, F., & Jurkat-Rott, K. (1999). Voltage-gated ion channels and hereditary disease. *Physiol.Rev., 79*, 1317-1372.

Lennox, W. G. (1947). The genetics of epilepsy. *Am J Psychiatry, 103*(4), 457-462.

Lerche, H., Shah, M., Beck, H., Noebels, J., Johnston, D., & Vincent, A. (2013). Ion channels in genetic and acquired forms of epilepsy. *J Physiol, 591*(Pt 4), 753-764. doi: 10.1113/jphysiol.2012.240606

Li, Z., Massengill, J. L., O'Dowd, D. K., & Smith, M. A. (1997). Agrin gene expression in mouse somatosensory cortical neurons during development *in vivo* and in cell culture. *Neuroscience, 79*, 191-201.

Liu, Y., Lopez-Santiago, L. F., Yuan, Y., Jones, J. M., Zhang, H., O'Malley, H. A., . . . Parent, J. M. (2013). Dravet syndrome patient-derived neurons suggest a novel epilepsy mechanism. *Ann.Neurol., 74*, 128-139.

Lossin, C. (2009). A catalog of *SCN1A* variants. *Brain Dev., 31*, 114-130.

Lossin, C., Wang, D. W., Rhodes, T. H., Vanoye, C. G., & George, A. L., Jr. (2002). Molecular basis of an inherited epilepsy. *Neuron, 34*, 877-884.

Mantegazza, M. (2011). Dravet syndrome: insights from in vitro experimental models. *Epilepsia, 52 (suppl. 2)*, 62-69.

Mantegazza, M., Rusconi, R., Scalmani, P., Avanzini, G., & Franceschetti, S. (2010). Epileptogenic ion channel mutations: from bedside to bench and, hopefully, back again. *Epilepsy Res, 92*(1), 1-29. doi: 10.1016/j.eplepsyres.2010.08.003

Mantegazza, M., Yu, F. H., Catterall, W. A., & Scheuer, T. (2001). Role of the C-terminal domain in inactivation of brain and cardiac sodium channels. *Proc.Natl.Acad.Sci.USA, 98*, 15348-15353.

Marchi, N., Granata, T., & Janigro, D. (2014). Inflammatory pathways of seizure disorders. *Trends Neurosci, 37*(2), 55-65. doi: 10.1016/j.tins.2013.11.002

Marini, C., Mei, D., Temudo, T., Ferrari, A. R., Buti, D., Dravet, C., . . . Guerrini, R. (2007). Idiopathic epilepsies with seizures precipitated by fever and *SCN1A* abnormalities. *Epilepsia, 48*, 1678-0685.

Marini, C., Scheffer, I. E., Nabbout, R., Mei, D., Cox, K., Dibbens, L. M., . . . Mulley, J. C. (2009). *SCN1A* duplications and deletions detected in Dravet syndrome: implications for molecular diagnosis. *Epilepsia, 50*, 1670-1678.

Marini, C., Scheffer, I. E., Nabbout, R., Suls, A., De Jonghe, P., Zara, F., & Guerrini, R. (2011). The genetics of Dravet syndrome. *Epilepsia, 52 (Suppl. 2)*, 24-29.

Markram, H., Toledo-Rodriguez, M., Wang, Y., Gupta, A., Silberberg, G., & Wu, C. (2004). Interneurons of the neocortical inhibitory system. *Nat.Rev.Neurosci., 5*, 793-807.

Martin, M. S., Dutt, K., Papale, L. A., Dubé, C. M., Dutton, S. B., de Haan, G., . . . Escayg, A. (2010). Altered function of the *SCN1A* voltage-gated sodium

channel leads to g-aminobutyric acid-ergic (GABAergic) interneuron abnormalities. *J.Biol.Chem., 285*, 9823-9834.

McKhann, G. M., 2nd, Wenzel, H. J., Robbins, C. A., Sosunov, A. A., & Schwartzkroin, P. A. (2003). Mouse strain differences in kainic acid sensitivity, seizure behavior, mortality, and hippocampal pathology. *Neuroscience, 122*(2), 551-561.

Meisler, M. H., Kearney, J., Ottman, R., & Escayg, A. (2001). Identification of epilepsy genes in human and mouse. *Annu.Rev.Genet., 35*, 567-588.

Meisler, M. H., & Kearney, J. A. (2005). Sodium channel mutations in epilepsy and other neurological disorders. *J.Clin.Invest., 115*, 2010-2017.

Menon, B., & Shorvon, S. D. (2009). Ischaemic stroke in adults and epilepsy. *Epilepsy Res, 87*(1), 1-11. doi: 10.1016/j.eplepsyres.2009.08.007

Miledi, R., & Slater, C. R. (1966). The action of calcium on neuronal synapses in the squid. *J Physiol, 184*(2), 473-498.

Mistry, A. M., Thompson, C. H., Miller, A. R., Vanoye, C. G., George, A. L., Jr., & Kearney, J. A. (2014). Strain- and age-dependent hippocampal neuron sodium currents correlate with epilepsy severity in Dravet syndrome mice. *Neurobiol.Dis., 65c*, 1-11. doi: 10.1016/j.nbd.2014.01.006

Mohajeri, M. H., Madani, R., Saini, K., Lipp, H. P., Nitsch, R. M., & Wolfer, D. P. (2004). The impact of genetic background on neurodegeneration and behavior in seizured mice. *Genes Brain Behav, 3*(4), 228-239. doi: 10.1111/j.1601-1848.2004.00073.x

Mulley, J. C., Scheffer, I. E., Petrou, S., Dibbens, L. M., Berkovic, S. F., & Harkin, L. A. (2005). *SCN1A* mutations and epilepsy. *Human Mutation, 25*, 535-542.

Nagao, Y., Mazaki-Miyazaki, E., Okamura, N., Takagi, M., Igarashi, T., & Yamakawa, K. (2005). A family of generalized epilepsy with febrile seizures plus type 2 - a new missense mutation of SCN1A found in the pedigree of several patients with complex febrile seizures. *Epilepsy Res., 63*, 151-156.

Nguyen, H. M., & Goldin, A. L. (2010). Sodium channel carboxy terminal residue regulates fast inactivation. *J.Biol.Chem., 285*, 9077-9089.

Noebels, J. L. (2001). Modeling human epilepsies in mice. *Epilepsia, 42 Suppl 5*, 11-15.

Ogiwara, I., Iwasato, T., Miyamoto, H., Iwata, R., Yamagata, T., Mazaki, E., . . . Yamakawa, K. (2013). Nav1.1 haploinsufficiency in excitatory neurons ameliorates seizure-associated sudden death in a mouse model of Dravet syndrome. *Hum.Molec.Genet., In press*.

Ogiwara, I., Miyamoto, H., Morita, N., Atapour, N., Mazaki, E., Inoue, I., . . . Yamakawa, K. (2007). $Na_v1.1$ localizes to axons of parvalbumin-positive inhibitory interneurons: a circuit basis for epileptic seizures in mice carrying an *Scn1a* gene mutation. *J.Neurosci., 27*, 5903-5914.

Organization, W. H. (2012). Epilepsy. from http://www.who.int/mediacentre/factsheets/fs999/en/

Pallin, D. J., Goldstein, J. N., Moussally, J. S., Pelletier, A. J., Green, A. R., & Camargo, C. A., Jr. (2008). Seizure visits in US emergency departments: epidemiology and potential disparities in care. *Int J Emerg Med, 1*(2), 97-105. doi: 10.1007/s12245-008-0024-4

Parihar, R., & Ganesh, S. (2013). The SCN1A gene variants and epileptic encephalopoathies. *J.Hum.Genet., 58*, 573-580.

Pellock, J. M. (2004). Defining the problem: psychiatric and behavioral comorbidity in children and adolescents with epilepsy. *Epilepsy Behav, 5 Suppl 3*, S3-9. doi: 10.1016/j.yebeh.2004.06.010

Racine, R. J. (1972). Modification of seizure activity by electrical stimulation. II. Motor seizure. *Electroencephalogr Clin Neurophysiol, 32*(3), 281-294.

Ragsdale, D. S. (2008). How do mutant Nav1.1 sodium channels cause epilepsy? *Brain Res.Rev., 58*, 149-159.

Rhodes, T. H., Vanoye, C. G., Ohmori, I., Ogiwara, I., Yamakawa, K., & George, A. L., Jr. (2005). Sodium channel dysfunction in intractable childhood epilepsy with generalized tonic-clonic seizures. *J.Physiol.(Lond.), 569*, 433-445.

Rogawski, M. A., & Löscher, W. (2004). The neurobiology of antiepileptic drugs. *Nat.Rev.Neurosci., 5*, 553-564.

Roopra, A., Dingledine, R., & Hsieh, J. (2012). Epigenetics and epilepsy. *Epilepsia, 53 Suppl 9*, 2-10. doi: 10.1111/epi.12030

Rusconi, R., Combi, R., Cestèle, S., Grioni, D., Franceschetti, S., Dalprà, L., & Mantegazza, M. (2009). A rescuable folding defective $Na_v1.1$ (*SCN1A*)

sodium channel mutant causes GEFS+: common mechanism in $Na_v1.1$ related epilepsies? *Hum.Mutat., 30*, E747-E760.

Savic, I., & Engel, J., Jr. (2014). Structural and functional correlates of epileptogenesis - does gender matter? *Neurobiol Dis, 70*, 69-73. doi: 10.1016/j.nbd.2014.05.028

Schauwecker, P. E. (2011). The relevance of individual genetic background and its role in animal models of epilepsy. *Epilepsy Res, 97*(1-2), 1-11. doi: 10.1016/j.eplepsyres.2011.09.005

Scheffer, I. E., & Berkovic, S. F. (1997). Generalized epilepsy with febrile seizures plus. A genetic disorder with heterogeneous clinical phenotypes. *Brain, 120*, 479-490.

Scheffer, I. E., Zhang, Y.-H., Jansen, F. E., & Dibbens, L. (2009). Dravet syndrome or genetic (generalized) epilepsy with febrile seizures plus? *Brain Dev., 31*, 394-400.

Schwartz, P. J., Ackerman, M. J., George, A. L., Jr., & Wilde, A. A. M. (2013). Impact of genetics on the clinical management of channelopathies. *J.Am.Coll.Cardiol., 62*, 169-180.

Schwartz, P. J., Priori, S. G., Locati, E. H., Napolitano, C., Cantu, F., Towbin, J. A., . . . Colatsky, T. J. (1995). Long QT syndrome patients with mutations of the *SCN5A* and *HERG* genes have differential responses to Na^+ channel blockade and to increases in heart rate. Implications for gene-specific therapy. *Circ., 92*, 3381-3386.

Shorvon, S., & Tomson, T. (2011). Sudden unexpected death in epilepsy. *Lancet, 378*(9808), 2028-2038. doi: 10.1016/s0140-6736(11)60176-1

Silvestri, L., Sacconi, L., & Pavone, F. S. (2013). The connectomics challenge. *Funct Neurol, 28*(3), 167-173. doi: 10.11138/FNeur/2013.28.3.167

Singh, R., Andermann, E., Whitehouse, W. P. A., Harvey, A. S., Keene, D. L., Seni, M.-H., . . . Scheffer, I. E. (2001). Severe myoclonic epilepsy of infancy: Extended spectrum of $GEFS^+$. *Epilepsia, 42*, 837-844.

Smithson, W. H., Colwell, B., & Hanna, J. (2014). Sudden unexpected death in epilepsy: addressing the challenges. *Curr Neurol Neurosci Rep, 14*(12), 502. doi: 10.1007/s11910-014-0502-4

Somjen, G. G. (2002). Ion regulation in the brain: implications for pathophysiology. *Neuroscientist, 8*(3), 254-267.

Spampanato, J., Escayg, A., Meisler, M. H., & Goldin, A. L. (2001). Functional effects of two voltage-gated sodium channel mutations that cause generalized epilepsy with febrile seizures plus type 2. *J.Neurosci., 21*, 7481-7490.

Spampanato, J., Kearney, J. A., de Haan, G., McEwen, D. P., Escayg, A., Aradi, I., . . . Meisler, M. H. (2004). A novel epilepsy mutation in the sodium channel *SCN1A* identifies a cytoplasmic domain for β subunit interaction. *J.Neurosci., 24*, 10022-10034.

Sperling, M. R. (2001). Sudden unexplained death in epilepsy. *Epilepsy Curr., 1*(1), 21-23.

Stafstrom, C. E. (2007). Persistent sodium current and its role in epilepsy. *Epilepsy Curr., 7*, 15-22.

Steinlein, O. K. (2002). Channelopathies can cause epilepsy in man. *Eur.J.Pain, 6 (Suppl. A)*, 27-34.

Sugawara, T., Mazaki-Miyazaki, E., Fukushima, K., Shimomura, J., Fujiwara, T., Hamano, S., . . . Yamakawa, K. (2002). Frequent mutations of SCN1A in severe myoclonic epilepsy in infancy. *Neurology, 58*(7), 1122-1124.

Sun, L., Gilligan, J., Staber, C., Schutte, R. J., Nguyen, V., O'Dowd, D. K., & Reenan, R. (2012). A knock-in model of human epilepsy in *Drosophila* reveals a novel cellular mechanism associated with heat-induced seizure. *J.Neurosci., 32*, 14145-14155.

Tang, B., Dutt, K., Papale, L., Rusconi, R., Shankar, A., Hunter, J., . . . Escayg, A. (2009). A BAC transgenic mouse model reveals neuron subtype-specific effects of a Generalized Epilepsy with Febrile Seizures Plus (GEFS+) mutation. *Neurobiol.Dis., 35*, 91-102.

Tomaselli, G. F., Marbán, E., & Yellen, G. (1989). Sodium channels from human brain RNA expressed in *Xenopus* oocytes. Basic electrophysiologic characteristics and their modification by diphenylhydantoin. *J.Clin.Invest., 83*, 1724-1732.

Tuchman, R. M. D., Hirtz, D. M. D., & Mamounas, L. A. P. (2013). NINDS epilepsy and autism spectrum disorders workshop report. *Neurology, 81*(18), 1630-1636.

Vanoye, C. G., Lossin, C., Rhodes, T. H., & George, A. L., Jr. (2006). Single-channel properties of human $Na_v1.1$ and mechanism of channel dysfunction in *SCN1A*-associated epilepsy. *J.Gen.Physiol., 127*, 1-14.

Verrotti, A., Laus, M., Coppola, G., Parisi, P., Mohn, A., & Chiarelli, F. (2010). Catamenial epilepsy: hormonal aspects. *Gynecol Endocrinol, 26*(11), 783-790. doi: 10.3109/09513590.2010.490606

Wallace, R. H., Marini, C., Petrou, S., Harkin, L. A., Bowser, D. N., Panchal, R. G., . . . Berkovic, S. F. (2001). Mutant $GABA_A$ receptor γ2-subunit in childhood absence epilepsy and febrile seizures. *Nat.Genet., 28*, 49-52.

Wallace, R. H., Wang, D. W., Singh, R., Scheffer, I. E., George, A. L., Jr., Phillips, H. A., . . . Mulley, J. C. (1998). Febrile seizures and generalized epilepsy associated with a mutation in the Na^+-channel β1 subunit gene *SCN1B*. *Nat.Genet., 19*, 366-370.

Wallingford, E., Ostdahl, R., Zarzecki, P., Kaufman, P., & Somjen, G. (1973). Optical and pharmacological stimulation of visual cortical neurones. *Nat New Biol, 242*(120), 210-212.

Wang, D. W., Yazawa, K., George, A. L., Jr., & Bennett, P. B. (1996). Characterization of human cardiac Na^+ channel mutations in the congenital long QT syndrome. *Proc.Natl.Acad.Sci.USA, 93*, 13200-13205.

Wang, Q., Shen, J., Splawski, I., Atkinson, D., Li, Z., Robinson, J. L., . . . Keating, M. T. (1995). *SCN5A* mutations associated with an inherited cardiac arrhythmia, long QT syndrome. *Cell, 80*, 805-811.

Waxman, S. G. (2001). Transcriptional channelopathies: An emerging class of disorders. *Nat.Rev.Neurosci., 2*, 652-659.

Waxman, S. G. (2013). Painful Na-channelopathies: an expanding universe. *Trends Mol.Med., 19*, 406-409.

Waxman, S. G., & Zamponi, G. W. (2014). Regulating excitability of peripheral afferents: emerging ion channel targets. *Nature Neuroscience, 17*(2), 153-163. doi: 10.1038/nn.3602

Weiss, L. A., Escayg, A., Kearney, J. A., Trudeau, M., MacDonald, B. T., Mori, M., . . . Meisler, M. H. (2003). Sodium channels *SCN1A*, *SCN2A* and *SCN3A* in familial autism. *Mol.Psychiatry, 8*, 186-194.

Westenbroek, R. E., Merrick, D. K., & Catterall, W. A. (1989). Differential subcellular localization of the R_I and R_{II} Na^+ channel subtypes in central neurons. *Neuron, 3*, 695-704.

WHO. (2009, 2009). Epilepsy. from http://www.who.int/mediacentre/factsheets/fs999/en/

Wilmshurst, J. M., Berg, A. T., Lagae, L., Newton, C. R., & Cross, J. H. (2014). The challenges and innovations for therapy in children with epilepsy. *Nat Rev Neurol, 10*(5), 249-260. doi: 10.1038/nrneurol.2014.58

Wingo, T. L., Shah, V. N., Anderson, M. E., Lybrand, T. P., Chazin, W. J., & Balser, J. R. (2004). An EF-hand in the sodium channel couples intracellular calcium to cardiac excitability. *Nature Struct.Mol.Biol., 11*, 219-225.

Wolf, P. (2010). Sociocultural history of epilepsy. In C. P. Panayiotopoulos (Ed.), *Atlas of epilepsies* (pp. 35-44). London: Springer-Verlag

Wu, Y. C., Du, X., van den Buuse, M., & Hill, R. A. (2014). Sex differences in the adolescent developmental trajectory of parvalbumin interneurons in the hippocampus: a role for estradiol. *Psychoneuroendocrinology, 45*, 167-178. doi: 10.1016/j.psyneuen.2014.03.016

Yang, N., Ji, S., Zhou, M., Ptácek, L. J., Barchi, R. L., Horn, R., & George, A. L., Jr. (1994). Sodium channel mutations in paramyotonia congenita exhibit similar biophysical phenotypes *in vitro*. *Proc.Natl.Acad.Sci.USA, 91*, 12785-12789.

Yu, F. H., Mantegazza, M., Westenbroek, R. E., Robbins, C. A., Kalume, F., Burton, K. A., . . . Catterall, W. A. (2006). Reduced sodium current in GABAergic interneurons in a mouse model of severe myoclonic epilepsy in infancy. *Nat.Neurosci., 9*, 1142-1149.

Zaydman, M. A., Silva, J. R., & Cui, J. (2012). Ion channel associated diseases: overview of molecular mechanisms. *Chem,Rev,, 112*, 6319-6333.

Zimmer, T., & Surber, R. (2009). *SCN5A* channelopathies - an update on mutations and mechanisms. *Prog.Biophys.Mol.Biol., 98*, 120-136.